GeoArabia, 2013, v. 18, no. 4, p. 85-132
Gulf PetroLink, Bahrain

Stratigraphic control of the Aptian–Early Turonian sequences of the Levant Platform, Coastal Range, northwest Syria

Hussam Ghanem and Jochen Kuss

ABSTRACT

The predominantly carbonate Aptian–Lower Turonian succession of the Coastal Range in northwest Syria represents the northern edge of the Levant Platform. It was divided into 28 lithostratigraphic units, mainly reflecting shallowing-up and deepening-up intervals. We combined lithostratigraphy, biostratigraphy and carbon-isotope measurements, with facies interpretations, to establish a sequence-stratigraphic framework, adapted from outcrop data along two transects. The sequence-stratigraphic evolution records major transgressions-regressions and hiatuses that are compared with regional sequences of the Arabian and Levant platforms and the Tethyan realm. Age control, based on planktonic and benthonic foraminifera and ammonite biostratigraphies, is relatively good, despite changing diversities and occurrences. The chronostratigraphic framework is based on seven benthonic foraminiferal biozones (Aptian to Early Turonian) and six planktonic foraminiferal biozones (with two subzones) (latest Albian to Cenomanian). The studied carbon-isotope fluctuations record significant perturbations that are comparable with several global changes of the carbon cycle: OAE1d, LCE I-III, MCE and OAE2. The combined chemostratigraphic and biostratigraphic approach permits correlating the carbon-isotope curve of the Coastal Range with those from the Tethyan realm, England and South Palmyrides.

INTRODUCTION

In this study we present sequence-stratigraphic interpretations of a relatively monotonous succession of limestones, marls and dolostones of Aptian–Early Turonian age in northwest Syria, representing the northwestern edge of the Levant Platform (Figure 1). The depositional record of the Cretaceous succession of the Coastal Range (CR) reflects fluctuating environmental conditions and different depositional settings that were analyzed with respect to regional comparisons and to the identification of different environmental settings. All biostratigraphic, lithostratigraphic and chemostratigraphic data were evaluated with respect to the sequence-stratigraphic and paleoenvironmental interpretations.

The western slopes of the CR dip gradually to the west towards the Mediterranean Sea, while its eastern slopes are cut by the Dead Sea Fault (Mouty and Saint-Marc, 1982; Krasheninnikov et al., 2005). Similar to neighboring areas of the Syrian Arc, the Aptian–Early Turonian succession of the CR is characterized by passive continental margin depositional sequences, commonly composed of mixed siliciclastics and carbonates, formed in shallow-ramp or in deeper-ramp settings (Mouty and Saint-Marc, 1982; Flexer et al., 1986; Kuss, 1992; Kuss and Bachmann, 1996; Alsharhan and Nairn, 1997; Bachmann and Kuss, 1998; Sharland et al., 2001; Schulze et al., 2003, 2004, 2005; Le Nindre et al., 2008; Gerdes et al., 2010; Wendler et al., 2010; Powell and Moh'd, 2011).

METHODS

The study is based on detailed bed-by-bed measurements and sampling of six sections, which crop out along road cuts and two quarries of the Coastal Range (CR). The Aptian–Lower Turonian deposits attain a maximum thickness of 360 m. In the North CR (north of the South Banyas Fault, Figure 1) three sections were measured, spanning an Aptian to Lower Turonian succession: Slenfeh (SL), Bab Abdallah (SB) and Sayno (SY). The Sayno Section represents a composite section, comprising three subsections: Ain Tina, Al-Bragh and Gobet Al-Berghal (Figure 1). In the South CR (south of the South

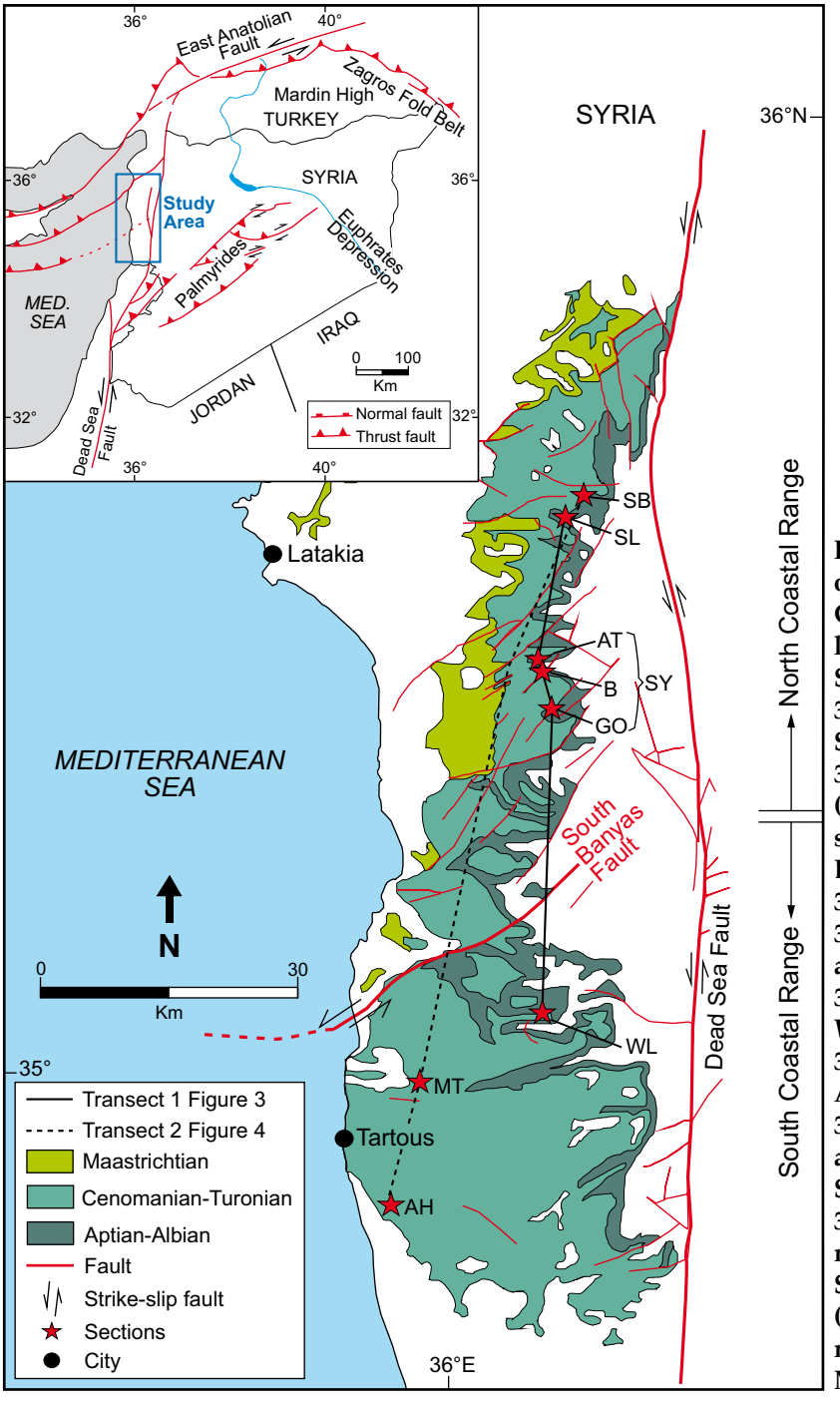

Figure 1: The Cretaceous outcrops of the Coastal Chain, showing the locations of the Slenfeh Section (SL: 35°35′74″N, 36°12′05″E); Bab Abdallah Section (SB: 35°37′11″N, 36°10′25″ E); Sayno Section (SY) is composed of three subsections; Gobet Al-Berghal (GO: 35°29′23″N, 36°09′50″E), Ain Tina (AT: 35°59′92″N, 36°11′62″E) and Al-Bragh Section (B: 35°32′39″N, 36°10′34″E); Wadi Layoun Section (WL: 34°59′53″N, 36°11′57″E); Al-Meten Section (MT: 34°59′27″N, 35°55′23″E); and Wadi Al-Haddah Section (AH: 34°49′18″N, 35°59′23″E). The solid line marks Transect 1 along SL-AT-B-GO-WL sections (Figure 3). The stippled line marks Transect 2 along SB-MT-AH sections (Figure 4).

Banyas Fault) three sections cover the Aptian to Lower Turonian: Wadi Layoun (WL), Al-Meten (MT) and Wadi Al-Haddah (AH, Figure 1). Approximately 600 rock samples were collected. Benthonic and planktonic foraminiferal biostratigraphy and microfacies were identified in ca. 400 thin sections using a standard transmitted light/polarized microscope. The microfacies analysis followed the classification of Dunham (1962) and the standard microfacies types of Flügel (2004).

The biostratigraphic framework is based on various descriptions of larger benthonic foraminifera (Mouty and Saint-Marc, 1982; Loeblich and Tappan, 1988; Banner and Simmons, 1994; Simmons et al., 2000; Velić, 2007; Boudagher-Fadel, 2009; Schroeder et al., 2010) and planktonic foraminifera (Verga and Premoli Silva, 2002; Premoli Silva and Verga, 2004; Premoli Silva et al., 2009). The biozone concept for the Coastal Range was correlated with those from other Tethyan areas proposed by the above-

mentioned authors, as well as Gradstein et al. (2012). Bulk rock samples (n = 340) for carbon-isotope analysis have been collected from SL, SB, AH and MT sections (Late Albian to Turonian). The carbon isotope *versus* depth plots have been compared with trends derived from published carbon-isotope curves (Paul et al., 1994; Gale et al., 1996; Kennedy et al., 2004; Jarvis et al., 2006; Gertsch et al., 2010).

LITHOSTRATIGRAPHY

The Cretaceous succession of the Coastal Range of Syria disconformably overlies Upper Jurassic limestones. In the North CR the following Aptian to Turonian formations were defined by Mouty and Saint-Marc (1982) in ascending order: Bab Janneh, Ain Elbeida, Slenfeh, Bab Abdallah and Aramo formations; and in the South CR: Bab Janneh, Blaatah, Slenfeh and Hannafiyah formations (Figure 2). 28 lithostratigraphic units are proposed for the Aptian–Lower Turonian succession of the CR, the reference section for the first 11 units is the SY Section, for units 12–19 the SL Section and for units 20 to 28 the SB Section (Figures 3 and 4). In the South CR, 17 subunits were defined in the fresh quarries of MT and AH sections (Hannafiyah Formation), comparable to the upper Slenfeh and Bab Abdallah formations (units 21–27 of North CR).

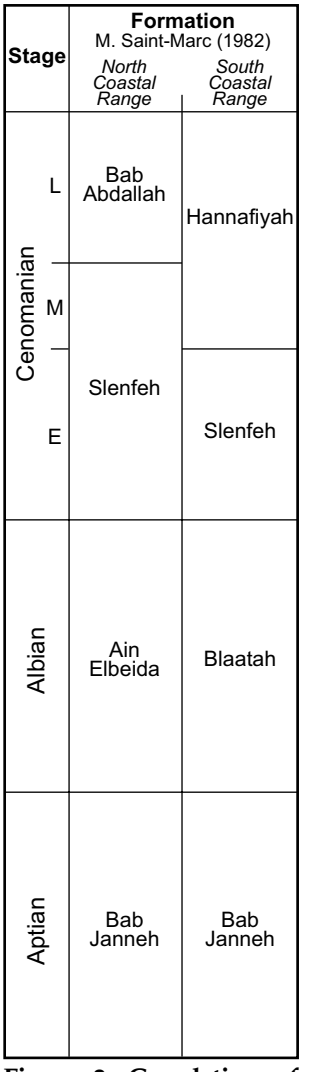

Figure 2: Correlation of formation names in South and North Coastal Range (after Mouty and Saint-Marc, 1982).

Bab Janneh Formation (North and South CR)

The Bab Janneh Formation attains a thickness of ca. 65 m in the northern part of CR and thins to ca. 20 m to the south. It was described by several authors as greenish-gray fossiliferous marls with thin limestones and dolomitic interbeds, alternating with fine-grained sandstones (Mouty and Saint-Marc, 1982; Krasheninnikov et al., 2005). In this study six lithostratigraphic units were defined from base to top (Figure 3):

Unit 1 comprises a ca. 7–8 m thick succession of greenish-gray marls with rare intercalations of sandstones in the north (SY Section) and predominantly thick intercalations of fluvial quartz sandstone in the south (WL Section Figure 5a). The marls are very rich in bivalves and echinoderms.

Unit 2 is ca. 1–3 m thick and mainly composed of thin-bedded bioclastic ooidal/peloidal limestones (calcareous algae, benthonic foraminifera, *Lithocodium* sp., ostracods and molluscs) with grain-supported texture in the SY Section and intercalated with dolomitic limestones in WL Section (Figure 5a).

Unit 3 is very similar to unit 1 in the SY Section (North CR) and is composed of 8 m-thick greenish-gray marls rich in molluscs. Thin intercalations of alluvial sandstones are present in the WL Section (South CR).

Unit 4 is 3.5 m thick and consists of 0.2–0.6 m thick beds of alternating dolomites and limestones. The lower and middle parts are composed of algal-, miliolid-, peloidal-wackestones or packstones, while the upper part is characterized by distinctive fenestral mudstones/wackestones and topped by a hardground. This unit of the North CR is correlated to 4 m of dolomitized limestones (wackestones and packstones with bivalves, calcareous algae, peloids and ooids) in WL Section (South CR).

Unit 5 is composed of an 11 m thick succession of green and gray marls with abundant bivalves, intercalated with thin beds of limestones (mudstones and wackestones with bivalves, gastropods, ostracods and miliolids) and a 0.70 m-thick glauconitic bed in the upper part of SY Section (partly similar to the south: WL Section).

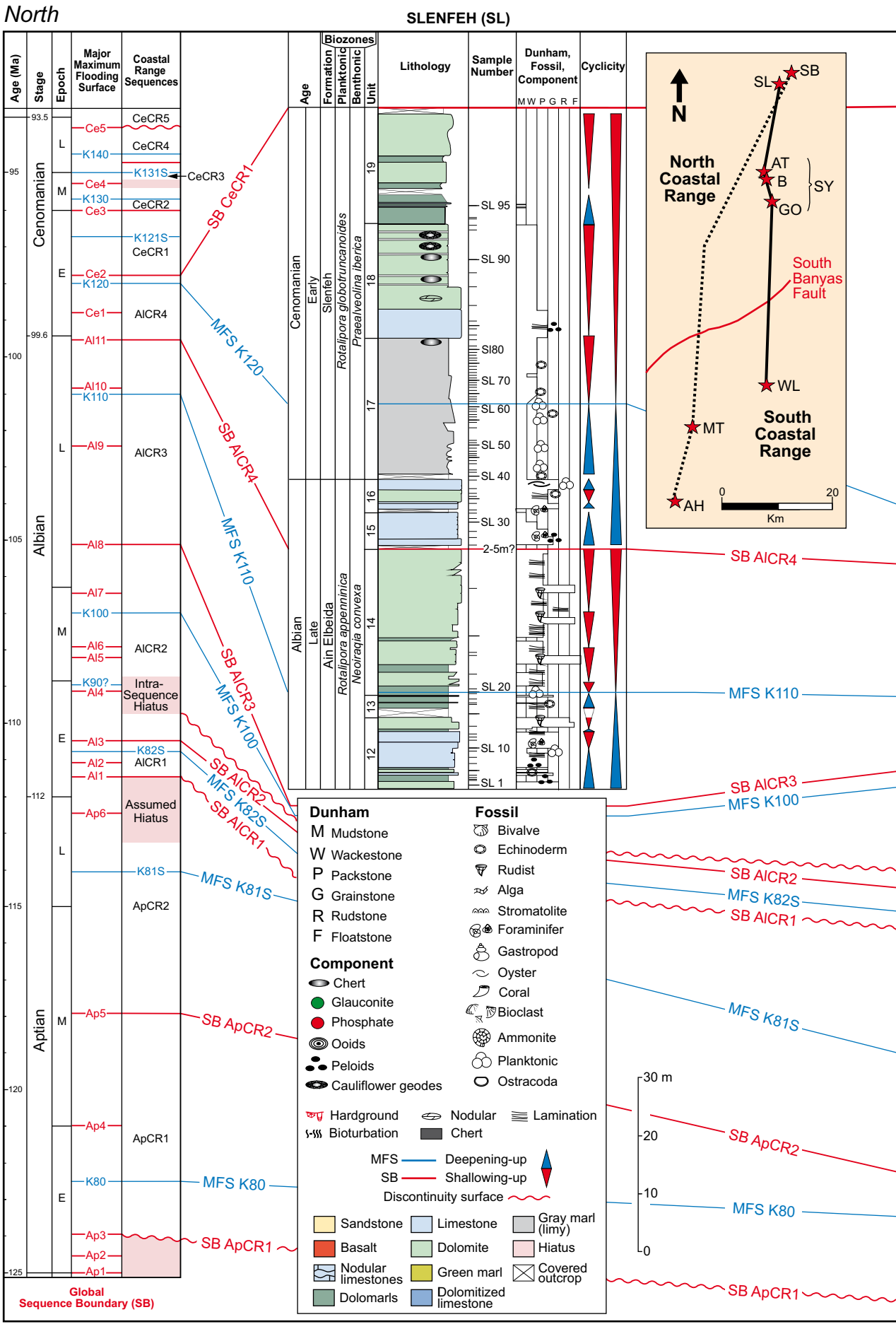
North
SLENFEH (SL)
Age (Ma)
Stage
Epoch
Major Maximum Flooding Surface
Coastal Range Sequences
Biozones
Age
Formation
Planktonic
Benthonic
Unit
Lithology
Sample Number
Dunham, Fossil, Component
Cyclicity
Cenomanian
Albian
Aptian
Early
Late
Slenfeh
Ain Elbeida
Rotalipora globotruncanoides
Praealveolina iberica
Rotalipora appenninica
Neoiraqia convexa
SL 95
SL 90
Sl80
SL 70
SL 60
SL 50
SL 40
SL 30
2-5m?
SL 20
SL 10
SL 1
CeCR5
CeCR4
CeCR3
CeCR2
CeCR1
AlCR4
AlCR3
AlCR2
Intra-Sequence Hiatus
AlCR1
Assumed Hiatus
ApCR2
ApCR1
Ce5
K140
K131S
Ce4
K130
Ce3
K121S
Ce2
K120
Ce1
Al11
Al10
K110
Al9
Al8
Al7
K100
Al6
Al5
K90?
Al4
Al3
K82S
Al2
Al1
Ap6
K81S
Ap5
Ap4
K80
Ap3
Ap2
Ap1
SB CeCR1
MFS K120
SB AlCR4
MFS K110
SB AlCR3
MFS K100
SB AlCR2
MFS K82S
SB AlCR1
MFS K81S
SB ApCR2
MFS K80
SB ApCR1
Global Sequence Boundary (SB)
N
North Coastal Range
South Coastal Range
SB
SL
AT
B
GO
SY
South Banyas Fault
WL
MT
AH
0
20
Km
Dunham
M Mudstone
W Wackestone
P Packstone
G Grainstone
R Rudstone
F Floatstone
Component
Chert
Glauconite
Phosphate
Ooids
Peloids
Cauliflower geodes
Fossil
Bivalve
Echinoderm
Rudist
Alga
Stromatolite
Foraminifer
Gastropod
Oyster
Coral
Bioclast
Ammonite
Planktonic
Ostracoda
Hardground
Bioturbation
Nodular
Chert
Lamination
MFS
SB
Deepening-up
Shallowing-up
Discontinuity surface
Sandstone
Limestone
Gray marl (limy)
Basalt
Dolomite
Hiatus
Nodular limestones
Green marl
Covered outcrop
Dolomarls
Dolomitized limestone
30 m
20
10
0

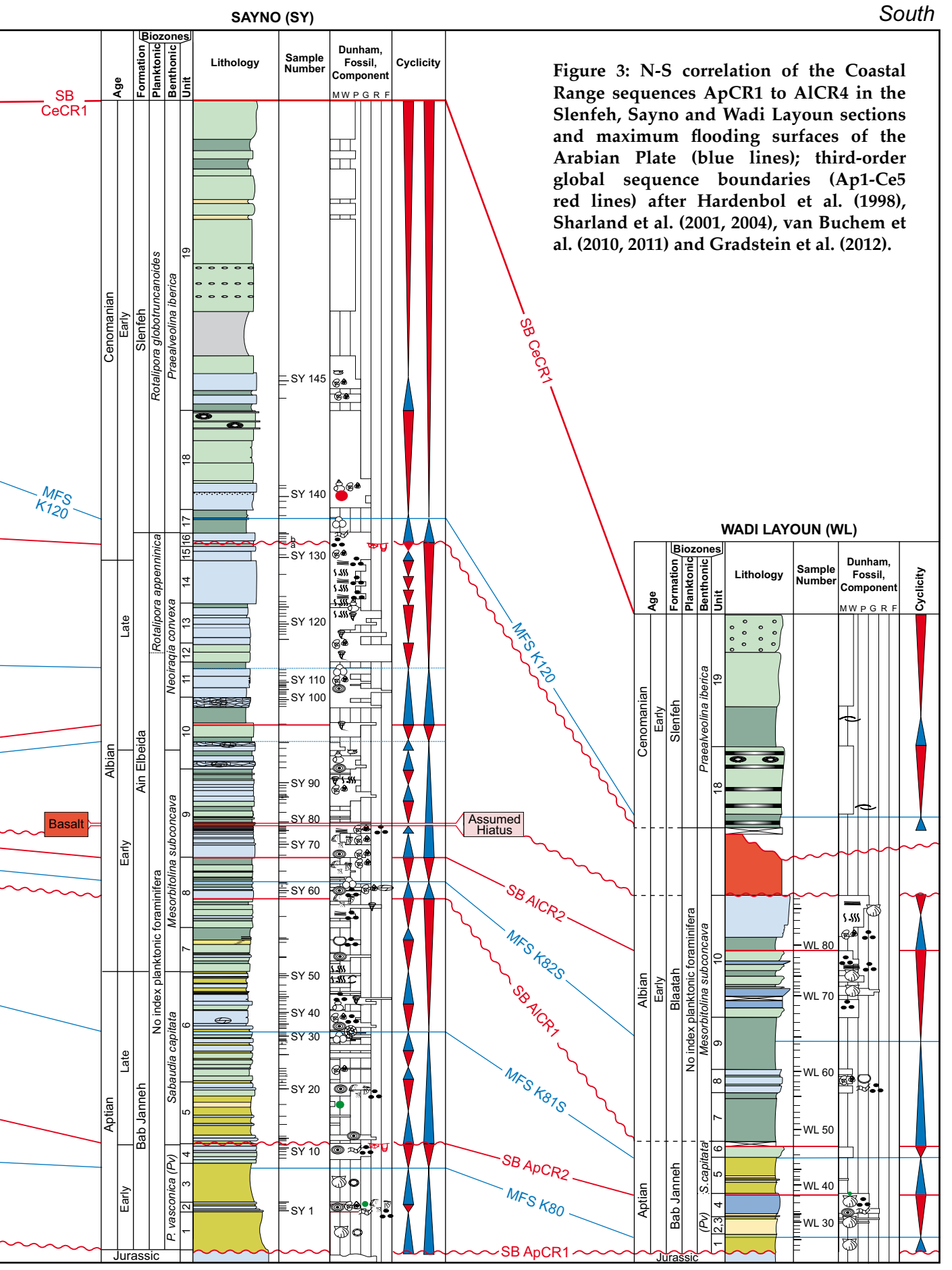

Figure 3: N-S correlation of the Coastal Range sequences ApCR1 to AlCR4 in the Slenfeh, Sayno and Wadi Layoun sections and maximum flooding surfaces of the Arabian Plate (blue lines); third-order global sequence boundaries (Ap1-Ce5 red lines) after Hardenbol et al. (1998), Sharland et al. (2001, 2004), van Buchem et al. (2010, 2011) and Gradstein et al. (2012).

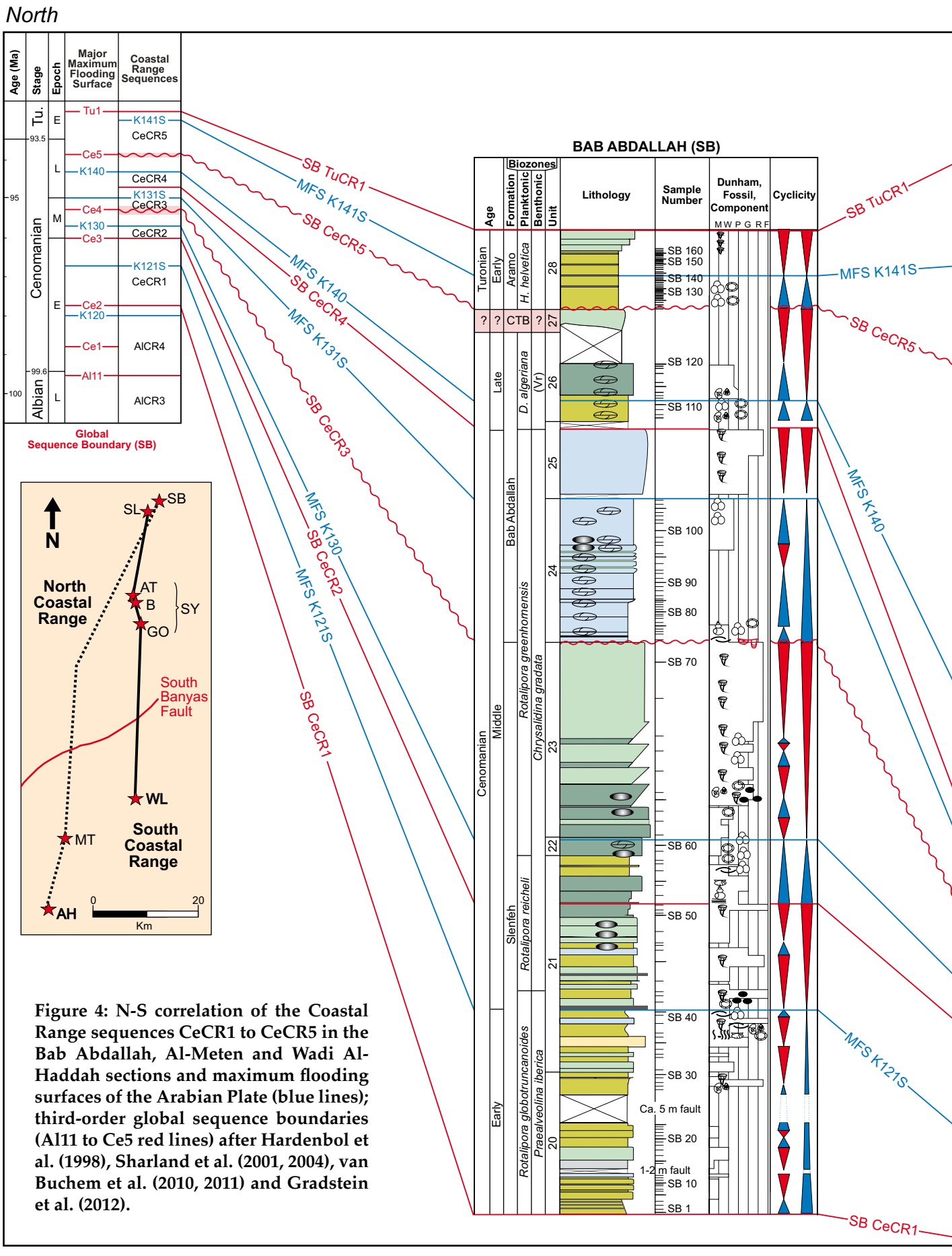

Figure 4: N-S correlation of the Coastal Range sequences CeCR1 to CeCR5 in the Bab Abdallah, Al-Meten and Wadi Al-Haddah sections and maximum flooding surfaces of the Arabian Plate (blue lines); third-order global sequence boundaries (Al11 to Ce5 red lines) after Hardenbol et al. (1998), Sharland et al. (2001, 2004), van Buchem et al. (2010, 2011) and Gradstein et al. (2012).

South

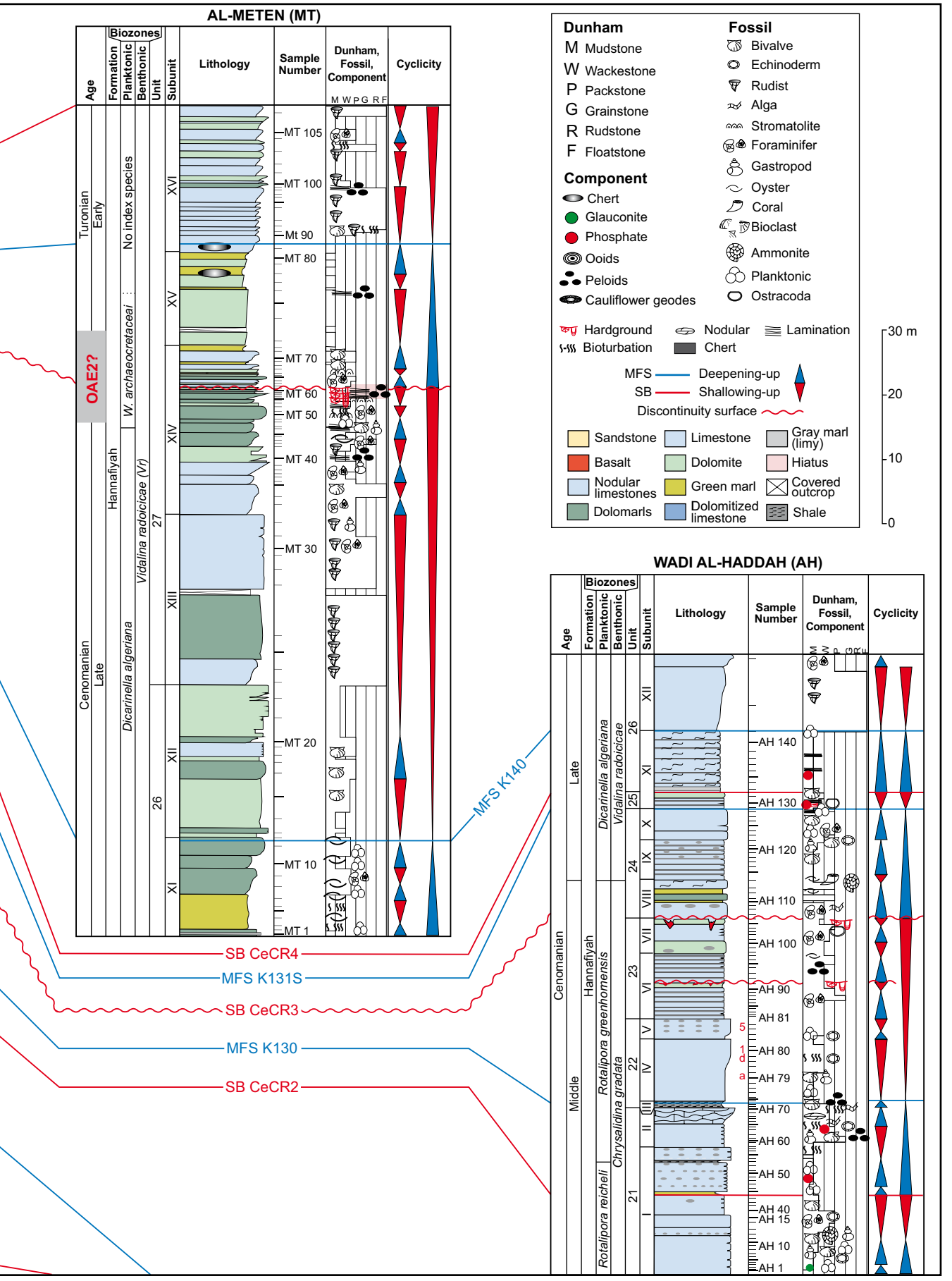
AL-METEN (MT)
Age
Biozones
Formation
Planktonic
Benthonic
Unit
Subunit
Lithology
Sample Number
Dunham, Fossil, Component
Cyclicity
M W P G R F
Turonian
Early
Cenomanian
Late
Hannafiyah
No index species
Dicarinella algeriana
W. archaeocretaceai
Vidalina radoicicae (Vr)
OAE2?
26
27
XVI
XV
XIV
XIII
XII
XI
MT 105
MT 100
Mt 90
MT 80
MT 70
MT 60
MT 50
MT 40
MT 30
MT 20
MT 10
MT 1
MFS K140
SB CeCR4
MFS K131S
SB CeCR3
MFS K130
SB CeCR2
Dunham
M Mudstone
W Wackestone
P Packstone
G Grainstone
R Rudstone
F Floatstone
Component
Chert
Glauconite
Phosphate
Ooids
Peloids
Cauliflower geodes
Fossil
Bivalve
Echinoderm
Rudist
Alga
Stromatolite
Foraminifer
Gastropod
Oyster
Coral
Bioclast
Ammonite
Planktonic
Ostracoda
Hardground
Bioturbation
Nodular
Chert
Lamination
MFS
SB
Deepening-up
Shallowing-up
Discontinuity surface
Sandstone
Basalt
Nodular limestones
Dolomarls
Limestone
Dolomite
Green marl
Dolomitized limestone
Gray marl (limy)
Hiatus
Covered outcrop
Shale
30 m
20
10
0
WADI AL-HADDAH (AH)
Age
Biozones
Formation
Planktonic
Benthonic
Unit
Subunit
Lithology
Sample Number
Dunham, Fossil, Component
Cyclicity
Cenomanian
Late
Middle
Hannafiyah
Dicarinella algeriana
Vidalina radoicicae
Rotalipora greenhornensis
Chrysalidina gradata
Rotalipora reicheli
26
25
24
23
22
21
XII
XI
X
IX
VIII
VII
VI
V
IV
III
II
I
5
1
d
a
AH 140
AH 130
AH 120
AH 110
AH 100
AH 90
AH 81
AH 80
AH 79
AH 70
AH 60
AH 50
AH 40
AH 15
AH 10
AH 1

Unit 6 is 19 m thick in the SY Section and is arranged in 0.3–1.0 m (average 0.9 m) thick beds. It comprises lower alternating dolomites and green marls with rare limestones and upper alternating limestones (occasionally nodular) and green marls with benthonic and planktonic foraminifera, ammonites, molluscs, calcareous algae, peloids and ooids. In the WL Section, unit 6 is either amalgamated in dolostones or partly missing due to later tectonic processes (Figures 3 and 5a).

Age: Most authors attributed an Aptian age for the Bab Janneh Formation (e.g. Mouty and Saint-Marc, 1982; Krasheninnikov et al., 2005), which is confirmed by our data (Early Aptian *Pseudocyclammina vasconica* range zone and the Late Aptian *Sabaudia capitata* interval zone).

Ain Elbeida Formation (North CR) and Blaatah Formation (South CR)

The Bab Janneh Formation is conformably overlain by a ca. 75 m-thick succession of limestones, marls and dolostones of the Ain Elbeida Formation (North CR) and by a ca. 56 m-thick succession of dolomitic marls, dolostones and limestones of the Blaatah Formation (South CR, Figure 3). Several basaltic layers in the upper Blaatah Formation were correlated with an interval spanning upper unit 9 to unit 16 of the Ain Elbeida Formation (SY Section). The lower interval (units 7 to lower unit 9) of the Ain Elbeida Formation were correlated with units 7 to 10 of the Blaatah Formation (WL Section, Figure 2).

Unit 7 of the Ain Elbeida Formation comprises ca. 8.5 m thick brownish-gray bedded dolostones and dolomitized limestones with a few intercalations of pure limestones. The latter contain ostracods and ooids. The beds are 0.10–1.40 m (average 0.5 m) thick; only in the lower two beds 0.08–0.1 m long horizontal burrows occur. This unit correlates with 9 m thick dolomarls of the WL Section in the eastern edge of South CR.

Unit 8 is 13.5 m thick in the SY Section. It includes several 0.40–2.1 m (average 0.8 m) thick beds of alternating dolostones, marls and fossiliferous white limestones with benthonic foraminifera, echinoderms, molluscs, calcareous algae, ooids, peloids, bioclast and algae debris. Packstone/grainstone textures prevail and occur within thicker limestone beds in the middle part of this unit. In the WL Section a 4.5 m thick alternation of limestones and dolo-limestones with ostracods, miliolids and calcareous algae occur which are comparable with unit 8 of the SY Section.

Unit 9 in the North CR is ca. 15 m thick and comprises predominantly sparitic limestones (packstones-grainstones). Bed thickness ranges from 0.1 to 0.85 m (average 0.2 m) of alternating limestones and subordinate marls and dolostones in the middle parts. Bioclasts and benthonic foraminifera are the most frequent fossils, while peloids are the most important non-skeletal grains. In the South CR unit 9 corresponds to 9.5 m thick dolomarls in the WL Section.

Unit 10 is represented in the SY Section by white limestones and nodular limestones with intercalated marly dolostones and massive dolomites. At the top, benthonic foraminifera are frequent. Peloids are the most common non-skeletal grains. This 13 m thick unit forms in the middle part of the Ain Elbeida Formation (average bed thickness of ca. 2 m) and is correlated with a 22 m-thick unit of massive dolostones and limestones in the Blaatah Formation of the South CR.

Unit 11 is ca. 6 m thick in the SY Section (North CR). It is mainly composed of wackestones-packstones. The lower 2 m are composed of 0.1–0.7 m (average 0.25 m) thick beds, while the upper 1.10 m is marly limestones with planktonic foraminifera. No corresponding lithofacies of units 11 to 18 occur in the WL Section of South CR (Figure 3); they may be replaced by a ca. 15 m thick basalt layer that disconformably overlies unit 10 (Figure 5b).

Unit 12 is 12.5 m thick in the SL Section and is predominantly composed of alternating dolostones, limestones and marls. Bed thickness ranges from 0.25–1.70 m (average 1.10 m). It comprises two groups of limestones: Planktonic foraminiferal mudstone/wackestone and peloidal packstone/grainstone, topped by a 1.1 m-thick rudist biostrome. These limestone lithologies are comparable to a 1.8 m interval dominated by rudists in the SY Section.

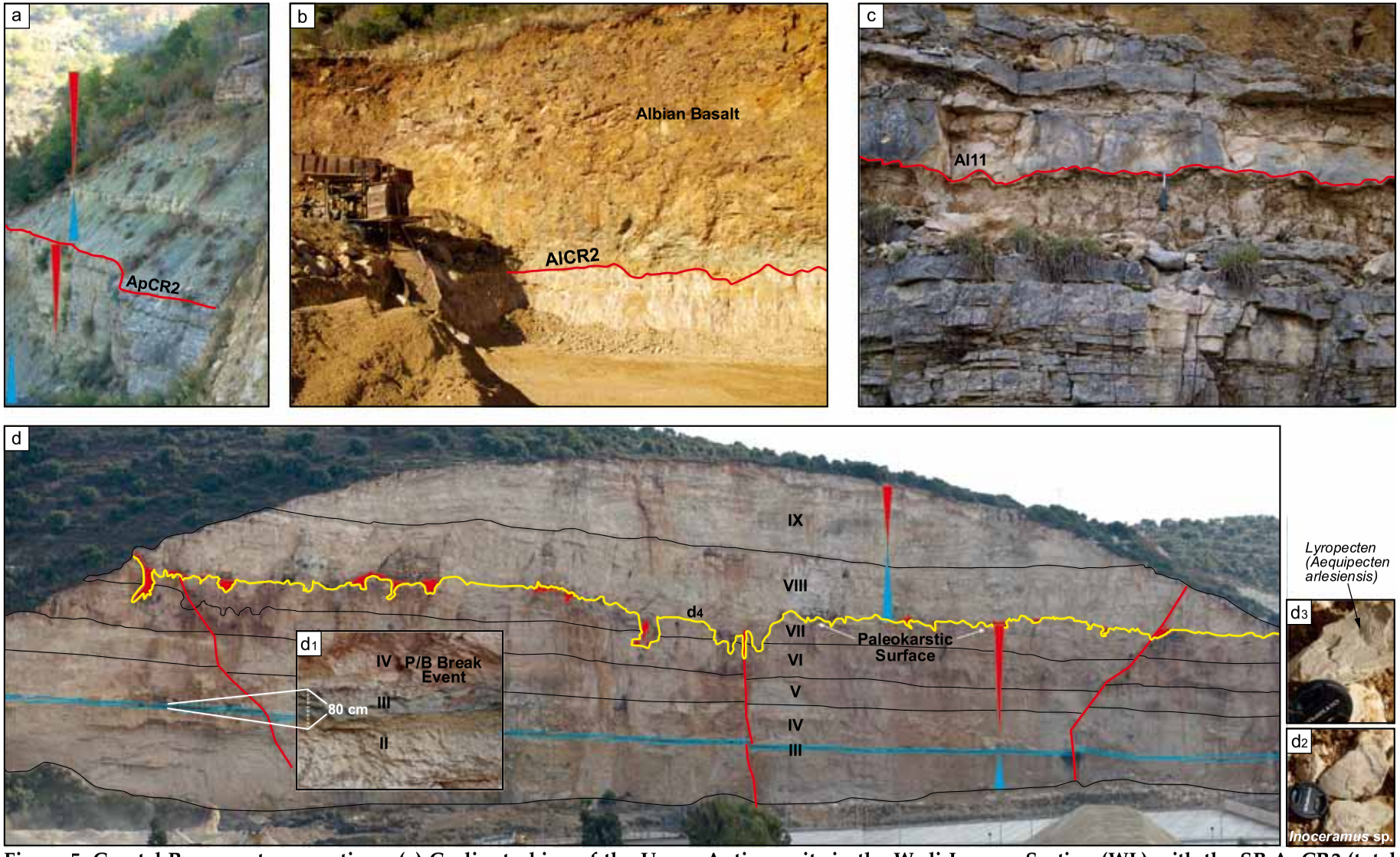

Figure 5: Coastal Range outcrop sections. (a) Cyclic stacking of the Upper Aptian units in the Wadi Layoun Section (WL) with the SB ApCR2 (total height ca. 15 m). (b) Approximately 20 m-thick Upper Albian basalt of South Coastal Range (Wadi Layoun) disconformably overlying SB AlCR2. (c) SB AlCR4 along an irregular surface corresponding to Al11 of Gradstein et al. (2012); Sayno Section, see hammer as scale. (d) Overview of Wadi Al-Haddah quarry exposing a ca. 75m thick mid-Upper Cenomanian succession of Hannafiyah Formation. (d1) close-up of unit III that represents the MFS of sequence CeCR2 (compare Figure 4) and probably corresponds with the P/B Break Event (Jarvis et al., 2006); (d2) *Inoceramus pictus* of unit III; (d3) *Lyropecten (Aequipecten) arlesiensis* of unit III; the yellow irregular line of (d4) traces a major paleokarstic surface, corresponding with SB CeCR3.

Unit 13 is ca. 4 m thick in the SL Section and comprises predominantly thin-bedded marly limestones (rich planktonic foraminifera and pelagic crinoids) with lenticular chert. In the SY Section, this 7.1 m-thick unit comprises massive limestones (average 1.2 m) with miliolids, bioclasts and rudists.

Unit 14 is ca. 22 m thick in the SL Section and 7.7 m thick in the SY Section. It is mainly composed of massive limestones or dolomitized limestones, alternating with marls in the lower part of the unit (SL Section, 1.0–3.5 m thick with average of 1.20 m). Bioturbation and lamination are most common sedimentary structures in the massive limestones of the SY Section, while rudist biostromes characterize unit 14 in the SL Section (Figure 6b).

Unit 15 comprises ca. 6 m thick bedded limestones 0.7–0.8 m thick in the SL Section. Benthonic foraminifera form the common fossils, while peloids are the most important non-skeletal grains. This characteristic unit is represented in the SY Section by 2.65 m-thick, thin-bedded limestones, topped by a hardground (Figure 5c).

Unit 16 is composed of ca. 4.8 m thick alternating dolostones and fossiliferous limestones in the SL Section. Bed thickness ranges from 0.50 to 1.30 m (average 1.2 m). The limestones hold benthonic foraminifera and abundant oysters in the upper 1.2 m. This unit correlates with 2.4 m-thick alternating dolostones and limestones in the SY Section (Figure 5c).

Age: Mouty and Saint-Marc (1982) attributed an Albian age for the Ain Elbeida and Blaatah formations. Benthonic foraminifera identified in limestones of both formations indicate Early Albian (*Mesorbitolina subconcava* Zone) and Late Albian (*Neoiraqia convexa* Zone) ages.

Slenfeh Formation (North and South CR) and Hannafiyah Formation (South CR)

The Slenfeh Formation is represented by massive bedded limestones, dolostones with marly intercalations, occasionally with chert lenses. Seven units (17–23) were defined in the North CR, with units 20 and 21 missing in the South CR. The lowermost part of Hannafiyah Formation in the South CR (AH Section) is correlated with the uppermost Slenfeh Formation in the North CR (Figures 2 and 4).

Unit 17 in the SL Section comprises basal 7 m light brown soft marls alternating with two horizons of platy marly limestones (the upper rich in oysters). The upper 15 m of this unit consist of platy marly limestones with few chert nodules occurring only in its uppermost part. Among very rare non-skeletal grains, planktonic foraminifera are by far the most important biota. Additionally, some fragments of pelagic echinoids and thin-shelled molluscs have been found. The 22 m-thick unit 7 of the SL Section correlates with 6 m in the SY Section and with 1.5 m thick limestones, disconformably overlying the basalt of the WL Section.

Unit 18 is 12.5 m thick in the SL Section, predominantly composed of massive dolostones that form cliff walls. Bed thickness ranges from 1.2 to 3.60 m (average 2.1 m). This unit is an important marker bed, comprising nodular chert and cauliflower-shaped cherts (Figure 6a). Unit 18 has similar thicknesses in the WL and SY sections, however, the lower part in the SY Section is marked by a 0.3 m-thick phosphatic bed.

Unit 19 consists of massive dolostones with intercalations of dolomarls. The ca. 50 m-thick unit comprises unfossiliferous dolomite with chert lenses and nodules (Figure 6c). Only the lower part of this unit is measured in the SL and WL sections.

Unit 20 is 19 m thick and comprises alternating limy and dolomitic marls, both unfossiliferous with chert lenses at the base. Bed thickness ranges from 0.3 to 2.4 m (average 0.8 m) in the SB Section.

Unit 21 is ca. 37 m thick and consists of 0.8–3.9 m (average 1.5 m) thick beds of alternating dolomites, marls, limestones with rudists, bivalves, benthonic and planktonic foraminifera. The lower part of unit 21 in the SB Section (North CR) includes a ca. 2 m limestone interval with quartz grains

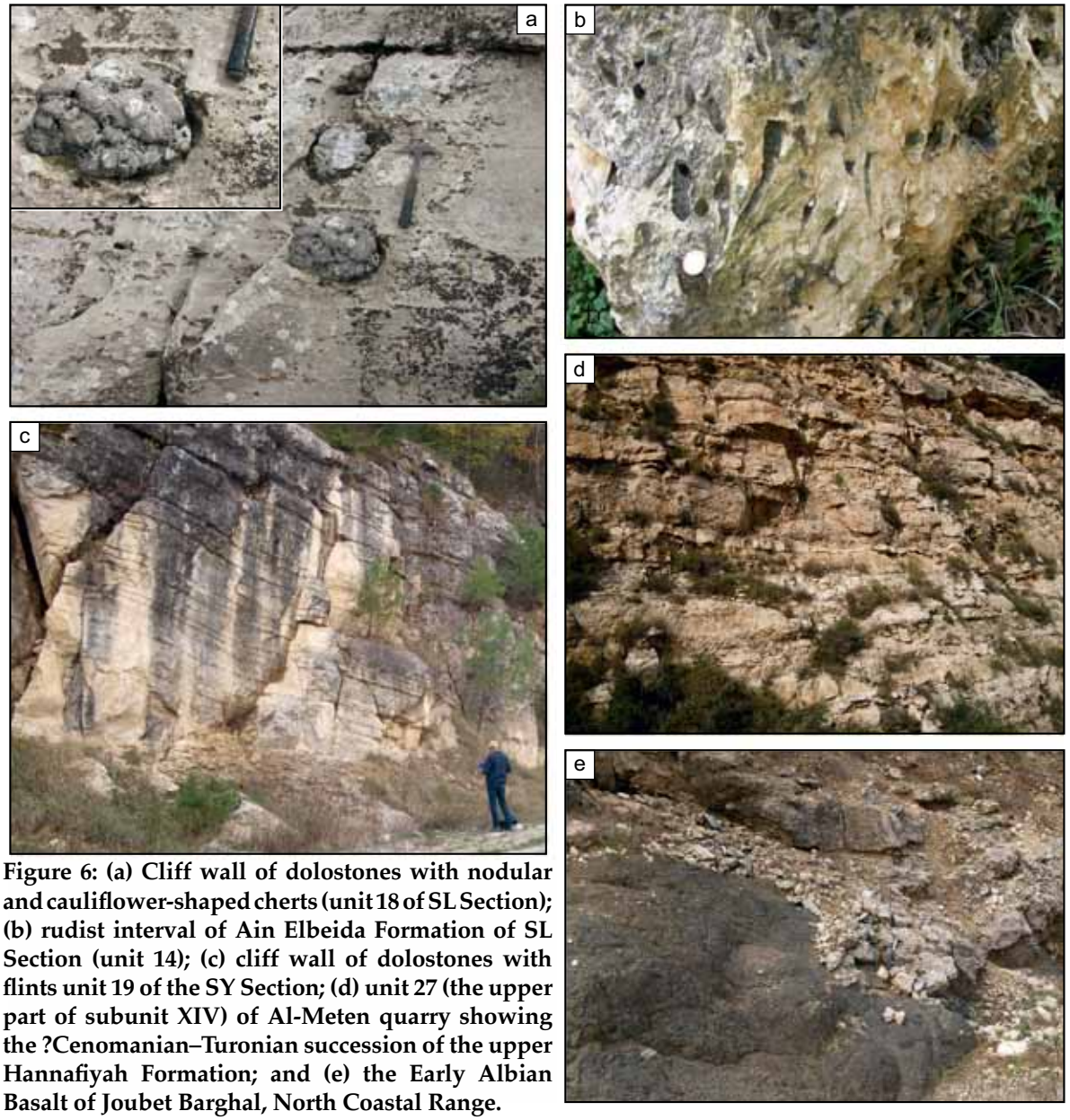

Figure 6: (a) Cliff wall of dolostones with nodular and cauliflower-shaped cherts (unit 18 of SL Section); (b) rudist interval of Ain Elbeida Formation of SL Section (unit 14); (c) cliff wall of dolostones with flints unit 19 of the SY Section; (d) unit 27 (the upper part of subunit XIV) of Al-Meten quarry showing the ?Cenomanian–Turonian succession of the upper Hannafiyah Formation; and (e) the Early Albian Basalt of Joubet Barghal, North Coastal Range.

(Figure 4), while the upper 8 m of this unit are correlated with ca. 26 m thick limestones (0.10–0.20 m-thick beds with thin bands of chert nodules) in the South CR (here: subunits I–II of the AH Section). The latter hold planktonic foraminifera, thin-walled molluscs and calcareous algal debris (Figures 4 and 5d).

Unit 22 is composed of 2 m-thick nodular limestones, rich in planktonic foraminifera and chert nodules (SB Section). The comparable unit of the South CR comprises 0.8 m-thick black shale with *Lyropecten (Aequipecten) arlesiensis* and large inoceramids shells (Figure 5d2) and is overlain by 12 m thick nodular limestones (0.1–0.2 m each bed) with planktonic foraminifera, thin-walled molluscs and chert nodules in the upper part. Unit 22 correlates with subunits III–V in the AH Section.

Unit 23 is 31 m thick and composed of ca. 1.9–6.0 m (average 2.6 m) thick rudist beds with few limestone intercalations (wackestone with planktonic foraminifera). This unit correlates with subunits VI–VII of the AH Section (South CR). The upper boundary of subunit VII is characterized by a regional unconformity marked by a distinctive paleokarstic surface (Figures 4 and 5d).

Age: Mouty and Saint-Marc (1982) attributed a latest Albian–Early to Middle Cenomanian age to the Slenfeh Formation in the North CR. In this study, the Slenfeh Formation of the North CR is correlated with the Slenfeh and the lower Hannafiyah Formation in the South CR, based on stratigraphic assumptions.

Bab Abdallah Formation (North CR) and Hannafiyah Formation (South CR)

Units 24 to 27 represent a more than 100 m thick succession of alternating well-bedded limestones, marls with chert nodules and massive dolomitized limestones (with rudists) that are attributed to the Bab Abdallah Formation in the North CR. This interval correlates with ca. 200 m-thick limestones and marls in the South CR of the Hannafiyah Formation (Figures 2 and 4).

Unit 24 is ca. 23 m thick and comprises 1.6–3.8 m (average 2.4 m) thick beds of nodular marly limestones. The base of unit 24 is marked by abundant oysters, gastropods (*Turritella* sp.) and planktonic foraminifera, while chert nodules are more frequent in the upper 9 m of the SB Section. In the AH Section (South CR), this unit (subunits VII–X) comprises 18 m-thick marls and nodular limestones (with corals, molluscs, calcareous algae, ammonites and benthonic and planktonic foraminifera).

Unit 25 is ca. 20 m thick and consists of massive dolomitized limestones composed of rudist rudstones (bed thicknesses between 1.8–3.1 m) in the North CR (SB Section). Unit 25 was correlated with a 1.0 m-thick massive dolomite bed at the base of subunit XI in the AH Section (South CR).

Unit 26 consists of ca. 50 m-thick marls and nodular limestones with abundant oysters, pelagic molluscs and planktonic foraminifera in the SB Section. It is correlated with subunits XI–XII in the AH and MT sections. The latter are composed of well-bedded limestones (wacke-/packstones with bed-thickness of 0.3–1.0 m), containing oysters, echinoderms and foraminifera (benthonic and planktonic). These limestones are overlain by marls rich in planktonic foraminifera and oysters.

Unit 27 comprises ca. 50 m-thick massive dolostones and limestones (rudist boundstones). The thickness of individual beds range between 1–8 m (average 4 m) in the SB and MT sections (subunits XII–XIII). Only in the MT Section, the overlying subunits XIV, XV and XVI are present and are composed of 25 m-thick platy limestones and dolostones, overlain by 37 m-thick massive bedded fossiliferous limestones, alternating with marls, dolomitic limestones and dolostones (Figures 4 and 6d). Benthonic foraminifera, molluscs, stromatolites (bindstones) and reworked rudists are frequent constituents of the wacke-/packstones and pack-/floatstones. Based on maximum values of $\delta^{13}C$ the Cenomanian/Turonian Boundary (CTB) is interpreted to occur in the platy limestone interval (Figure 6d).

Unit 28 has a thickness of 20 m and is composed of 0.05–0.1 m-thick alternating limestones and chert, containing pelagic echinoids, thin-walled molluscs and planktonic foraminifera. These marly limestones are argillaceous in some intervals and are overlain by 3 m massive limestones with rudists. This unit forms the base of the Turonian Aramo Formation.

Age: Most authors attributed a mid-Late Cenomanian age for the Bab Abdallah and Hannafiyah formations and a Turonian age for the Aramo Formation (e.g. Mouty and Saint-Marc, 1982). This is consistent with our results. In addition we attribute an earliest Turonian age for the uppermost Hannafiyah Formation (MT Section).

BIOSTRATIGRAPHY

Biostratigraphic control of the mainly shallow-water carbonates of the Coastal Range of Syria is mainly based on foraminifera, identified in thin sections. Planktonic foraminifera reflect shallow environments and high-stress conditions, as indicated by generally low diversity, dwarfing and sporadic presence of index species. However, several intervals of the studied Aptian–Lower Turonian succession show more diverse and abundant assemblages and permit a good resolution, when all biostratigraphic data (benthonic and planktonic foraminifera plus macrofossils) are combined (Figure 7).

Benthonic Foraminifera Biostratigraphy

Numerous benthonic foraminifera are useful index fossils of the Cretaceous carbonate platforms (Loeblich and Tappan, 1988; BouDagher-Fadel, 2009). They show a widespread distribution, high diversity and abundance in the studied sections of the Coastal Range (Figures 7 to 14) and thus are important for the biostratigraphic subdivision. Based on the concepts of Velić (2007), Schroeder et al. (2010), Gradstein et al. (2012) and Ghanem et al. (2012) the following seven biozones (overlapping most planktonic zonal boundaries, Figure 7) were defined.

Early Aptian Pseudocyclammina vasconica (Palorbitolina lenticularis) partial-range zone

Diagnosis*:* This biozone is defined by the total range of the zonal markers *Pseudocyclammina vasconica* and *Voloshinoides murgensis,* according to the range of co-occurring benthonic foraminifera in the Tethys and the Adriatic platforms (Velić, 2007; Ogg and Ogg, 2008; Figure 7).

Description: This biozone spans a long Early Aptian stratigraphic interval. However, the lower part of the Lower Aptian is missing (compare Sequence ApCR1). In addition to the zonal marker species, the following taxa occur within the *P. vasconica* range zone of the present study**:** *Voloshinoides murgensis*, *Sabaudia minuta, Sabaudia auruncensis, Vercorsella arenata, Vercorsella immaturata, Rumanoloculina robusta, Ammobaculites celatus, Dukhania conica, Praechrysalidina infracretacea, Charentia cuvillieri, Pseudonummoloculina aurigerica, Derventina* sp., including few miliolids. Mouty and Saint-Marc (1982) described two marker species (*Palorbitolina lenticularis* and *Choffatella decipiens*) from units 1 and 3 (Figures 3, 7 and 8).

Correlation: The benthonic assemblages of the *P. vasconica* range zone of the CR correlates well with the Early Aptian benthonic foraminiferal assemblages of the Adriatic Platform and Tethyan realm, described by Loeblich and Tappan (1988), Velić (2007) and Gradstein et al. (2012). Therefore it is comparable to the stratigraphic range of the *Palorbitolina lenticularis* Zone of the Arabian Platform (Schroeder et al., 2010).

Age and Occurrence*:* The Early Aptian *P. vasconica* range zone documents the first benthonic foraminifera of the Cretaceous succession of the Coastal Range. It is recorded from 22 m thick green marls, dolostones and limestones, representing units 1, 2, 3 and 4 (Bab Janneh Formation) of the SY and WL sections (Figure 3, 7 and 9).

Late Aptian Sabaudia capitata interval zone

Diagnosis: The lower boundary of this interval zone has been determined by the first occurrence (FO) of *S. capitata* and *Nezzazata isabellae*. The FO of *Nezzazatinella picardi*, *Cuneolina parva* and *C. pavonia* mark the upper boundary of this biozone (Figure 7).

Description: The benthonic index fossils of the Late Aptian (*Mesorbitolina parva* and *M. texana*) biozones (Velić, 2007; Ogg and Ogg, 2008; Schroeder et al., 2010; Figure 7) are not present in the studied sections. We therefore suggest the *S. capitata* interval zone as index zone for the Late Aptian. Besides the FOs of the two marker species, this biozone is characterized by the last occurrences (LOs) of *Voloshinoides murgensis, Pseudocyclammina vasconica* and *Ammobaculites celatus*. Moreover, the *S. capitata* Zone is associated with rich assemblages of the following wide ranging species: *Charentia cuvillieri*, *Dukhania conica, Praechrysalidina infracretacea, Sabaudia minuta*, *Sabaudia auruncensis*, *Vercorsella arenata*, *Vercorsella immaturata*, *Rumanoloculina robusta*, *Pseudonummoloculina aurigerica* (Figures 7 and 9).

Correlation: The Late Aptian *S. capitata* interval zone is equivalent to the stratigraphic range of both *Mesorbitolina parva* and *M. texana* biozones (Schroeder et al., 2010) of the Arabian Platform.

Age and Occurrence: The *S. capitata* interval zone comprises a Late Aptian interval in the northern part of the Coastal Range (SY Section). It is represented by 30 m thick shallow-marine limestones intercalating with green marls and dolomites and occurs in units 5 and 6, respectively the upper Bab Janneh Formation (Figure 7).

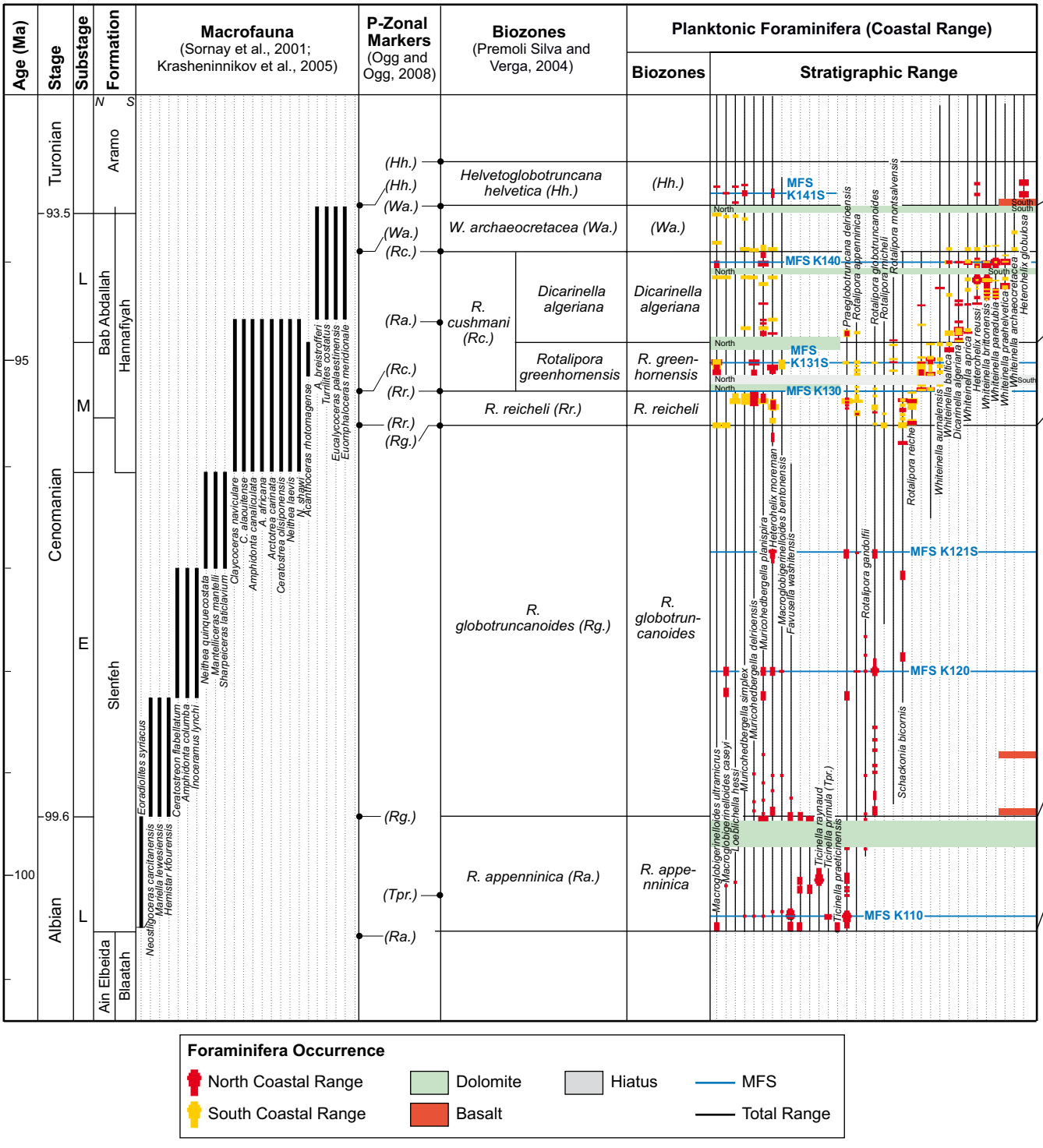

Figure 7: Stratigraphic concept and standard biozones (planktonic and benthonic foraminifera). Red/ yellow dots represent the foraminiferal occurrence of North/South Coastal Range, the thick line indicates the total range of foraminifera species, and the blue line represents maximum flooding surfaces.

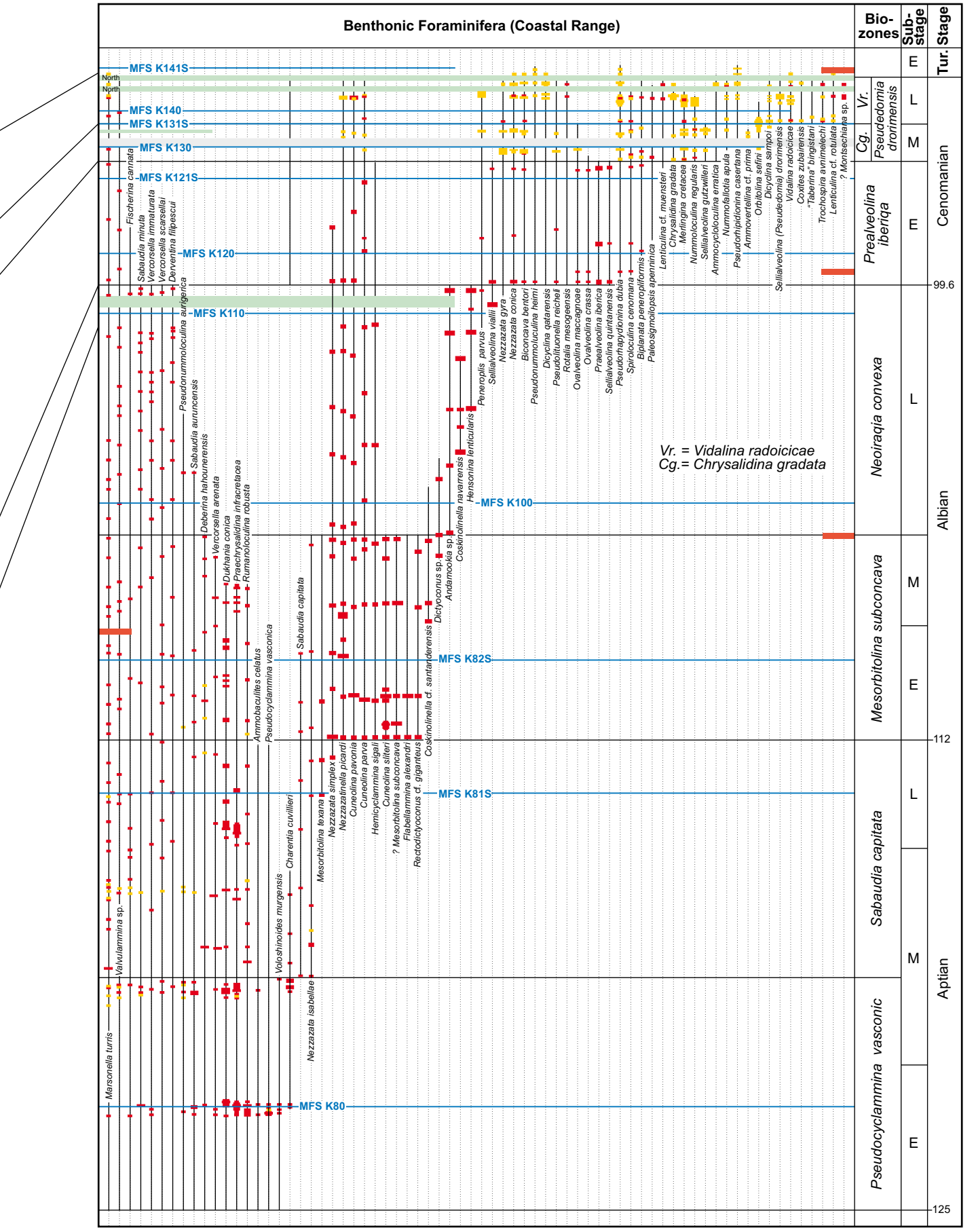
Benthonic Foraminifera (Coastal Range)
Bio-zones
Sub-stage
Tur. Stage
MFS K141S
MFS K140
MFS K131S
MFS K130
MFS K121S
MFS K120
MFS K110
MFS K100
MFS K82S
MFS K81S
MFS K80
North
North
Fischerina cannata
Sabaudia minuta
Vercorsella immaturata
Vercorsella scarsellai
Derventina filipescui
Pseudonummoloculina aurigerica
Sabaudia auruncensis
Deberina hahounerensis
Vercorsella arenata
Dukhania conica
Praechrysalidina infracretacea
Rumanoloculina robusta
Ammobaculites celatus
Pseudocyclammina vasconica
Sabaudia capitata
Voloshinoides murgensis
Charentia cuvillieri
Mesorbitolina texana
Nezzazata simplex
Nezzazatinella picardi
Cuneolina pavonia
Cuneolina parva
Hemicyclammina sigali
Cuneolina sliteri
? Mesorbitolina subconcava
Flabellammina alexandri
Rectodictyoconus cf. giganteus
Coskinolinella cf. santanderensis
Dictyoconus sp.
Andamookia sp.
Coskinolinella navarrensis
Hensonina lenticularis
Peneroplis parvus
Sellialveolina viallii
Nezzazata gyra
Nezzazata conica
Biconcava bentori
Pseudonummoloculina heimi
Dicyclina qatarensis
Pseudolituonella reicheli
Rotalia mesogeensis
Ovalveolina maccagnoae
Ovalveolina crassa
Praealveolina iberica
Sellialveolina quintanensis
Pseudorhapydionina dubia
Spiroloculina cenomana
Biplanata peneropliformis
Paleosigmoilopsis apenninica
Lenticulina cf. muensteri
Chrysalidina gradata
Merlingina cretacea
Nummoloculina regularis
Sellialveolina gutzwilleri
Ammocyclocloculina erratica
Nummofallotia apula
Pseudorhipidionina casertana
Ammovertellina cf. prima
Orbitolina sefini
Dicyclina sampoi
Sellialveolina (Pseudedomia) dorimensis
Vidalina radoicicae
Coxites zubairensis
"Taberina" bingistani
Trochospira avnimelechi
Lenticulina cf. rotulata
? Montsechiana sp.
Marsonella turris
Valvulammina sp.
Nezzazata isabellae
Vr. = Vidalina radoicicae
Cg.= Chrysalidina gradata
Vr.
Cg.
Pseudedomia dorimensis
Prealveolina iberiga
Neoiraqia convexa
Mesorbitolina subconcava
Sabaudia capitata
Pseudocyclammina vasconic
E
L
M
E
L
M
E
Cenomanian
Albian
Aptian
99.6
112
125

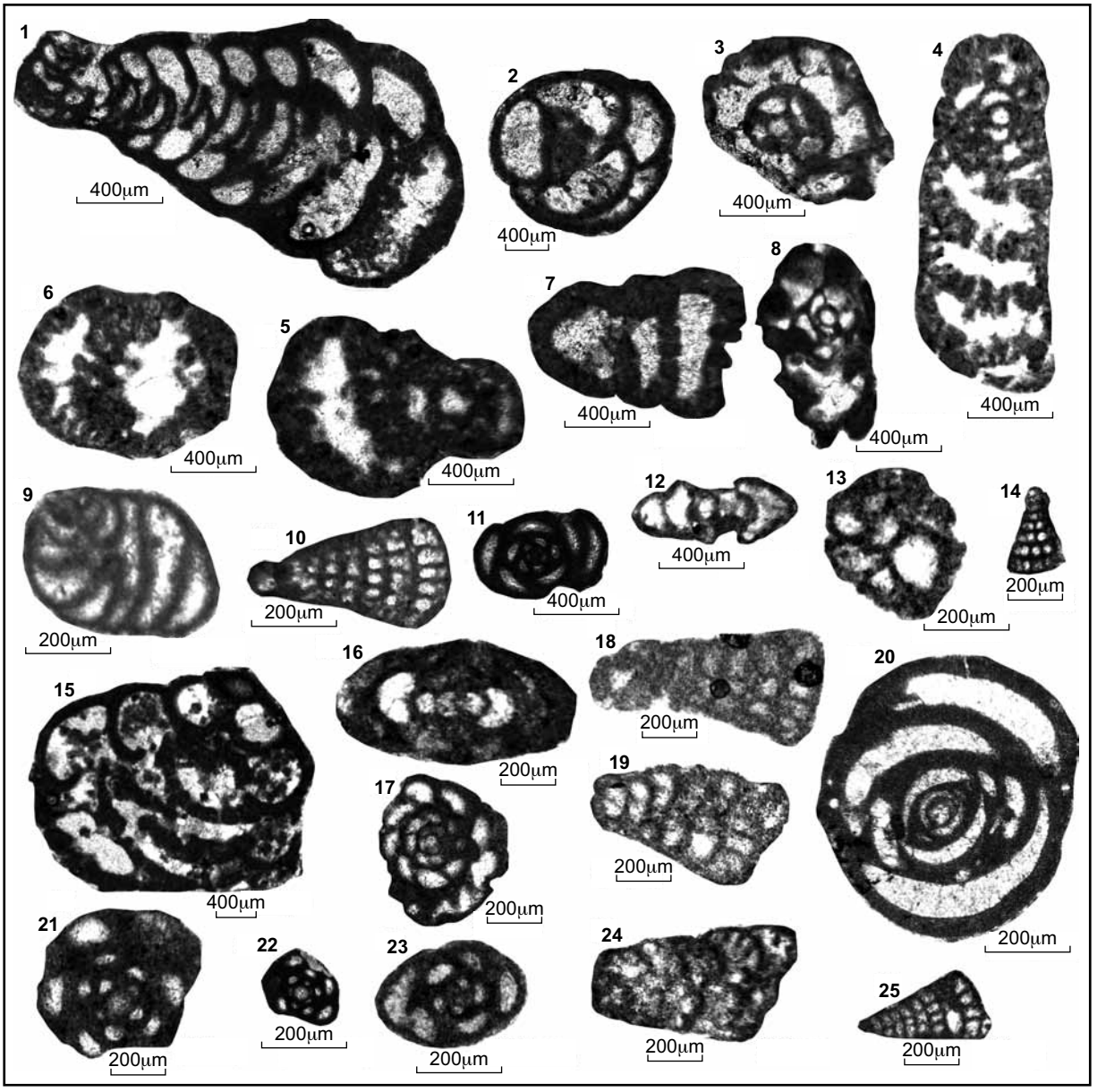

Figure 8: **Benthonic foraminifera of the Early Aptian *Pseudocyclammina vasconica* Zone (as = axial section; sas = subaxial section; es = equatorial section; ses = subequatorial section; ob = oblique section; ts = transversal section; ls = longitudinal section).**
(1 and 2) *Praechrysalidina infracretacea*, (1) [ls], (2) [es] (Ain Tina). (3) *Hemicyclammina* sp., [es] (Sayno).
(4, 5 and 6) *Pseudocyclammina vasconica*, (4) [as], (5) [sls], (6) [es] (Sayno).
(7 and 8) *Ammobaculites celatus*, (7) [ls], (8) [as] (Sayno). (9) *Nezzazatinella* sp.?, [ses] (Sayno).
(10) *Vercorsella* sp., [os] young megalospheric form (Sayno). (11) *Pseudorhapydionina* sp.?, [ses] (Sayno).
(12, 16 and 17) *Charentia cuvillieri*, (12) [sas], (16) [as], (17) [es] (Sayno).
(13) *Voloshinoides* cf. *murgensis*, [ses] (Sayno).
(14) *Sabaudia capitata*, [os] young megalospheric form (Sayno). (15) *Dukhania conica*, [ls] (Sayno).
(18) *Vercorsella* cf. *immaturata*, [os] young megalospheric form (Sayno).
(19) *Sabaudia auruncensis*, [os] young megalospheric form (Sayno).
(20) *Pseudonummoloculina aurigerica*, [as] (Sayno).
(21 and 22) *Rumanoloculina robusta*, [as] (Sayno). (23) miliolid indet., [sas] (Sayno).
(24) *Cuneolina* sp., [os] young megalospheric form (Sayno).
(25) *Vercorsella arenata*, [os] young megalospheric form (Sayno).

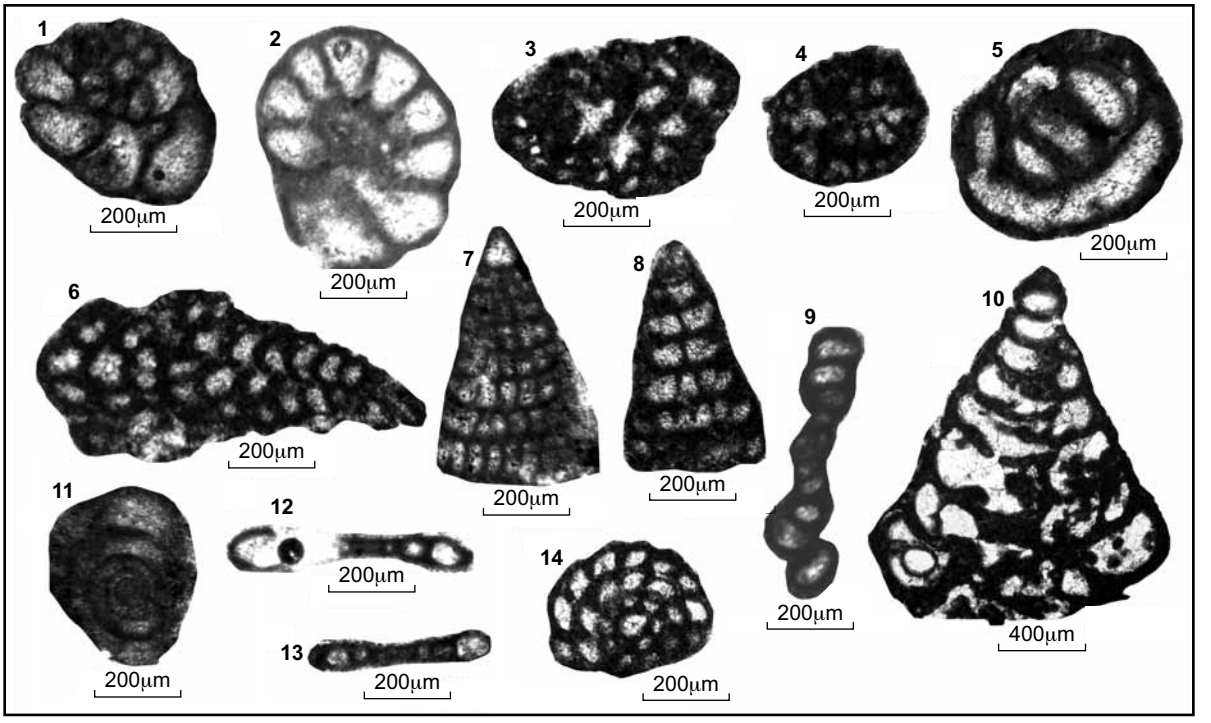

Figure 9: Benthonic foraminifera of the Late Aptian Assemblage Zone (as = axial section; sas = subaxial section; es = equatorial section; ses = subequatorial section; ob = oblique section; ts = transversal section; ls = longitudinal section).
(1 and 2) *Nezzazatinella picardia*, (1) [as], (2) [sas] (Sayno). (3) *Voloshinoides* cf. *murgensis*, [sas] (Sayno).
(4) *Cuneolina sliteri*, [sas] (Sayno). (5) *Pseudonummoloculina aurigerica*, [sas] (Sayno).
(6 and 7) *Vercorsella scarsellai*, [os] young megalospheric form (Sayno).
(8) *Vercorsella arenata*, [os] young megalospheric form (Sayno). (9) *Derventina filipescui*, [sas] (Sayno).
(10) *Praechrysalidina infracretacea*, [ls] (Sayno).
(11, 12 and 13) *Vidalina* cf. *radoicicae*, (11) [ses], (12, 13) [sas] (Sayno).
(14) *Nezazzata* sp., [es] (Sayno).

Early Albian Mesorbitolina subconcava range zone

Diagnosis*:* This biozone spans the total range of *Mesorbitolina subconcava* (Velić, 2007; Schroeder et al., 2010; Ghanem et al., 2012).

Description: The following Early Albian index taxa, such as *Mesorbitolina texana*, *Cuneolina sliteri, C. pavonia, C. parva, Dukhania conica, Praechrysalidina infracretacea, Flabellammina alexandri, Hemicyclammina sigali, Sabaudia minuta, Nezzazata simplex*, *N. isabellae, Vercorsella arenata*, *V. immaturata* and *Nezzazatinella picardi* as well as some miliolids, *Dictyoconus* sp. and different *Orbitolina* spp. occur in the *Mesorbitolina subconcava* Zone (Figures 7 and 10).

Correlation: The benthonic foraminifera assemblage described coincides with the *Mesorbitolina subconcava* Biozone of South Pamyrides after Ghanem et al. (2012) and the same zone in the Adriatic Platform (Velić, 2007) (Figure 7).

Age and Occurrence: The *M. subconcava* Zone comprises the Early to Middle Albian (Simmons et al., 2000; Velić, 2007; Ghanem et al., 2012). The *M. subconcava* Biozone is evident in 65-m-thick limestones (units 7–10) of the Ain Elbeida Formation. It occurs in the SY Section, northern part of the North CR (Figure 3).

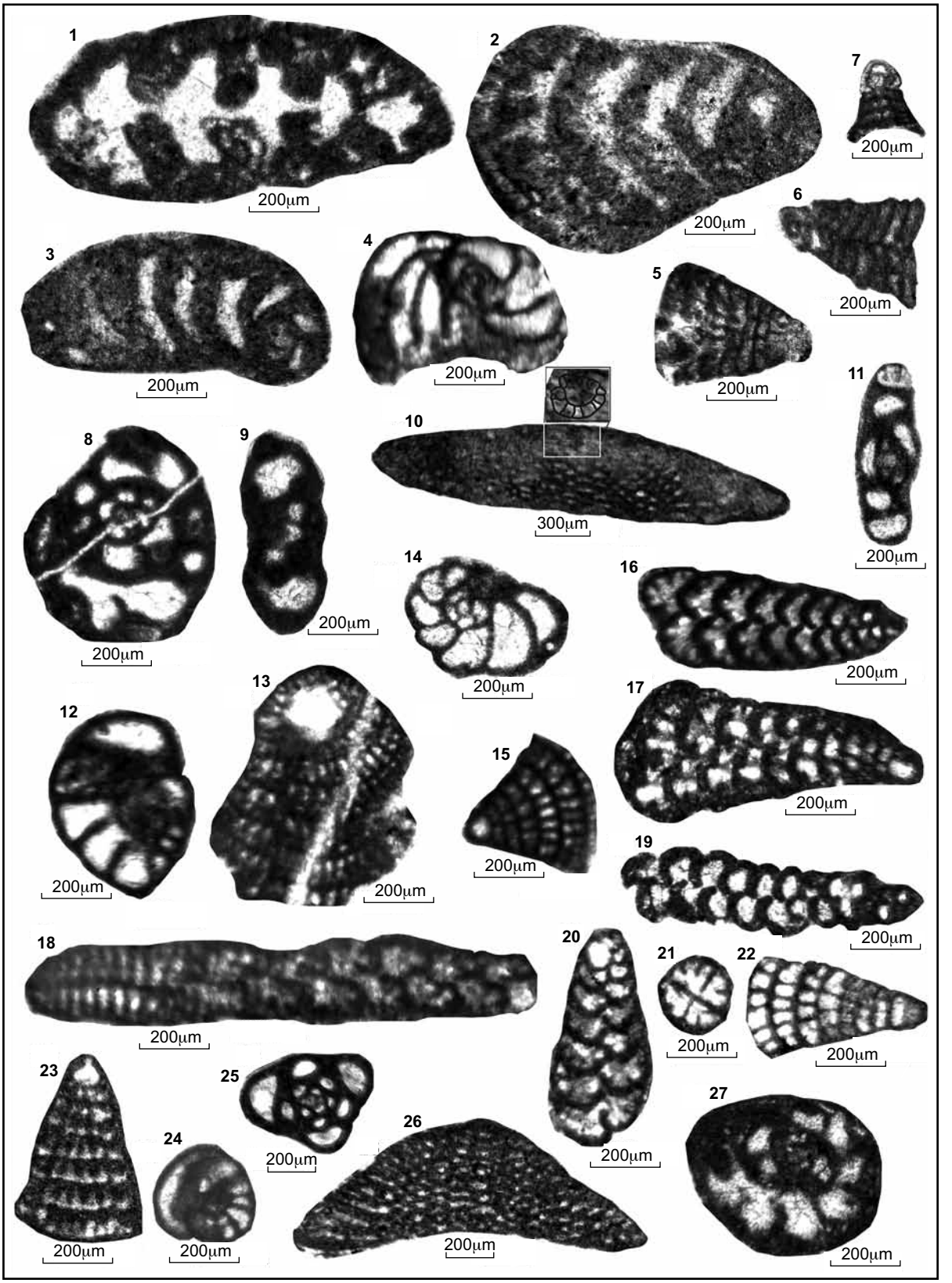

Figure 10 (facing page): Benthonic foraminifera of the Early Albian *Mesorbitolina subconcava* Zone (as = axial section; sas = subaxial section; es = equatorial section; ses = subequatorial section; ob = oblique section; ts = transversal section; ls = longitudinal section).
(1, 2 and 3) *Flabellammina* cf. *alexanderi*, (1 and 3) [es], (2) [as] (Sayno).
(4) *Peneroplis* sp.?, [es] (Sayno). (5 and 6) *Sabaudia capitata*, [as] (Sayno).

Late Albian Neoiraqia convexa taxon-range zone

Diagnosis: Total range zone of zonal marker (Velić, 2007; Ghanem et al., 2012).

Description: The base of this biozone is defined by the FO of the zonal marker and of *Andamookia* sp. and the LOs of *Cuneolina sliteri, Hemicyclammina sigali, Debarina hahounerensis, Nezzazata isabellae, Mesorbitolina texana, M. subconcava, Flabellammina alexandri* and *Rectodictyoconus* sp. The top of this biozone corresponds to the FO of the following Early Cenomanian species: *Praealveolina iberica, Pseudolituonella reicheli, Biconcava bentori* and *Nezzazata conica*. Additional taxa within that biozone are: *Coskinolinella navarrensis, C. santanderensis* and *Hensonina lenticularis.* Moreover, further taxa of wide stratigraphic range occur such as: *Dukhania conica, Praechrysalidina infracretacea, Nezzazata simplex, Nezzazatinella picardi, Cuneolina pavonia, C. parva, Vercorsella arenata, V. immaturata, Derventina filipescui, Spiroloculina* sp., *Rumanoloculina* cf. *robusta, Fischerina* sp., *Sabaudia minuta, Bolivinobsis* sp., *Vercorsella* sp., *Vidalina* sp., *Voloshinoides* sp. and few miliolids (Figures 7 and 11).

Correlation: The *Neoiraqia convexa* Biozone is equivalent to both biozones: *Valdanchella dercourti* partial range zone and *Neoiraqia* taxon-range zone of Velić (2007). It is delineated by the overlapping ranges of co-occurring species (Loeblich and Tappan, 1988; Velić, 2007; Figure 7).

Age and Occurrence: In the North CR this biozone occurs in restricted shallow marine limestones of the upper Ain Elbeida Formation (units 10–16). The interval is composed of ca. 42 m thick limestones, marly limestones and dolomitic limestones in the SY Section and of 53 m thick limestones and dolostones in the SL Section.

Early Cenomanian Praealveolina iberica interval zone

Diagnosis: Total range zone of the zonal marker. Furthermore, this biozone is determined by the range between the FO of *Praealveolina iberica* and the FO of *Chrysalidina gradata, Selliaveolina gutzwilleri,* (Ogg and Ogg, 2008; Vicedo et al., 2011; Ghanem et al., 2012).

Description: Besides the zonal marker, additional foraminifera (known as Early Cenomanian index taxa) occur, such as: *Nezzazata gyra, N. conica, Biconcava bentori, Ovalveolina crassa, Selliaveolina viallii, S. quintanensis, Peneroplis parvus, Biplanata peneropliformis, Dicyclina qatarensis, Pseudonummoloculina heimi, Pseudorhapydionina dubia* and *Pseudolituonella reicheli.* They co-occur with some wide range species: *Nezzazata simplex, Cuneolina pavonia, C. parva, Nezzazatinella picardi, Nummoloculina* sp., *Fischerina* sp., *Marsonella* sp. and miliolids div. spp. (Figures 7 and 12).

Correlation: This biozone is equivalent to the *Praealveolina iberica* Biozone in the South Palmyrides proposed by Ghanem et al. (2012); it also coincides with the *Conicorbitolina conica/Conicorbitolina cuvillieri* range zone of the Adriatic Platform of Velić (2007).

Age and Occurrence: The *Praealveolina iberica* interval zone spans the restricted Early Cenomanian shallow marine carbonates of the uppermost Ain Elbeida to Slenfeh formations (units 17–21). It is represented by 109 m-thick limestones in the SL Section (North CR).

(Figure 10 caption continued from facing page):
(7) *Sabaudia minuta*, [as] (Sayno). (8 and 9) *Debrina hahounerensis*, (8) [es], (9) [as] (Sayno).
(10) *Orbitolina* (Ms) cf. *texana*, [as] through a megalospheric form (Sayno).
(11) *Derventina filipescui*, [as] (Sayno). (12) *Nezazzatinella icardi*, [sas] (Sayno).
(13) *Cuneolina parva*, [os] through a young megalospheric form (Sayno).
(14) *Nezazzata isabellae*, [es] (Sayno). (15) *Vercorsella* sp., [as] (Sayno).
(16, 17 and 18) *Cuneolina sliteri*, [os] through a young megalospheric form (Sayno).
(19) *Voloshinoides* sp., [os] through a young megalospheric form (Sayno).
(20 and 21) *Vecorsella immaturata*, (20) [as], (21) [ts] (Sayno). (22) *Vecorsella arenata*, [as] (Sayno).
(23) *Dictyoconus* sp.?, [as] (Sayno). (24) *Nezazzatinella* sp., [sas] (Sayno).
(25) *Rumanoloculina robusta*, [as] (Sayno). (26) *Orbitolina* sp., [as] through a megalospheric form (Sayno).
(27) *Hemicyclamina sigali*, [es] (Sayno).

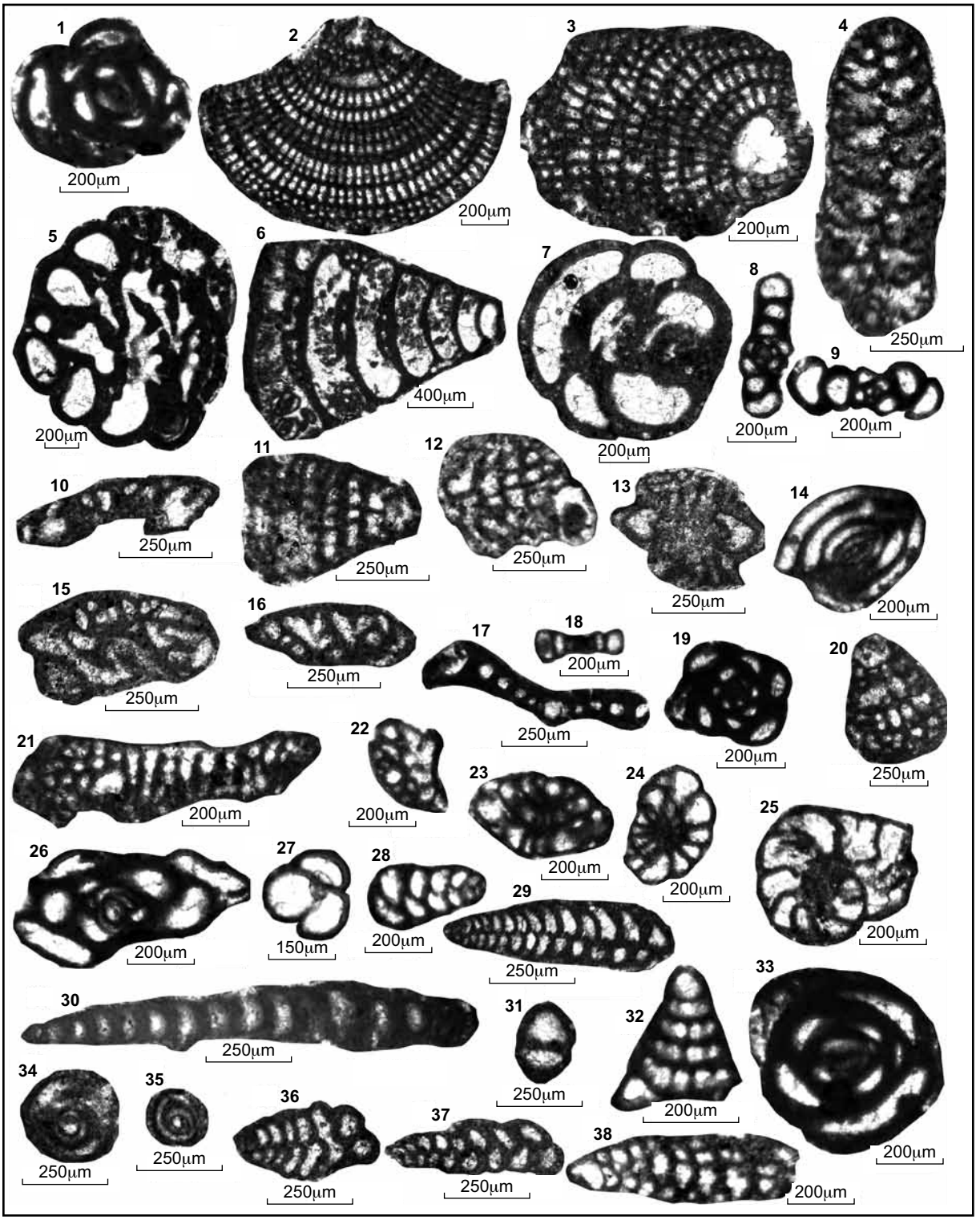

Figure 11: Benthonic foraminifera of the Late Albian *Neoiraqia convexa* Zone (as = axial section; sas = subaxial section; es = equatorial section; ses = subequatorial section; ob = oblique section; ts = transversal section; ls = longitudinal section).
(1 and 33) *Pseudonummoloculina aurigerica*, [sas] (Sayno).
(2, 3 and 4) *Cuneolina pavonia*, (2, 3) [os] through the megalospheric form (Sayno), (4) [ls] (Slenfeh).

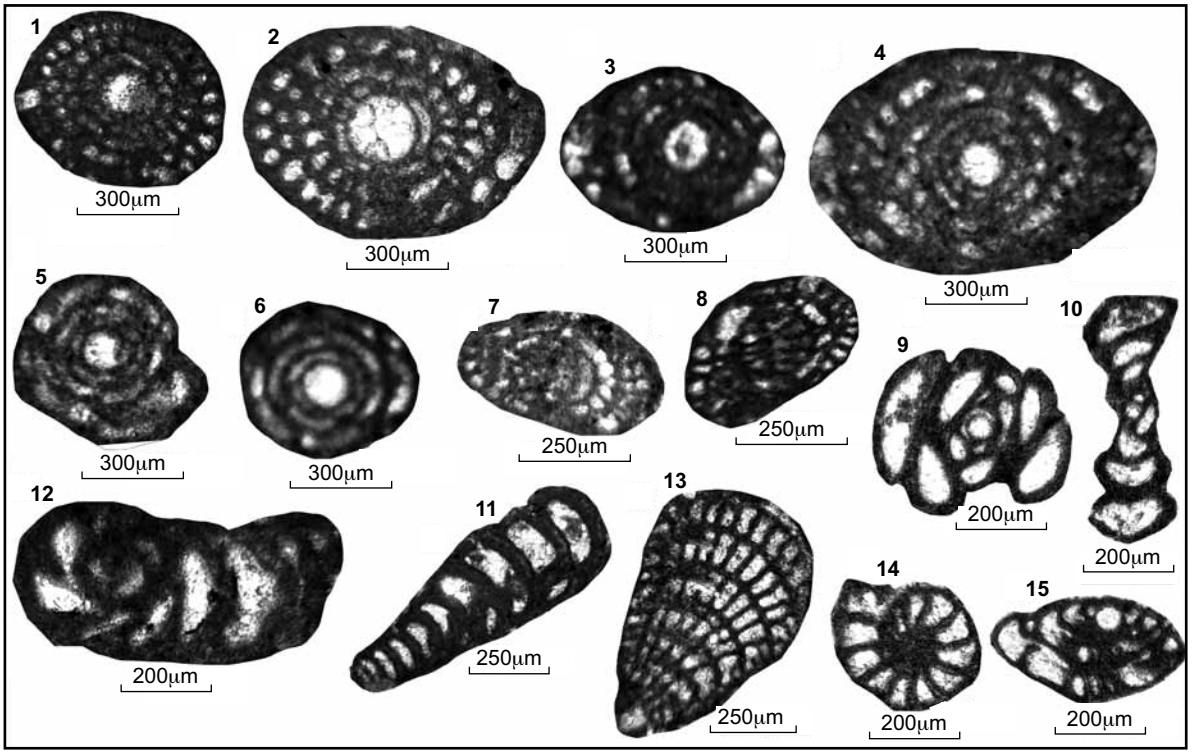

Figure 12: Benthonic foraminifera of the Early Cenomanian *Praealveolina iberica* interval zone (as = axial section; sas = subaxial section; es = equatorial section; ses = subequatorial section; os = oblique section; ts = transversal section; ls = longitudinal section).
(1 and 2) *Praealveolina iberica*, [os] (Slenfeh).
(3, 4 and 5) *Sellialveolina viallii*, (3 and 4) [as], (5) [ses] (Slenfeh).
(6, 7 and 8) *Ovalveolina crassa*, (6) [ses] (Sayno), (7 and 8) [ts] (Slenfeh). (9) miliolid indet., [as] (Sayno).
(10) *Fischerina cannata*, [es] (Sayno). (11) *Pseudolituonella reicheli*, [ls] (Slenfeh).
(12) *Pseudorhipidionina dubia*, [es] (Slenfeh). (13) *Cuneolina parva*, [os] the megalospheric form (Slenfeh).
(14) *Biconcava bentori*, [sas] (Sayno). (15) *Nezazzata simplex*, [sas] (Sayno).

(Figure 11 caption continued from facing page):
(5) *Dokhania conica*, [ls] (Sayno). (6 and 7) *Praechrysalidina infracretacea*, (6) [ls], (7) [es] (Sayno).
(8 and 9) *Derventina filipescui*, (8) [sas] (Sayno), (9) [sas] (Slenfeh).
(10) *Coskinolinella navarrensis*, [os] (Slenfeh).
(11 and 12) *Sabaudia minuta*, [os] through the megalospheric form (Slenfeh).
(13) *Hensonina lenticularis*, [as] (Slenfeh).
(14, 17 and 18) *Spiroloculina* sp., (14) [sas] (Sayno), (17) [as] (Slenfeh), (18) [es] (Sayno).
(15 and 16) *Andamookia* sp., [os] (Slenfeh). (19) *Rumanoloculina robusta*, [sas] (Sayno).
(20) *Vecorsella* sp., [os] megalospheric form (Slenfeh). (21) *Coskinolinella* cf. *santanderensis*, [os] (Sayno).
(22) *Nezzazata isabellae*, [as] (Sayno). (23 and 24) *Nezzazata simplex*, (23) [as], (24) [sas] (Sayno). (25) *Nezzazatinella picardia*, [sas] (Sayno). (26) miliolid indet., [as] (Sayno).
(27 and 28) textularid foraminifera, (27) [es], (28) [ls] (Slenfeh). (29, 30 and 31) *Bolivinopsis* sp., (29, 30) [ls], (31) [es] (Slenfeh). (32) *Vercorsella* sp., [os] young the megalospheric form (Sayno). (34 and 35) *Vidalina* sp., [es] (Slenfeh). (36 and 37) *Voloshinoides* sp.?, [ls] (Slenfeh).
(38) *Vecorsella arenata*, [os] through the megalospheric form (Sayno).

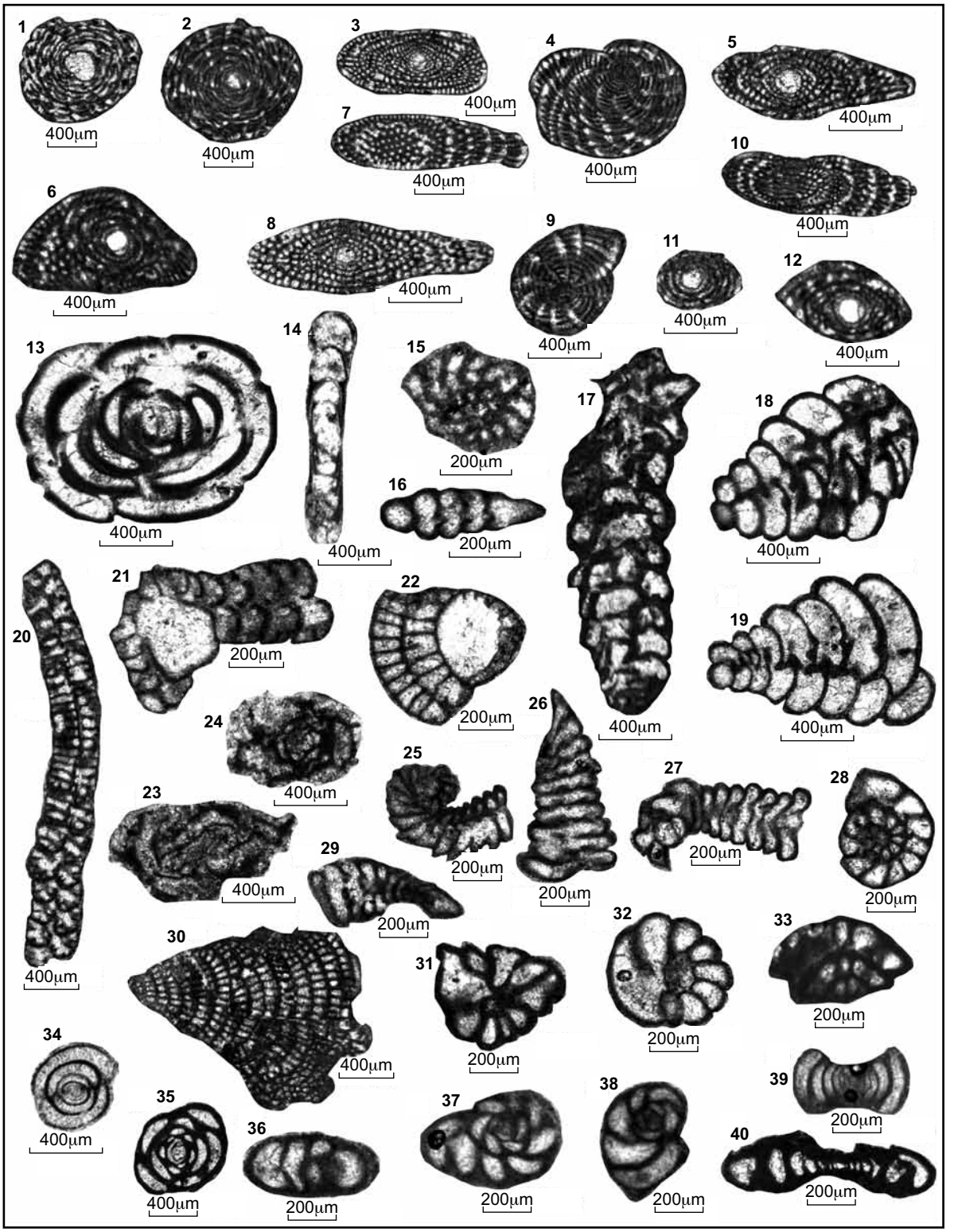

Figure 13: Benthonic foraminifera of the Middle Cenomanian *Chrysalidina gradata* partial zone (as = axial section; sas = subaxial section; es = equatorial section; ses = subequatorial section; os = oblique section; ts = transversal section; ls = longitudinal section).
(1, 2, 3, 4 and 7) *Sellialveolina gutzwilleri*, (1) [as], (2, 3 and 7) [sas], (4) [ses] (Wadi Al-Haddah).
(5, 6, 8, 9 and 10) *Sellialveolina quintanensis*, (5, 8 and 10) [sas], (6) [os], (9) [ses] (Wadi Al-Haddah).
(11 and 12) *Ovalveolina maccagnoae*, (11) [ses] (Wadi Al-Haddah), (12) [os] (Bab Abdallah).
(13 and 14) *Nummoloculina regularis*, (13) [as], (14) [ses] (Wadi Al-Haddah).
(15 and 16) *Biconcava* cf. *bentori*, (15) [ses], (16) [ses] (Wadi Al-Haddah).

Middle Cenomanian Chrysalidina gradata partial range zone

Diagnosis: Interval range of the zonal marker to the FO of *Vidalina radoicicae*.

Description: This biozone is defined by the FO of the index fossil *Chrysalidina gradata,* associated with a rich assemblage of further Cenomanian benthonic foraminifera like *Selliaveolina gutzwilleri, Ovalveolina maccagnoae, Merlingina cretacea, Nummoloculina regularis, Nezzazata gyra, N. simplex, N. conica, Biconcava bentori, Biplanata peneropliformis, Orbitolina sefini, Dicyclina qatarensis, Nummofallotia apula, Peneroplis parvus, Pseudonummoloculina heimi, Pseudorhipidionina casertana, Pseudorhapydionina dubia, Spiroloculina cenomana* and *Rotalia mesogeensis*. These species co-occur with some wide range species: *Cuneolina pavonia, C. parva, Nezzazatinella picardi, Valvulammina* sp., *Marsonella* sp. and miliolids div. sp. (Figures 7 and 13).

Correlation: The described biozone correlates with the *Chrysalidina gradata* partial range zone and the *Broeckinella (Pastrikella) balcanica* Zone of the Adriatic Platform described by Velić (2007). It also correlates with the mid-Cenomanian marker species of the Tethyan realm of Gradstein et al. (2012). This biozone is comparable with the lower part of *Selliaveolina* (*Pseudedomia*) *drorimensis* range zone in the South Palmyrides (Ghanem et al., 2012; Figure 7).

Age and Occurrence: The Middle Cenomanian *Chrysalidina gradata* partial range zone is determined by the FO of *Chrysalidina gradata* to the FO *Vidalina radoicicae* (Ogg and Ogg, 2008). This biozone is represented by 76 m thick marly limestones of the Hannafiyah Formation in the AH Section (units 22–24) and by a ca. 80 m-thick succession of limestones, intercalated with marls and dolostones in the SB Section (60 m of Slenfeh Formation and 20 m of Bab Abdallah Formation units 22–25) (Figure 4).

Late Cenomanian Vidalina radoicicae range zone

Diagnosis*:* Total range zone of the zonal marker.

Description: The *Vidalina radoicicae* Biozone is delineated by the total range of the zonal marker together with *Selliaveolina drorimensis* and *"Taberina" bingistani,* originally described from Tethyan carbonate platforms (Loeblich and Tappan, 1988; Velić, 2007). This biozone is associated with several other benthonic taxa like: *Orbitolina sefini, Dicyclina sampoi, D. qatarensis, Biplanata peneropliformis, Pseudorhapydionina dubia, Pseudorhipidionina casertana, Montsechiana* sp.?, *Chrysalidina gradata, Nummofallotia apula, Spiroloculina cenomana, Ammocycloloculina erratica, Trochospira avnimelechi, Nezzazata gyra, N. conica, Nezzazatinella picardi, Biconcava bentori, Lenticulina* cf. *rotulata, L.* cf. *muensteri Pseudonummoloculina heimi, Nummoloculina regularis, Cuneolina pavonia, C. para* and miliolids div. sp. (Figures 7 and 14).

Correlation: The *Vidalina radoicicae* range zone correlates with the same zone of the Adriatic Platform (compare Velić, 2007).

Age and Occurrence: According to Velić (2007), the *Vidalina radoicicae* Biozone comprises the Upper Cenomanian. It is identified within a 35 m-thick succession of marls and limestones of the Hannafiyah Formation (AH Section units 24–27), within 110 m of marls, dolostones and limestones of the Hannafiyah Formation (MT Section, Figure 4) and within 15 m of marly limestones and limestones of Bab Abdallah Formation of the SB Section (units 26–27).

(Figure 13 caption continued from facing page):
(17, 18 and 19) *Chrysalidina gradate*, [ls] (Wadi Al-Haddah).
(20 and 21) *Dicyclina sampoi*, (20) [ses], (21) [as] (Wadi Al-Haddah).
(22) *Cuneolina* sp., [as] (Wadi Al-Haddah). (23 and 24) *Ammovertellina* cf. *prima*, [sas] (Wadi Al-Haddah).
(25, 26, 27 and 29) *Merlingina cretacea*, (25, 29) [es], (26, 27) [os] (Wadi Al-Haddah, Bab Abdallah).
(28 and 33) *Nezazzata gyra*, (28) [es], (33) [os] (Wadi Al-Haddah).
(30) *Dicyclina* sp., [os] (Bab Abdallah). (31 and 32) *Nezazzatinella picardi*, [sas] (Wadi Al-Haddah).
(34 and 35) miliolid indet., [sas] (Bab Abdallah, Wadi Al-Haddah).
(36, 37 and 38) *Pseudorhapydionina dubia*, (36) [os] (Bab Abdallah), (37 and 38) [ses] (Wadi Al-Haddah).
(39 and 40) *Spiroloculina cenomana*, [as] (Wadi Al-Haddah).


1
500µm
2
500µm
3
500µm
4
500µm
5
400µm
6
400µm
7
400µm
8
400µm
9
400µm
10
300µm
11
300µm
12
150µm
13
150µm
16
400µm
7
250µm
4
300µm
15
400µm
19
300µm
20
500µm
18
250µm
21
400µm
22
400µm
25
400µm
27
300µm
23
400µm
24
400µm
26
400µm
29
300µm
31
200µm
28
200µm
32
300µm
33
300µm
35
400µm
30
300µm
34
400µm
37
125µm
38
300µm
36
200µm
47
150µm
49
39
500µm
42
300µm
44
200µm
45
300µm
40
300µm
43
300µm
48
300µm
50
300µm
41
500µm
46
150µm
500µm

Planktonic Foraminifera Biostratigraphy

Planktonic foraminifera occur with changing frequencies in units 12 to 26 of the SL, AH and MT sections. The high variety of planktonic foraminifera permits defining six biozones (with two subzones), based on the first (FO) and last occurrence (LO) of several index taxa. They range from latest Albian to Early Turonian and are well comparable to the standard global assemblages of planktonic foraminifera (Premoli Silva and Verga, 2004; Ogg and Ogg, 2008).

Latest Albian Rotalipora appenninica Zone

Diagnosis: Interval zone of *Rotalipora appenninica*.

Description: The marly limestones of that biozone are characterized by the FO of *Rotalipora appenninica,* associated with the Late Albian index species such as *Muricohedbergella albiana, Ticinella raynaudi* and *T. madecassiana* (Premoli Silva and Verga, 2004, Premoli Silva et al., 2009). Those co-occur with some wide range species: *Muricohedbergella planispira, Heterohelix moremani, Rotalipora gandolfii, Macroglobigerinelloides ultramicrus* and *Favusella washitensis* (Figures 7 and 15).

Correlation: The described assemblage holds several index species of the *Rotalipora appenninica* Zone (Premoli Silva and Verga, 2004; Ogg and Ogg, 2008).

Age and Occurrence: Premoli Silva and Verga (2004) and Gradstein et al. (2012) attributed a latest Albian age for that biozone. In the present study, the *Rotalipora appenninica* Biozone occurs in a 50-m-thick succession of marly limestones, limestones and dolostones, corresponding with units 12–16 of the Ain Elbeida Formation in the SL Section (Figure 3).

Figure 14 (facing page): Benthonic foraminifera of the Late Cenomanian *Vidalina radoicicae* range zone (as = axial section; sas = subaxial section; es = equatorial section; ses = subequatorial section; os = oblique section; ts = transversal section; ls = longitudinal section).
(1 and 2) *Sellialveolina drorimensis*, (1) [es], (2) [sas] (Al-Meten).
(3 and 4) *Chrysalidina gradata*, [ls] (Al-Meten).
(5, 6, 7 and 9) *Orbitolina sefini*, (5, 6) [as], (7) [os], (9) [sas] (Wadi Al-Haddah).
(8) *"Taberina" bingistani*, [ses] (Wadi Al-Haddah).
(10) *Peneroplis parvus*, [es](Al-Meten, Wadi Al-Haddah).
(11) *Coxites zubairensis*, [sas] (Al-Meten). (12) *Binconcava bentori*, [sas] (Al-Meten, Wadi Al-Haddah, Slenfeh/Bab Abdallah).
(13, 21 and 22) *Merlingina cretacea*, (13) [sas], (21) [es], (22) [as] (Al-Meten, Wadi Al-Haddah).
(14) *Montsechiana* sp.?, [es] (Slenfeh/Bab Abdallah).
(15, 16, 44 and 45) *Pseudorhipidionina casertana*, (15) [es], (16) [as], (44, 45) [os] (Wadi Al-Haddah).
(17 and 18) *Dicyclina* sp., (17) [ses], (18) [sas], (Slenfeh/ Bab Abdallah).
(19) *Ammocycloloculina erratica*, [sas] (Al-Meten).
(20, 48, 49 and 50) *Dicyclina qatransis*, (20) [sas], (48, 50) [as], (49) [ses] (Al-Meten).
(23, 24 and 32) *Nezzazata gyra*, (23, 24) [sas] (Wadi Al-Haddah), (32) [sas] (Al-Meten).
(25 and 26) *Pseudolituonella reicheli*, (25) [ls], (26) [as] (Wadi Al-Haddah).
(27) *Trochospira avnimelechi*, [ses] (Slenfeh/ Bab Abdallah).
(28) *Lenticulina* cf. *rotulata*, [sas] (Wadi Al-Haddah).
(29 and 30) *Lenticulina* cf. *muensteri*, (29) [sas], (30) [es] (Bab Abdallah).
(31) *Lenticulina* sp., [sas] (Wadi Al-Haddah). (33) *Nezzazata conica*, [sas] (Al-Meten).
(34) *Nezzazatinella picardi*, [as] (Slenfeh/Bab Abdallah). (35) *Nezzazata* sp., [as] (Wadi Al-Haddah).
(36 and 37) *Nummofallotia* cf. *apula*, (36) [os], (37) [es] (Al-Meten).
(38) *Pseudonummoloculina heimi*, [es] (Al-Meten).
(39, 40 and 41) *Biplanata peneropliformis*, [as].
(42 and 43) *Pseudorhapydionina* cf. *dubia*, (42) [es], (43) [as] (Al-Meten).
(46) miliolids indet., [as] (Al-Meten). (47) *Vidalina radoicicae*, [es] (Al-Meten).

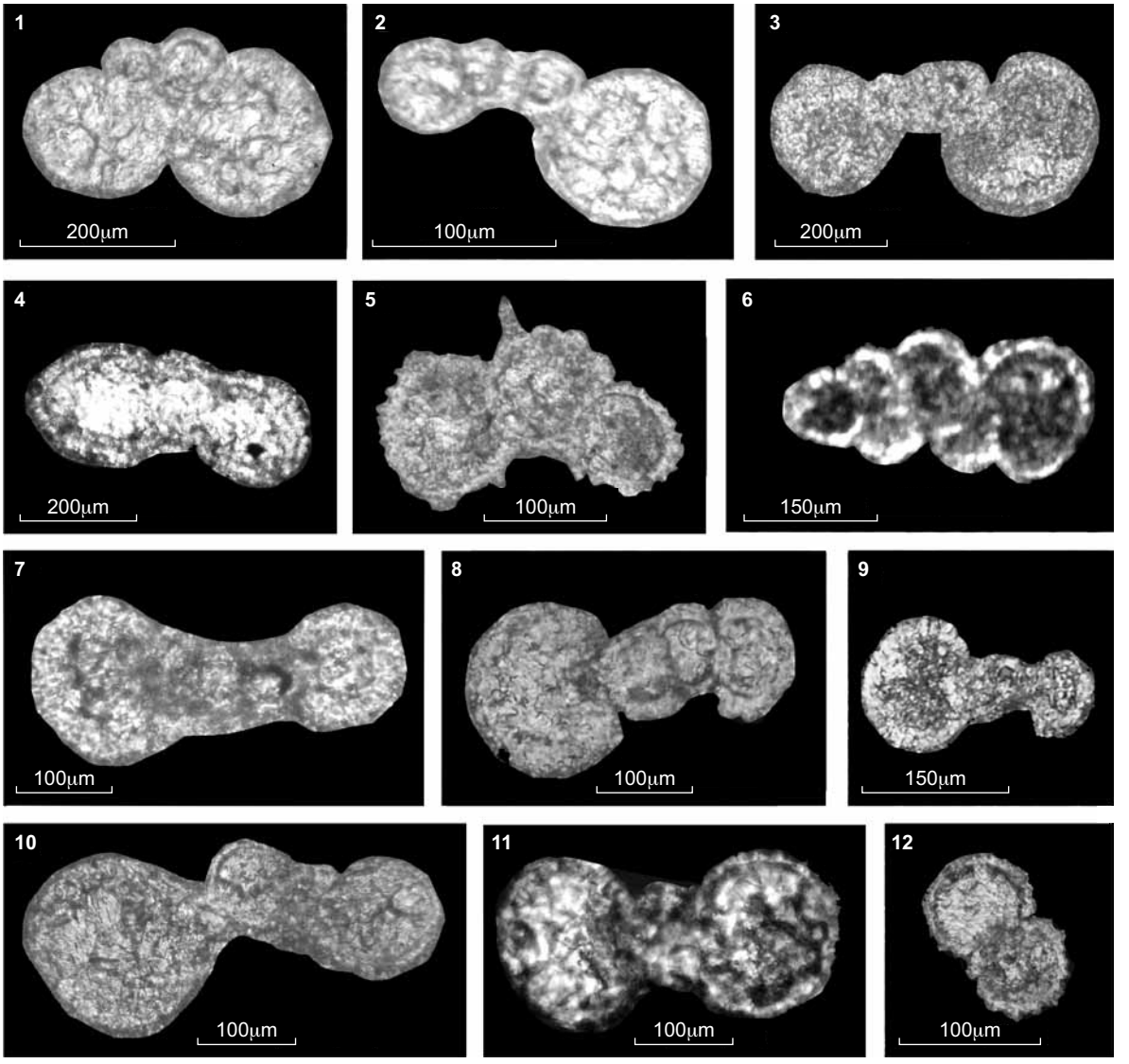

Figure 15: Planktonic foraminifera of latest Albian *Rotalipora appenninica* Zone (as = axial section; sas = subaxial section; ts = transversal section).
(1) *Ticinella madecassiana*, [as] (SL). (2 and 10) *Muricohedbergella planispira*, [as] (SL).
(3) *Ticinella praeticinensis*, [as] (SL). (4) *Ticinella raynaudi*, [sas] (SL).
(5 and 12) *Favusella washitensis*, [as] (SL). (6) *Heterohelix moremani*, [ts] [as] (SL).
(7) *Macroglobigerinelloides ultramicrus*, [as] (SL). (8) *Muricohedbergella albiana*, [as] (SL).
(9 and 11) *Muricohedbergella* sp., [sas] (SL).

Early Cenomanian Rotalipora globotruncanoides Zone

Diagnosis: Interval zone comprising the range between the FO of the zonal marker to the FO of *Rotalipora reicheli*.

Description: The following planktonic foraminifera co-occur together with the zonal marker: *Rotalipora globotruncanoides, R. gandolfii, R. montsalvensis, Macroglobigerinelloides ultramicrus, M. "caseyi", Heterohelix moremani, Muricohedbergella planispira* and *Praeglobotruncana delrioensis* (Premoli Silva and Verga, 2004; Premoli Silva, et al., 2009; Figures 7 and 16).

Correlation: The described *Rotalipora globotruncanoides* Zone of the Coastal Range correlates with the same zone of the standard global planktonic foraminifera (Premoli Silva and Verga, 2004; Ogg and Ogg, 2008).

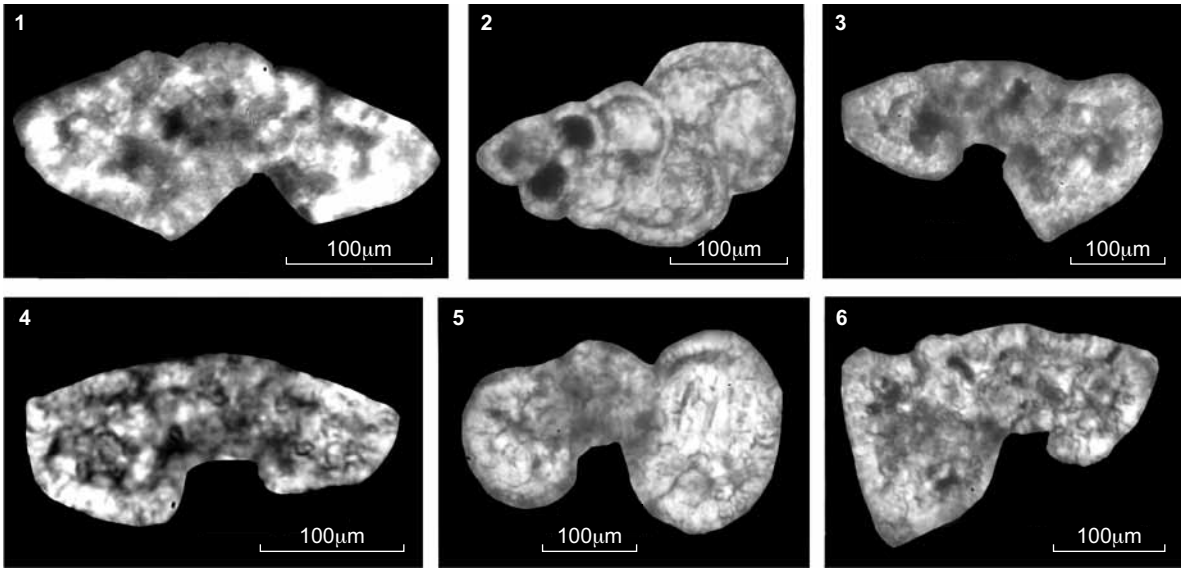

Figure 16: Planktonic foraminifera of Early Cenomanian *Rotalipora globotruncanoides* Zone (as = axial section; sas = subaxial section; ts = transversal section).
(1) *Rotalipora* cf. *globotruncanoides*, [as] (SB). (2) *Heterohelix moremani*, [ts] (SB).
(3) *Praeglobotruncana* cf. *delrioensis*, [as] (SB). (4) *Rotalipora montsalvensis*, [sas] (SL).
(5) *Muricohedbergella delrioensis*, [sas] (SL). (6) *Rotalipora gandolfi*, [sas] (SL).

Age and Occurrence: The *Rotalipora globotruncanoides* Zone corresponds to the Early Cenomanian (Premoli Silva and Verga, 2004; Ogg and Ogg, 2008). This biozone is evident in 79 m thick marly limestones, alternating with limestones and dolomites of units 17–19 and the lower part of unit 20 of the Slenfeh Formation in the SL and SB sections.

Middle Cenomanian Rotalipora reicheli Zone

Diagnosis: Total range zone of the zonal marker (Ogg and Ogg, 2008).

Description: This biozone is delineated by *Rotalipora reicheli*, associated with *R. montsalvensis, R. appenninica, R. micheli, R. globotruncanoides, Macroglobigerinelloides"caseyi", M. ultramicrus, M. bentonensis, Heterohelix moremani, Praeglobotruncana delrioensis, Muricohedbergella planispira M. simplex, M. delrioensis, Loeblichella hessi* and *Schackoina bicornis* (Premoli Silva and Verga, 2004; Premoli Silva et al., 2009) (Figures 7 and 17).

Correlation: The *Rotalipora reicheli* Biozone in the Syrian CR correlates with the standard global zone, defined by Premoli Silva and Verga (2004) and Ogg and Ogg (2008) (Figure 7).

Age and Occurrence: This biozone was attributed to the early Middle Cenomanian according to Premoli Silva and Verga (2004) and Ogg and Ogg (2008). The *Rotalipora reicheli* Biozone appears in 24 m thick marly limestones in the upper part of Slenfeh Formation (unit 21 of the SB Section). It also occurs in 13 m thick chalky limestones of unit 21 of Hannafiyah Formation (lower part of the AH Section).

Middle to Late Cenomanian Rotalipora cushmani Zone

The *R. cushmani* total range zone corresponds to the upper Middle to Late Cenomanian (Premoli Silva and Verga, 2004; Ogg and Ogg, 2008). This biozone contains two subzones: *Rotalipora greenhornensis* Subzone and *Dicarinella algeriana* Subzone, both defined by Premoli Silva and Verga (2004) (Figure 7).

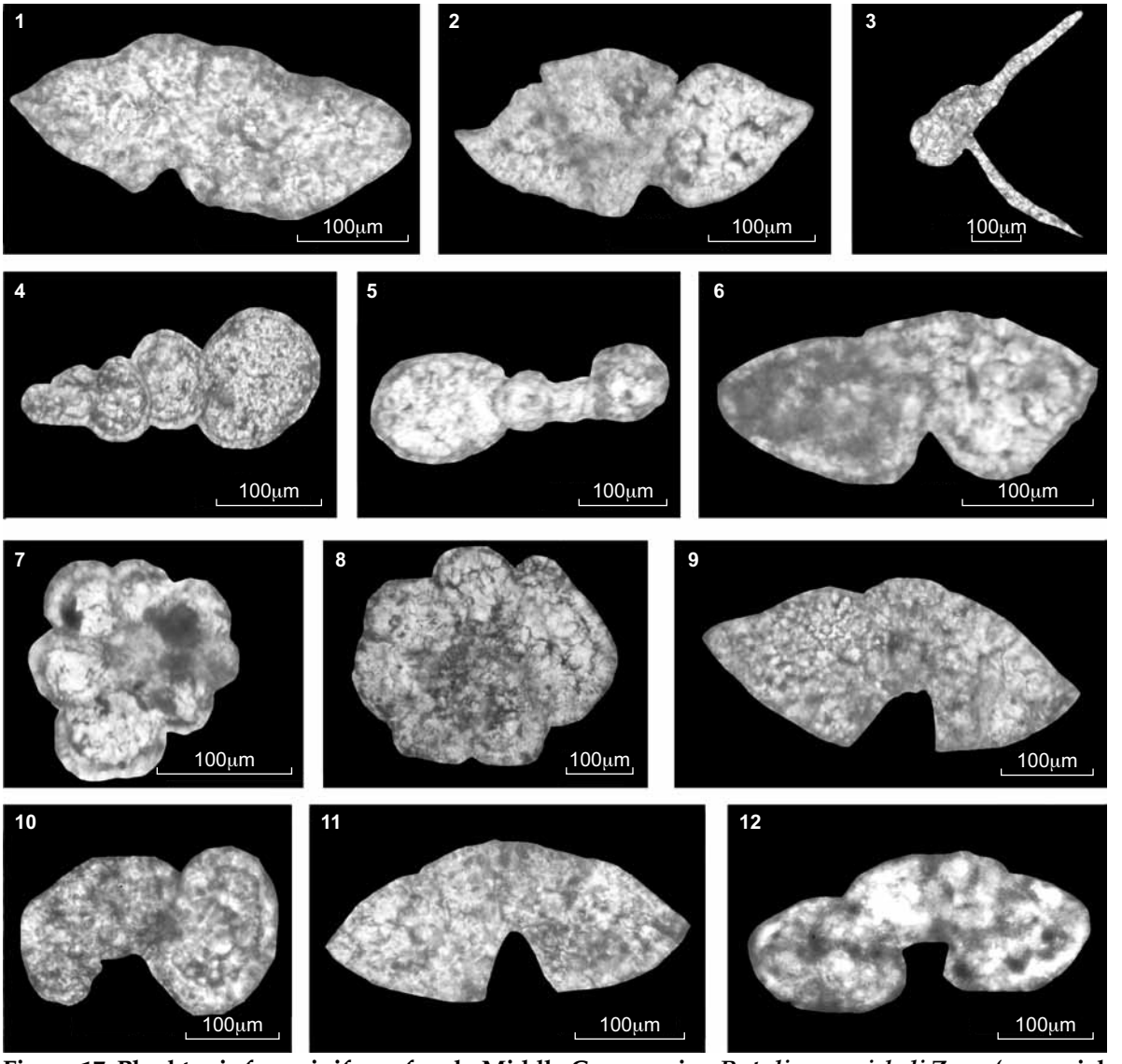

Figure 17: Planktonic foraminifera of early Middle Cenomanian *Rotalipora reicheli* Zone (as = axial section; sas = subaxial section; es = equatorial section; ts = transversal section).
(1, 8, 9 and 11) *Rotalipora reicheli*, (1, 9, 11) [as] (AH), (8) [es] (SB).
(2 and 6) *Rotalipora appenninica*, [as] (AH). (3) *Schackoina bicornis*, [sas] (AH).
(4) *Heterohelix moremani*, [ts] (AH). (5) *Macroglobigerinelloids caseyi*, [as] (AH).
(7) *Macroglobigerinelloids ultramicrus*, [es] (AH). (10) *Muricohedbergella delrioensis*, [as] (SB).
(12) *Praeglobotruncana delrioensis*, [as] (SB).

(a) late Middle Cenomanian Rotalipora greenhornensis Subzone

Diagnosis: Interval subzone ranging from the FO of *Rotalipora greenhornensis* and *R. cushmani* to the FO of *Dicarinella algeriana*.

Description: the *Rotalipora greenhornensis* Subzone is delineated by the sub-zonal marker together with *R. cushmani*, associated with *R. montsalvensis, R. appenninica, Muricohedbergella planispira, M. simplex, Heterohelix moremani, Praeglobotruncana delrioensis, Macroglobigerinelloides bentonensis, M. ultramicrus* and *Loeblichella hessi* (Premoli Silva and Verga, 2004; Premoli Silva et al., 2009) (Figures 7 and 18).

Correlation: This subzone correlates with the Middle Cenomanian part of *R. cushmani* Zone of Premoli Silva and Verga (2004) and Ogg and Ogg (2008), equivalent to the *Rotalipora greenhornensis* Subzone after Premoli Silva and Verga (2004).

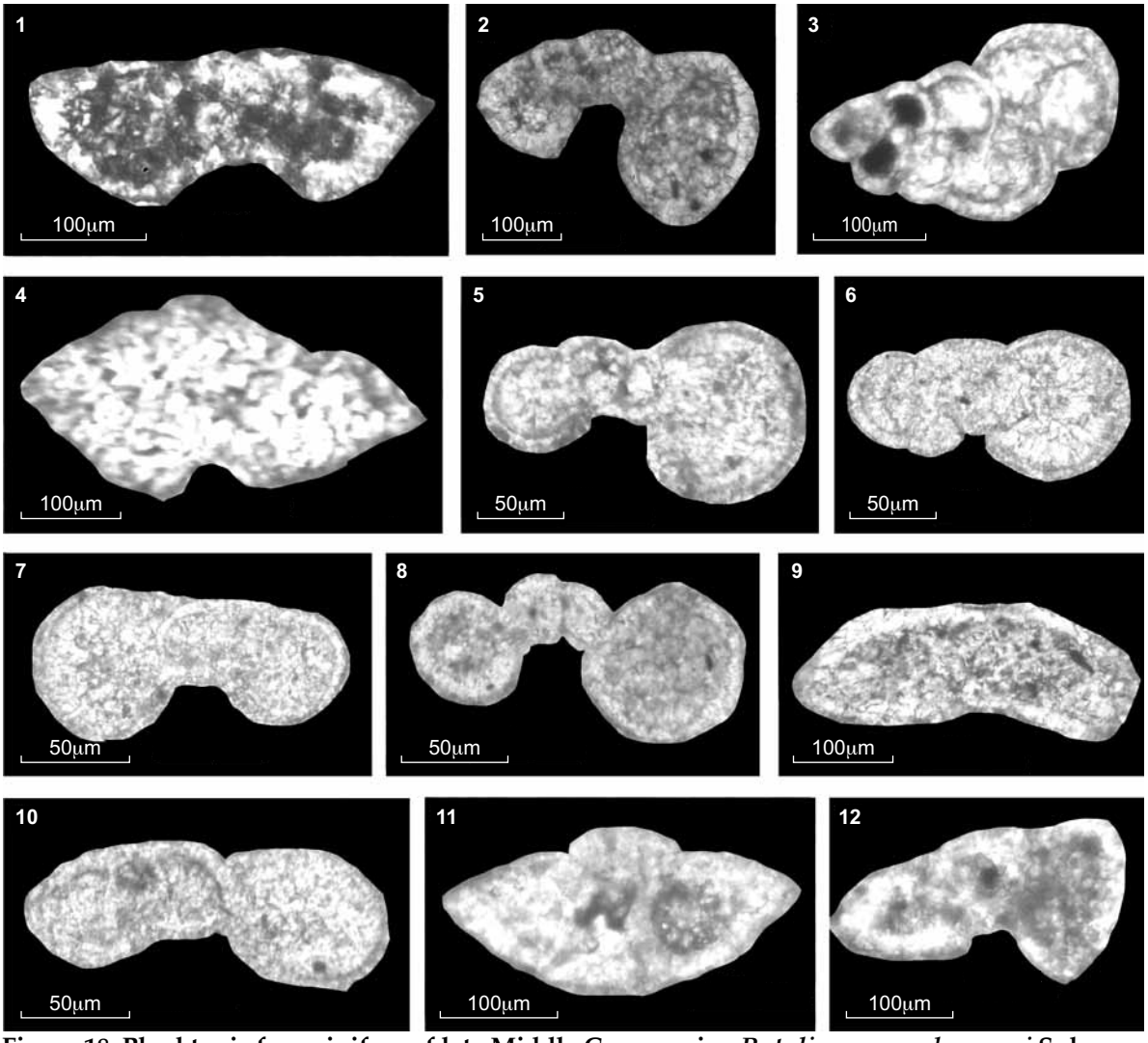

Figure 18: Planktonic foraminifera of late Middle Cenomanian *Rotalipora greenhornensi* Subzone (*Rotalipora cushmani* Zone) (as = axial section; sas = subaxial section; ts = transversal section). (1) *Rotalipora greenhornensis*, [as] (SB). (2) *Muricohedbergella delrioensis*, [as] (SB). (3) *Heterohelix moremani*, [ts] (SB). (4) *Rotalipora cushmani*, [as] (AH). (5 and 6) *Loeblichella hessi*, (5) [as], (6) [sas] (AH). (7 and 10) *Muricohedbergella simplex*, [as] (AH). (8) *Muricohedbergella planispira*, [as] (AH). (9) *Rotalipora montsalvensis*, [sas] (SB). (11) *Rotalipora appenninica*, [as] (AH). (12) *Rotalipora* sp., [as] (SB).

Age and Occurrence: The *Rotalipora greenhornensis* Subzone indicates the late Middle Cenomanian age (Premoli Silva and Verga, 2004). It occurs in 47 m of chalky limestones with chert and dolostones from the uppermost part of unit 21 to unit 24 of Hannafiyah Formation in the AH Section. This subzone is also present in units 22–25 of Slenfeh Formation and Bab Abdallah Formation of the SB Section.

(b) Late Cenomanian Dicarinella algeriana Subzone

Diagnosis: This subzone comprises the range between the FO of the *Dicarinella algeriana* to the FO of *Whiteinella archaeocretacea* or the LO of *Rotalipora cushmani*.

Description: The FO of *Dicarinella algeriana* is accompanied by the gradual disappearance of the genus *Rotalipora* to the end of this subzone and by the diversification of the genus *Whiteinella,* including *W. baltica, W. aprica, W. paradubia, W. praehelvetica, W. aumalensis,* associated with *W. brittonensis,*

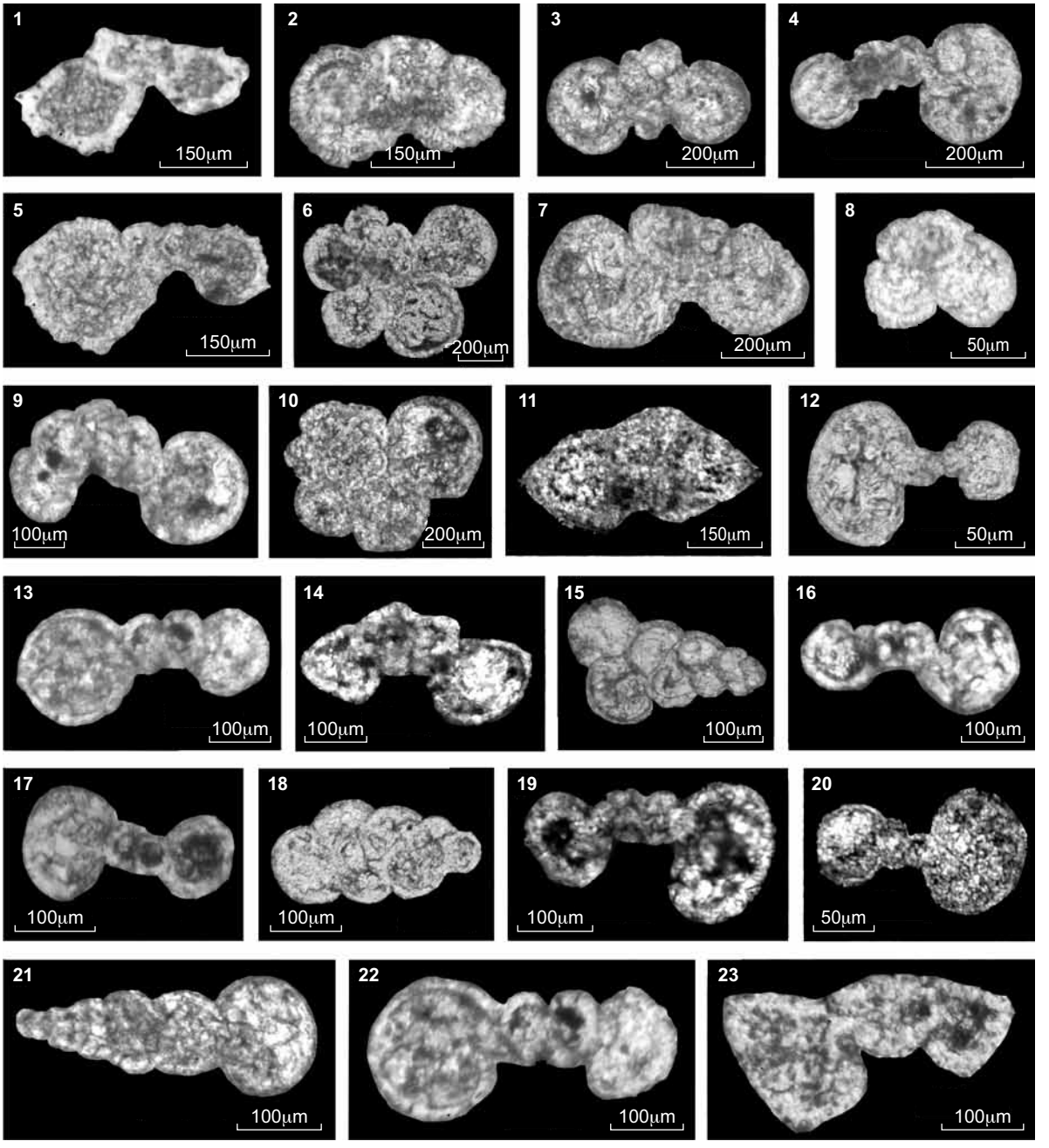

Figure 19: Planktonic foraminifera of Late Cenomanian *Dicarinella algeriana* Subzone (*Rotalipora cushmani* Zone) (as = axial section; sas = subaxial section; es = equatorial section; ses = subequatorial section; ob = oblique section; ts = transversal section).
(1 and 5) *Dicarinella algeriana*, [as] (SB). (2 and 3) *Whiteinella baltica*, [as] (SB).
(4, 7 and 13) *Whiteinella praehelvetica*, [as] (SB). (6 and 10) *Whiteinella* sp., [es] (SB).
(8) *Whiteinella* cf. *paradubia*, [sas] (AH). (9) *Whiteinella brittonensis*, [as] (SB).
(11) *Rotalipora* cf. *cushmani*, [as] (AH).
(12 and 20) *Macroglobigerinelloides bentonensis*, (12) [as] (SB), (20) [as] (AH).
(14) *Praeglobotruncana delrioensis*, [as] (SB). (15 and 21) *Heterohelix reussi*, [ts] (AH).
(16 and 19) *Muricohedbergella planispira*, [as] (AH, SB).
(17) *Macroglobigerinelloides ultramicrus*, [as] (SB).
(18) *Heterohelix moremani*, [ts] (SB).
(22) *Whiteinella aprica*, [as] (AH). (23) *Rotalipora* sp., [as] (AH).

Heterohelix reussi, H. moremani, Rotalipora cushmani, R. montsalvensis, Muricohedbergella planispira, Macroglobigerinelloides bentonensis, M. ultramicrus and *Praeglobotruncana delrioensis* (Figures 7 and 19).

Correlation: Both, the marker species and the planktonic assemblage correlate with the upper *Rotalipora cushmani* Zone, defined by Ogg and Ogg (2008) and correlate with the *Dicarinella algeriana* Subzone according to Premoli Silva and Verga (2004).

Age and Occurrence: The *Dicarinella algeriana* Subzone corresponds to the Late Cenomanian (Premoli Silva and Verga, 2004). It occurs in units 24–27 of the Hannafiyah Formation of the AH Section and units 26–27 of Bab Abdallah Formation (SB Section).

Latest Cenomanian to earliest Turonian Whiteinella archaeocretacea Zone

Diagnosis*:* This biozone is defined by the FO of the zonal markers.

Description: This zone is delineated by *Whiteinella archaeocretacea,* associated with *W. baltica, W. aprica, W. praehelvetica, Heterohelix moremani, H. reussi, Muricohedbergella planispira, M. delrioensi* and *Hedbergella* sp. (Figure 20).

Correlation: This biozone coincides with the Cenomanian/Turonian Boundary interval (Ogg and Ogg, 2008) and was correlated with the *W. archaeocretace* Biozone after Premoli Silva and Verga (2004).

Age and Occurrence: The *W. archaeocretacea* Biozone corresponds to the latest Cenomanian to earliest Turonian (Premoli Silva and Verga, 2004; Ogg and Ogg, 2008). It appears in 30 m thick platy limestones of unit 27 of the Hannafiyah Formation, including the upper dolostones of unit 27 of Bab Abdallah Formation of the MT Section (Figures 4 and 20). The overlying (pelagic) limestones of the Aramo Formation contain Early Turonian planktonic foraminifera (*Helvetoglobotruncana helvetica* Zone).

Early Turonian Helvetoglobotruncana helvetica Zone

Diagnosis: This interval zone is defined in the CR by the first occurrence of *Hetrohelix globolusa* - the nominal taxon is missing.

Description: Besides *Hetrohelix globolusa*, the following taxa were evidenced: *H. reussi. H. moremani, Hedbergella* sp. and *Muricohedbergella delrioensis* (Figure 20).

Correlation: This biozone in the North CR correlates with the *Helvetoglobotruncana helvetica* Zone, defined by Premoli Silva and Verga (2004) and Gradstein et al. (2012) (Figure 7).

Age and Occurrence: The *H. helevetica* Biozone corresponds to the Early Turonian (Premoli Silva and Verga, 2004; Ogg and Ogg, 2008). It was evidenced in ca. 20 m thick white limestones of the Aramo Formation in the upper part of the Slenfeh Section (Figures 4 and 20).

SEQUENCE STRATIGRAPHY

The Aptian–Early Turonian succession of the Coastal Range is characterized by a cyclic organization of sequences/cycles at different scales. Each of these sequences/cycles and their bounding surfaces are interpreted to be unique chronostratigraphic units that developed through rising/falling sea level. The here-defined sequences are based on the lateral comparison of stratigraphic sections and their stacking patterns within the new high-resolution biostratigraphic framework. The applied genetic model of sequence stratigraphy is derived from field observations and thin section analysis. A multitude of high-frequency cycles and half-cycles are defined by changes of the depositional environments that are expressed by different facies associations.

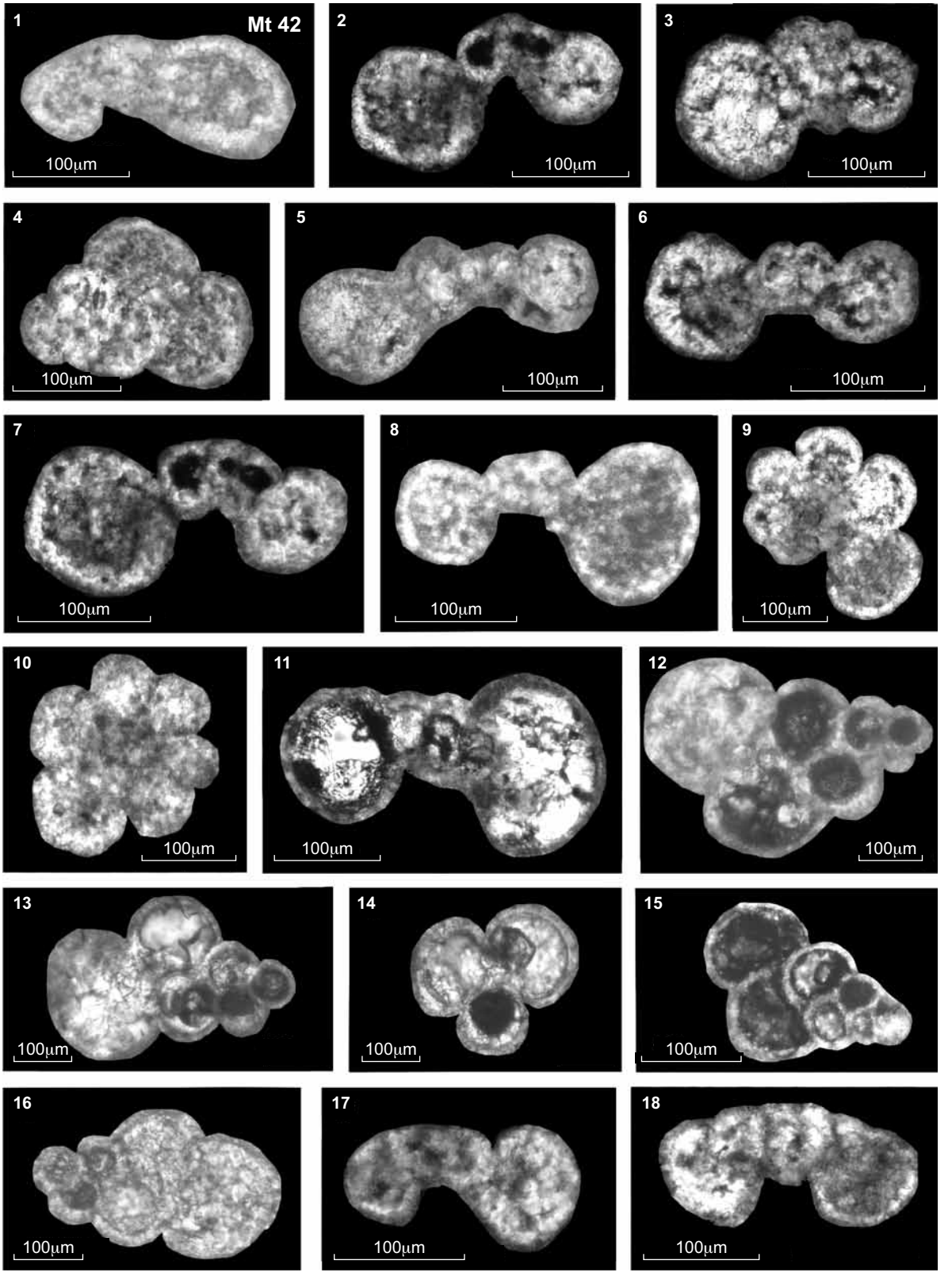

Figure 20: Planktonic foraminifera of latest Cenomanian–Early Turonian *Whiteinella archaeocretacea* Zone and *Helvetoglobotruncana helvetica* Zone (as = axial section; sas = subaxial section; es = equatorial section; ses = subequatorial section; ob = oblique section; ts = transversal section).
(1 and 9) *Whiteinella archaeocretacea*, [as], [es] (MT). (2, 7, 11 and 18) *Muricohedbergella delrioensis*, [sas] (MT).
(3) *Whiteinella baltica*, [as] (MT). (4 and 15) *Heterohelix moremani*, [ts] (MT, SB).
(5) *Whiteinella* cf. *praehelvetica*, [sas] (MT). (6) *Whiteinella aprica*, [as] (MT).
(8) *Muricohedbergella planispira*, [as] (MT). (10) *Hedbergella* sp., [ses] (AH).
(12, 13 and 14) *Heterohelix globulosa*, (12, 13) [ts], (14) [es] (SB). (16) *Heterohelix reussi*, [ts] (SB).
(17) *Muricohedbergella delrioensis*, [sas] (SB).

Comparisons with the "global sequence stratigraphy" (Hardenbol et al., 1998; Gradstein et al., 2012) and the "Arabian Platform sequence stratigraphy" (Sharland et al., 2001, 2004; van Buchem et al., 2010, 2011), permitted determining eleven "Coastal Range (CR) sequences": two Aptian second-order sequences (ApCR1 and ApCR2), four Albian second-order sequences (AlCR1 to AlCR4) and five Cenomanian to Early Turonian third-order sequences (CeCR1-CeCR5). These CR sequences are tied by biostratigraphic criteria to the Arabian maximum flooding surfaces (MFS K) of van Buchem et al. (2010, 2011), to the global sequences boundaries of Gradstein et al. (2012), and to sequence boundaries of the neighboring South Palmyrides (Ghanem et al., 2012), Jordan (Schulze et al., 2004, Wendler et al., 2010) and Sinai (Bachmann et al., 2010). The vertical stacking patterns and lithologic characteristics (including microfacies data) support our new sequence-stratigraphic interpretations, including two "Syrian mfs" (MFS K81S and MFS K82S, Figures 3, 4 and 21). A major outcome of this study is a unified sequence-stratigraphic model, which significantly increases the chronostratigraphic resolution for the Aptian–Early Turonian succession of the Coastal Range (northwest Syria).

Coastal Range Sequence ApCR1 (including MFS K80)

The Upper Jurassic carbonate rocks are separated from the overlying Lower Aptian marls by a regional unconformity that forms the lower sequence boundary of the first Aptian Sequence of the Coastal Range (ApCR1). This Sequence corresponds to the lower Bab Janneh Formation (units 1–4) in the North Coastal Range of the SY Section and in the South CR of the WL Section. An Early Aptian age is confirmed by benthonic foraminifera assemblages of the long-range *Pseudocyclammina vasconica* Biozone (compare Figures 7 and 21).

Sequence ApCR1 represents two Lower Aptian shallowing/deepening-up cycles in both SY and WL sections (Figures 3 and 5a). The basal cycle of the SY Section represents a deepening-up trend with green marls (rich in bivalves and echinoids). The overlying limestones are composed of grainstones to packstones with bioclasts, ooids, benthonic foraminifera and green algae that are attributed to a shallowing-up cycle (unit 2 of the SY Section). A second shallowing/deepening-up cycle above correlates with a major MFS that was compared with MFS K80 of van Buchem et al. (2010), based on biostratigraphic correlation. Dolomite-limestone intercalations above are characterized by high-energy microfacies (grainstones) with benthonic foraminifera, bioturbations and may thus form the shallowest part of Sequence ApCR1 of the SY Section. They correlate with sandy limestones/sandstones and dolomitic limestones of the WL Section (Figures 3 and 5a).

The lower Aptian sequence boundaries Ap1 to Ap3 of Gradstein et al. (2012) coincide with the disconformable lower contact of ApCR1 at the Upper Jurassic–Lower Aptian boundary of the Coastal Range. MFS K80 of van Buchem et al. (2010) is interpreted to correlate with a layer that holds free specimens of *Palorbitolina lenticularis* (Mouty, personal communication), within the upper green marls of unit 3 (Figures 3 and 21).

Coastal Range Sequence ApCR2 (including MFS K81S)

The lower boundary of the ApCR2 in the North CR (SY Section) is defined by a hardground surface, associated with thin caliche crusts. This boundary is correlated to the global sequence boundary Ap5 according to Gradstein et al. (2012) (Figures 3 and 21).

Sequence ApCR2 is correlated with the upper Bab Janneh Formation and the lower part of the Ain Elbeida Formation in the SY Section, and with the upper Bab Janneh Formation in the WL Section of the South Coastal Range. Up to five shallowing/deepening-up cycles can be recognized in the North Coastal Range (SY Section) that are comparable with only one deepening-up cycle in the South Coastal Range (WL Section). The lower three cycles of the SY Section are composed of fossiliferous green marls intercalated with thin-bedded fine- to coarse-grained limestones. The latter hold molluscs, ooids, bioclast and benthonic foraminifera. The shallowing-up cycles include marls and dolostones in the North CR. In the South CR (WL Section) fossiliferous green marls with thin sandstones prevail in the WL Section (Figure 3).

Syrian MFS K81S is represented by ammonite-bearing limestones (with planktonic foraminifera) of the SY Section, respectively by a mollusc-rich interval of the upper green marls of the WL Section (Figure 3) and by marls of the lower Zbeideh Formation of the Southern Palmyrides (Figure 21). It correlates well with the MFS between SBs Ap5 and of Ap6 of Gradstein et al. (2012).

Mouty and Saint-Marc (1982) demonstrated a complete Late Aptian succession in the Coastal Range (based on echinoid-stratigraphy). However we doubt its stratigraphic completeness because of the prevailing shallow-water (partly dolomitic) lithologies in the upper part of Sequence ApCR2 (Figure 21). This is supported by a major hiatus in the Palmyrids, spanning the upper *texana* to lower *subconcava* biozones (Ghanem et al., 2012). Consequently, we interpret a latest Aptian hiatus around the *S. capitata – M. subconcava* boundary (Figure 21) that most likely coincides with the Late Aptian glacio-eustatic lowstand, described by Maurer et al. (2012) from the Arabian Plate.

Coastal Range Sequence AlCR1 (including MFS K82S)

The lower boundary of Sequence AlCR1 may be erosional, as evidenced by mixing of caliche and syn-sedimentary karstic filling (SY Section). It is, moreover, delineated by a rapid facies change from a stromatolitic (laminated) and dolomitic facies (below) to intertidal/shallow subtidal limestones (above); the latter are attributed to a deepening-up cycle (Figure 3). In the WL Section, however, the lower boundary of AlCR1 is obscured by talus at outcrop. The Early Albian sequence boundary AlCR1 correlates well with SB Al1 of Gradstein et al. (2012), based on biostratigraphic comparisons.

Sequence AlCR1 corresponds to the lower part of the Ain Elbeida Formation in North CR and to most of the Blaatah Formation in the South CR. It is represented by a major deepening/shallowing-up cycle in both SY and WL sections. The transgressive part in the SY Section is characterized by thin-bedded oolithic grainstones to packstones. These limestones contain benthonic foraminifera, green algae and bioclasts, indicating open lagoonal environments. The overlying shallowing-up subcycle contains packstone-wackestones with miliolids, laminated dolo-peloidal or pure dolostones (Figure 3).

Syrian MFS K82S is represented by *Orbitolina*–bearing marly limestones at the top of a nodular limestone unit of the SY Section. Biostratigraphically, MFS K82S is situated in the middle part of the *Mesorbitolina subconcava* Zone and may correlate with the global MFS between SBs Al2 and Al3 of Gradstein et al. (2012).

Coastal Range Sequence AlCR2 (including MFS K100)

Two second-order sequences of the Arabian Platform are amalgamated within Sequence AlCR2, due to a major hiatus around MFS K90 *sensu* van Buchem et al. (2010). SB AlCR2 has been identified in both SY and WL sections by a sharp vertical facies change from dolostones (including restricted peritidal carbonates) to pure limestones that represent mid-ramp environments (Figure 3). This SB is correlated with the Early Albian SB Al3 of Gradstein et al. (2012).

The varying lithologies of the Early Albian Sequence AlCR2 (including basaltic rocks) represent the lower part of the Ain Elbeida Formation (SY Section). They correlate with the Blaatah Formation, underlying the basalt of the WL Section (compare Mouty et al., 1992) (Figures 3, 5b and 21).

The cyclic stacking patterns of Sequence AlCR2 of the SY Section exhibits three shallowing/deepening-up cycles, composed of rhythmic beds of dolostones and dolomitized limestones with intercalated

Figure 21 (facing page): Correlation chart of the Aptian–Early Turonian succession based on integrated bistratigraphy and depositional sequences in the Coastal Range (N-S), South Palmyrides (Ghanem et al., 2012) and neighboring areas (Sinai, Jordan). Comparison with regional and global sequence boundaries on the left and maximum flooding surfaces (Arabian Plate) on the right.

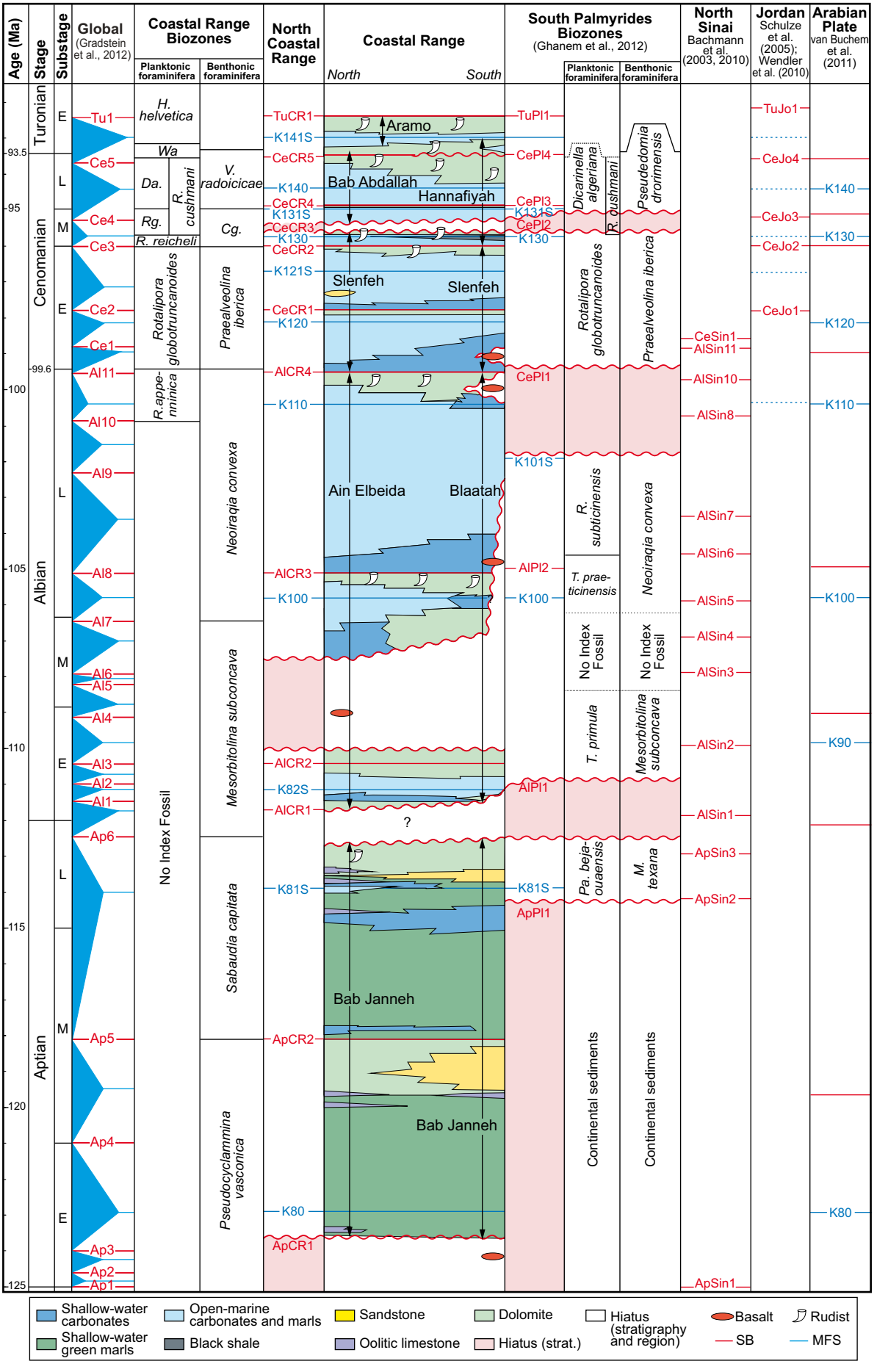
Age (Ma)
Stage
Substage
Global (Gradstein et al., 2012)
Coastal Range Biozones
Planktonic foraminifera
Benthonic foraminifera
North Coastal Range
Coastal Range
North
South
South Palmyrides Biozones (Ghanem et al., 2012)
North Sinai Bachmann et al. (2003, 2010)
Jordan Schulze et al. (2005); Wendler et al. (2010)
Arabian Plate van Buchem et al. (2011)
Turonian
Cenomanian
Albian
Aptian
Aramo
Bab Abdallah
Hannafiyah
Slenfeh
Ain Elbeida
Blaatah
Bab Janneh
No Index Fossil
Continental sediments
Shallow-water carbonates
Shallow-water green marls
Open-marine carbonates and marls
Black shale
Sandstone
Oolitic limestone
Dolomite
Hiatus (strat.)
Hiatus (stratigraphy and region)
Basalt
SB
Rudist
MFS

rudists. They are correlated with one minor deepening/shallowing-up cycle in the WL Section. The latter is composed of thin to massive well-bedded and nodular limestones with abundant benthonic foraminifera, bioclasts, ooids and echinoids (Figure 3).

In both SY and WL sections a major intra-AlCR2 hiatus is represented by volcanic rocks. A basalt, up to 3 m thick (Joubet Barghal, Figure 6e), was dated 108.9 ± 2.6 Ma by Mouty et al. (1992). It is overlain by ca. 50 m-thick Upper Albian strata of Sequence ALCR3 that are, however, completely missing in the South CR. Instead, an up to 24 m-thick basalt flow rests disconformably on Lower Albian limestones of the Blaatah Formation and is disconformably overlain by Lower Cenomanian marls of the Slenfeh Formation in the WL Section (Figures 3 and 5b). Consequently, we assume a major hiatus around 108.9 Ma that comprises a shorter interval (intra-AlCR2) in the North CR and a much longer interval (AlCR2 to AlCR3) in the south, based on sequence-stratigraphic comparisons (Figures 3 and 21). This intra-Albian (volcanic-derived) hiatus spans a maximum-interval from Al3 to Al8 (Gradstein et al., 2012). MFS K90 of van Buchem et al. (2011) lies within that hiatus (Figure 21).

MFS K100 is represented in the SY Section by nodular limestones with planktonic foraminifera. This MFS lies directly above the Lower/Upper Albian boundary, defined by the base of the *Neoiraqia convexa* Zone (Figure 7) and the *Simplorbitolina manasi* Zone of Schroeder et al. (2010), respectively. It is correlated with MFS K100 (ca. 106 Ma) of van Buchem et al. (2011) and is also recognized in the South Palmyrides (Figure 21). The biostratigraphic evidence for that interval (including the whole overlying Sequence AlCR3) is poorly represented in the South CR (Figures 3 and 21).

Coastal Range Sequence AlCR3 (including MFS K110)

Sequence boundary SB AlCR3 in the North CR is formed by a sharp facies change from rudist-bearing dolostones to open lagoon and inner shelf environments. It may correlate with the Late Albian SB Al8 of Gradstein et al. (2012) (Figure 21). In the South CR (WL Section) no age-equivalent sediments of Sequence AlCR3 were evidenced. Thus we assume that this sequence amalgamated with the hiatal surfaces at the base and the top of the 24 m-thick basalts of the WL Section. The basal disconformable contact of the basalts accounts for a correlation with SB AlCR3 (Figures 3 and 21).

The second-order Sequence AlCR3 corresponds to the upper Ain Elbeida Formation of SY and SL sections. It is composed of one major deepening/shallowing cycle that was subdivided into up to seven smaller cycles (Figure 3). Three smaller deepening-up and four smaller shallowing-up half-cycles of the SL Section correlate with one smaller deepening-up cycle and five shallowing-up half-cycles (including one smaller deepening-up cycle) of the SY section. The deepening-up cycles of both sections are composed of nodular and well-bedded to laminated, micritic limestones (wacke-/packstone, with planktonic foraminifera). On the other hand, the shallowing-up half-cycles are composed of massive limestones and dolostones with rudists, often characterized by interbedded laminated and bioturbated limestones (Figure 3). Sequence AlCR3 is well comparable to a regional transgression, expressed by the lower part of Sannine Formation in Lebanon (Nader et al., 2006). The second-order Sequence AlCR3 may correspond with four third-order sequences (AlSin5 to AlSin10) of the northern Sinai (Bachmann et al., 2010).

The Late Albian MFS K110 (van Buchem et al., 2011) corresponds in both sections of the North CR (Slenfeh and Sayno) to an interval rich in planktonic foraminifera of the middle *Rotalipora appenninica* Zone. In the South Palmyrides, a major hiatus spans that interval (Figure 21). Powell and Moh'd (2011) correlated MFS K110 with the initial transgressive phase of "Mega Sequence 2" in Jordan (corresponding to Wadi Juhra Member).

Sequence AlCR4 (including MFS K120)

The Late Albian SB AlCR4 is represented by a hardground surface in the SY Section (Figure 5c), while in the SL Section (South CR), a major facies change from intertidal to subtidal environments is interpreted to represent that surface. SB AlCR4 lies in the uppermost *Neoiraqia convexa* Zone, and thus

is well comparable to the global Late Albian SB Al11 of Gradstein et al. (2012) and to SB CePL1 of the South Palmyrides (Figure 21).

The Late Albian to Early Cenomanian Sequence AlCR4 corresponds to the uppermost Ain Elbeida Formation and lower Slenfeh Formation of both SY and SL sections of the North CR. In the South CR the lower part is missing, due to the hiatus on top of the basalt (WL Section Figures 3 and 5b).

The second-order Sequence AlCR4 is composed of five deepening-up cycles and four shallowing-up cycles in the SL Section that are correlated with three deepening-up and three shallowing-up subcycles of the SY Section and with two shallowing-up cycles of the WL Section (Figure 3). The lower deepening-up cycles of both SY and SL sections are composed of well-bedded, fine-grained limestones (wacke-/packstones with benthonic foraminifera, calcareous algae and peloids), while the upper deepening-up cycle(s) consist of limestones and marly limestones with planktonic foraminifera. Most shallowing-up cycles are characterized by massive dolomites (with minor lamination), chert laminae and nodules and cauliflower quartz geodes (possibly replacing supratidal evaporites of the late highstand (Chowns and Elkins, 1974) (Figures 3 and 6a).

The rapid increase of planktonic foraminifera in unit 17 of SY and SL sections (*Rotalipora globotruncanoides* Biozone) corresponds to MFS K120 (van Buchem et al., 2011). It is also evidenced from the South Palmyrides (Ghanem et al., 2012). In Jordan, Powell and Moh'd (2011) compared MFS K120 with their "mfs1" of the lower Fuheis Formation. According to Schulze et al. (2005), however, MFS 120 lies within the Naur Formation below, as evidenced by SB CeJo1 at the top of the Naur Formation (Figure 21).

Sequence CeCR1 (including MFS K121S)

SB CeCR1 was defined on the top of a massive carbonate unit composed of dolostone-dominated facies. It lies in the middle *Rotalipora globotruncanoides* Biozone and thus is well comparable to the lower Cenomanian SB Ce2 of Gradstein et al. (2012) (Figure 21).

The third-order Sequence CeCR1 corresponds to the middle Slenfeh Formation of the SB Section (Figure 4) and is composed of five shallowing/deepening-up cycles. The shallowing-up cycles are characterized by unfossiliferous marls, dolostones, marls with rudists and chert nodules, and sandstones in the SB Section, whereas the deepening-up cycles are marked by marly limestones and limestones (mudstones to packstones with benthonic foraminifera) at the base and by planktonic foraminifera at the top. In the South CR (AH Section), the uppermost CeCR1 is represented by two deepening-up subcycles (chalky limestones rich in planktonic foraminifera) and only one minor shallowing-up subcycle (an interval of dolostones and limestones with benthonic foraminifera).

The MFS K121S of Sequence CeCR1 corresponds to a marly limestone bed, rich in planktonic foraminifera of the upper *Rotalipora globotruncanoides* Biozone. It is well comparable to an MFS between SBs CeJo1 and CeJo2 *sensu* Schulze et al. (2005) (compare stippled blue line in Figure 21) and may correspond to an MFS between SBs Ce2 and Ce3 *sensu* Gradstein et al. (2012) (Figures 3, 4 and 21).

Sequence CeCR2 (including MFS K130)

SB CeCR2 is situated at the top of massive limestones rich in rudist biostromes of unit 21 (Figure 4) and is overlain by open shelf sediments. This SB lies ca. 15 m above the Lower/Middle Cenomanian Boundary of the SB Section, within the *Rotalipora reicheli* Zone and was compared with the global SB Ce3 according to Gradstein et al. (2012) and with a major SB of the Arabian Platform (below K130 *sensu* van Buchem et al., 2011) (Figures 4 and 21).

Sequence CeCR2 coincides with the upper part of Slenfeh Formation in the northern CR (SB Section) and with the lower Hannafiyah Formation in the southern CR (AH Section, Figure 4). We identified four deepening-up cycles in the SB Section, corresponding to eight deepening-up (half) cycles and

plus six shallowing-up cycles in the AH Section. The deepening-up cycles of both sections are composed of intermediate to thick bedded limestones and marls with thin-walled molluscs, planktonic foraminifera and ammonites, while the shallowing-up subcycles contain massive dolostones rich in rudists in the SB Section. In the AH Section, they are composed of dolostones and limestones with benthonic foraminifera and bivalves. Two shallowing-up cycles are topped by two karstic horizons, due to subaerial exposure (Figures 4 and 5d); the upper karstification bed represents SB CeCR3.

A major Middle Cenomanian MFS of Sequence Ce3 *sensu* Gradstein et al. (2012) coincides with MFS K130 of the Eastern Arabian Plate after van Buchem et al. (2011). In the CR, this MFS corresponds to nodular limestones at the base of unit 22, rich in planktonic foraminifera of the basal *Rotalipora greenhornensis* Subzone (SB Section), and to a conspicuous dm-thick black shale interval (subunit III of the AH Section) with *Lyropecten* sp. and inoceramids (Tröger, personal communication) (Figures 4 and 5d2). In Jordan, MFS K130 was correlated with organic-rich marls in the lower part of the Fuheis Formation (Schulze et al., 2005) (compare stippled blue line in Figure 21) and may correspond with "mfs1" of Powell and Moh'd (2011).

Sequence CeCR3 (including MFS K131S)

SB CeCR3 is regionally significant and recognized by a paleokarstic surface in the upper *R. greenhornensis* Subzone (AH Section, Figures 4 and 5d). This unconformity was correlated with the major global SB Ce4 *sensu* Hardenbol et al. (1998) and Gradstein et al. (2012), and may correspond with a similar exposure surface in Iran (Hajikazemi et al., 2010), Sinai (Gertsch et al., 2010), Egypt (Wilmsen and Nagm, 2012, 2013) and NW Europe (Wilmsen et al., 2005) (Figure 21).

The third-order Sequence CeCR3 corresponds to the lower part of Bab Abdallah Formation (SB Section), and to the middle part of Hannafiyah Formation in the AH Section. It is composed of (nodular) limestones with local chert layers. Vertical stacking patterns reflect three deepening-up and one shallowing-up (half) cycles in the North CR (SB Section). They correspond with three deepening-up and one shallowing-up (half) cycles in the South CR (AH Section, Figure 4).

The deepening-up cycles of the AH Section are characterized by alternating marls (rich in oysters) and limestones with chert nodules and flint lenses (bivalves, corals, ammonites, benthonic and planktonic foraminifera), while nodular limestones, occasionally dolomitized, with planktonic foraminifera prevail in the SB Section. The shallowing-up cycles indicate regressive trends from shallow shelf to very restricted environments, as indicated by dolostones, rich in rudists (both AH and SB sections). The upper Middle Cenomanian MFS K131S corresponds in the AH Section to an interval rich in planktonic foraminifera of the uppermost *Rotalipora greenhornensis* Subzone (Figure 4).

Sequence CeCR3 is well exposed in the Palmyrids (CePl2, Ghanem et al., 2012) with a conspicuous hardground at its base. The latter may correspond with coal-bearing lowstand deposits of CeJo3 (lower part of Fuheis Formation) in Jordan (Schulze et al., 2005, Wendler et al., 2010).

Sequence CeCR4 (including MFS K140)

A sharp facies change between massive dolostones (rich in rudists) and overlying nodular limestones with planktonic foraminifera reflects SB CeCR4 in the North and South CR (Figure 4). This SB is situated between both SBs Ce4 and Ce5 *sensu* Gradstein et al. (2012) (Figures 4 and 21).

Sequence CeCR4 is composed of (nodular) limestones, marls and dolomites; the latter prevail in the upper parts. It corresponds to the upper part of Bab Abdallah Formation of the SB Section, and to the upper part of Hannafiyah Formation in both AH and MT sections. In the North CR (SB Section), Sequence CeCR4 is composed of two deepening-up and one shallowing-up cycles (corresponding to the upper part of Bab Abdallah Formation from a section that was previously collected by Mouty and Saint-Marc (1982). In the South CR (MT Section), within Sequence CeCR4 a total of seven deepening-up and eight shallowing-up (half) cycles were identified (Figure 4).

The deepening-up cycles in South CR are characterized by nodular and well-bedded limestones and marly limestones with nodules and lenses of chert (especially in the lowermost part), while the upper part of the sequence is characterized by a lagoonal environment. The deepening subcycles of North CR are composed of nodular limestones and marly limestones (with planktonic foraminifera and ammonites). The shallowing-up subcycles are characterized by restricted lagoonal facies (bioclastic wackestone). They consist of abundant rudist limestones (in both South and North CR) and dolostones, overlain by thin bedded to platy limestones with benthonic foraminifera, molluscs, stromatolites, laminated packstones and dolomites (MT Section, Figures 4 and 21).

Sequence CeCR4 ranges from the early Late Cenomanian to the latest Cenomanian (*Dicarinella algeriana* Subzone). The rapid increase of planktonic foraminifera in all three sections, AH, MT and SB, at the middle *Dicarinella algeriana* Subzone represents MFS K140 (Figure 4). It correlates to the global MFS between SBs Ce4 and Ce5 of Gradstein et al. (2012, around 94.6 Ma), however, has no equivalent in the Arabian Platform (Figures 4 and 21). In Jordan it is compared to an MFS between CeJo3 and CeJo4 (blue stippled lines in Figure 21), near the Jukes-Browne Event (Wendler et al., 2010). According to the stratigraphic concept of Powell and Moh'd (2011), MFS K140 was placed in the upper part of "Large Scale Depositional Sequence Ajlun 2" (Early Turonian).

Sequence CeCR5 (including K141S)

Several thin hardgrounds within the platy limestones of subunit XVI of the MT Section (South CR) delineate SB CeCR5, coinciding with similar karstic surfaces in the Eastern Arabian Plate (van Buchem et al., 2011). Stratigraphically, it is situated a few meters above the base of *Whiteinella archaeocretacea* Biozone, below the Cenomanian/Turonian Boundary. Moreover, this SB is defined by a sharp facies change from the uppermost dolostones of Bab Abdallah Formation to the deeper-shelf limestones of Aramo Formation (units 27 and 28 of North CR, Figure 4). SB CeCR5 is well comparable to the global SB Ce5 according to Gradstein et al. (2012), to CePl4 (Ghanem et al., 2012), and to CeJo4 directly below OAE2 (Wendler et al., 2010) (Figures 4 and 21).

Sequence CeCR5 is composed of four deepening-up subcycles and four shallowing-up (half) cycles in the MT Section that are correlated with one deepening-up and one shallowing-up cycle of the SB Section (Figure 4). The deepening-up subcycles of South CR (MT Section) comprise limestones with bivalves (abundant oysters) or planktonic foraminifera, and marls. These transgressive deposits are correlated with deeper-shelf limestones and cherts with planktonic foraminifera, pelagic echinoids, sponges and phosphatic grains in the North CR (Aramo Formation). The overlying massive limestones with rudists indicate restricted environments during a shallowing-up cycle of Sequence CeCR5 of both North and South CR, equivalent to SB TuCR1 at the top of Aramo Formation, defined by several hardgrounds in the MT Section (Figure 4). No outcrops occur above in the area, and therefore we could not study the section higher up. Sequence CeCR5 of both the SB and MT sections was not sampled in detail; its stratigraphic importance with respect to the Cenomian/Turonian Boundary became obvious only after studying the isotopic signature. However, a renewed sampling was not possible.

A conspicuous argillaceous marly limestone bed, rich in planktonic foraminifera and siliceous sponges of the lower *Helvetoglobotruncana helvetica* Biozone represents MFS K141S (Figure 21). According to the here-suggested terminology, this MFS corresponds to a third-order MFS *sensu* Gradstein et al. (2012) between SBs CeCR5 and TuCR1 that, however, has no equivalent in the Arabian Platform (Figures 4 and 21). MFS K141S may correspond in Jordan with an intra-OAE2 MFS of the Shueib Formation (Wendler et al., 2010; compare stippled blue line in Figure 21).

Summary of Sequence Stratigraphy

The stratigraphic attribution of the here-discussed second- and third-order sequences of the North Levant Platform was compared with the recently published global sequence boundaries of Gradstein et al. (2012) and with those from the neighboring Arabian Platform (van Buchem et al., 2011), and from adjacent areas of Jordan and Egypt (Figure 21). The major MFS K80, K100, K110, K120, K130

and K140 of the Arabian Plate (Sharland et al., 2001; van Buchem et al., 2011) are well discernable in the Syrian record and allow for an excellent correlation. Moreover, we defined five additional Syrian MFSs: K81S, K82S, K121S, K131S and K141S. K81S and K82S are well comparable with two major flooding surfaces of Gradstein et al. (2012). K121S is well comparable to the Early Cenomanian MFS in Jordan (between CeJo1 and CeJo2 *sensu* Schulze et al., 2005), while MFS K131S has no equivalent in Jordan or the Arabian Peninsula. K141S is well comparable with Gradstein et al. (2012) and Wendler et al. (2010), however, it has no equivalent in the Arabian Plate.

Within the second-order sequences, SB ApCR1 and SB AlCR2 are of regional importance, as they have no equivalents in the neighboring areas. SB AlCR1 and SB AlCR3 are of "global" importance, because they show well comparable age-eqivalent SBs from the Arabian Plate and from Sinai.

Within the third-order sequences AlCR4 to CeCR5, SBs AlCR4, CeCR2, CeCR3 and CeCR5 are well comparable with age-eqivalent SBs from the Arabian and Jordanian record. CeCR1 is comparable with CeJo1 from Jordan only, and thus is interpreted to be of local importance. The sequence-stratigraphic concepts of Powell and Moh'd (2011) are mainly based on facies and lithostratigraphic concepts and therefore do not allow for a good correlation with the here-presented sequence-stratigraphic concept that is based on a high-resolution biostratigraphic framework.

The Aptian sequences of the Coastal Range are characterized by siliciclastically influenced carbonates similar to those of the Sinai, Galilee and Golan heights (Bachmann et al., 2010). In contrast predominantly fluvial lithofacies prevail in Jordan, Lebanon and the Palmyrides (Nader et al., 2006; Powell and Moh'd, 2011; Ghanem et al., 2012).

The late Early Aptian to early Middle Aptian regressive deposits of the Coastal Range are topped by SB ApCR2, equivalent to the hiatus below SB ApPl1 of the Palmyrides (*Muricohedbergella planispira* Biozone, Ghanem et al., 2012, Figure 21). This may correspond to the Late Aptian lowstand of the Arabian Plate and the coincident stratigraphic gap described e.g. by Maurer et al. (2012).

The Albian period of Syria was subdivided into four second-order depositional sequences (AlCR1 to AlCR4) corresponding to two Palmyride sequences (AlPl1 and AlPl2) that were correlated to 10 (mainly third-order) sequences in the northern Sinai (Bachmann et al., 2003, 2010). They are represented by the upper fluvial sandstone in Jordan ("Megasequence 1 Kurnub" *sensu* Powell and Moh'd, 2011; Figure 21). The Cenomanian depositional sequences of the Levant Platform are similar in both areas, Jordan and Syria, compared with the "global sequence boundaries" of Gradstein et al. (2012). A conspicuous Mid-Cenomanian paleokarstic surface of the Coastal Range (SB CeCR3, Figure 5d) and the hardground at SB CePl2 (Palmyrides, Ghanem et al., 2012) coincides with the lowstand of SB CeJo3 of Jordan (Schulze et al., 2005; Wendler et al., 2010) (Figure 21).

CARBON-ISOTOPE STRATIGRAPHY

Carbon-isotope fluctuations may reflect global oceanic perturbations and thus are useful proxies for stratigraphic interpretations of shallow-water carbonate successions (Parente et al., 2007). Several authors tested the carbon-isotope signals of various Cretaceous carbonate platforms (Grötsch et al., 2002; Vahrenkamp, 1996, 2010) and contributed to an Albian to Turonian reference curve that was summarized by Jarvis et al. (2006), where boreal bioevents and global oceanic perturbations are correlated with carbon-isotope excursions. Although not all of the here-described events occur in the Tethyan realm (Parente et al., 2007; Ghanem et al., 2012) several major events of Jarvis et al. (2006) and Kennedy et al. (2004) are comparable on a global scale.

The studied isotope samples are from four sections of the Coastal Range, spanning an Upper Albian to Lower Turonian interval (Figure 22). To exclude diagenetic alteration, all samples were selected from micritic lithologies (after microscopic investigations). The correlation of the four studied sections SL, SB, AH and MT with other references permits biostratigraphic comparisons and the determination of C_{org}-rich intervals that correlate with major global events (Figure 22). We follow Allan and Matthews (1982) for the interpretation of carbon-isotope values in a sequence-stratigraphic context. These

authors suggested that negative $\delta^{13}C$ values may be associated with shallowing, due to alteration by meteoric fluids that resulted in increasing isotopically light carbon from soil zone CO_2 during sea-level fall and subaerial exposure.

Sequence Stratigraphy and Isotope Signatures

The Upper Albian–Cenomanian strata of the Coastal Range were deposited in shallow-marine to hemipelagic environments. $\delta^{13}C$ values range from -1.9‰ to 2.5‰ in the northern SL section and from -4.3‰ to 3.2‰ in the southern AH and MT sections (Figure 22), and thus reflect a characteristic range known from marine limestones, dolomitic limestones and marls (Jenkyns et al., 1994). The carbon-isotope record of six sequences, Upper Albian AlCR3 to Cenomanian CeCR4, comprises the late Albian to Cenomanian succession of the Coastal Range (Figure 22). The main negative-isotope excursions occur during an interval with several subaerial exposures (compare with Hajikazemi et al., 2010).

The late Albian $\delta^{13}C$ excursion during the early *R. appenninica* Zone reached maximum values of ca. 2‰ and was compared with "peak c" of the same age of Mont Risou (Kennedy et al., 2004); it represents the upper part of the Albian/Cenomanian Boundary Event. The following decline of $\delta^{13}C$ values is equivalent to shallower-water depths in the upper part of Sequence AlCR3 (including dolomitic lithologies).

Sequence AlCR4 starts with similar carbon-isotope values in the uppermost *R. appenninica* Zone (around 1.5‰), increasing to a first peak during the lowermost *R. globotruncanoides* Zone that was correlated with "peak d" of the Mont Risou (Figure 22). A short decline of the $\delta^{13}C$ values above is followed by rising $\delta^{13}C$ values (around 2.5‰, Figure 22). This interval was subdivided into two positive plateaus (Figure 22), probably equivalent to LCE I and LCE II of Jarvis et al. (2006). A short-term decrease of $\delta^{13}C$ is correlated with deepening during AlCR4, whereas the topmost 45 m of dolostones have not been sampled (Figure 4; compare unit 19 of SL and SY sections). Within the upper part of Sequence CeCR1, a short positive excursion was correlated with LCE III, while both events, virgatus and Mid-dixoni of Jarvis et al. (2006) are reflected by two characteristic negative excursions in the Coastal Range, all within the upper *R. globotruncanoides* Zone (Figure 22).

At the lower part of Sequence CeCR2 (mid *Rotalipora reicheli* Biozone), a characteristic double-peak (around 1.8‰) was correlated with "peak a" and "peak b" of the Mid-Cenomanian Event after Jarvis et al. (2006). This event was evidenced from limestones in the North CR, while in the South CR, this event occurs within a 0.05 m-thick bed of marly clays and the overlying marly limestone interval. The P/B Break Event of Jarvis et al. (2006) correlates with a minor increase of $\delta^{13}C$ values at the base of the *R. greenhornensis* Zone. It is comparable to a small positive excursion within a 0.4–0.6 m-thick black shale bed, rich in inoceramids and another bivalves species (MFS of CeCE2, compare Figure 5d2) of the AH Section. This event correlates with pelagic marls in the SB Section (Figures 4 and 22). In the upper *R. greenhornensis* Zone of the AH Section, an abrupt decline of $\delta^{13}C$ coincides with two karstic surfaces, including highstand deposits in between. Dolomites prevail in that interval in the SB Section. A major hiatus in the uppermost *R. greenhornensis* Zone occurs in both the North and South CR regions.

Sequence CeCR3 is characterized by slightly decreasing $\delta^{13}C$ values, corresponding to a deepening half-cycle that coincides with the FO of *Dicarinella algeriana* and *Whiteinella* sp. Higher upsection the increasing $\delta^{13}C$ values reach maximum values of 1.8‰ that are correlated with the Jukes-Browne Event of Jarvis et al. (2006). Dolomitic lithologies prevail in a major rudist biostrome above that correspond to the HST of Sequence CeCR3.

Sequence CeCR5 corresponds to the upper *Dicarinella algeriana* Zone and may include the Cenomanian/Turonian Boundary within platy limestones at the top of the MT Section (Figures 4 and 22). Furthermore, it marks an inflection in the long-term $\delta^{13}C$ trend from slightly rising to decreasing values. The short-term rising excursion of the Amphidonte Bed Event of Jarvis et al. (2006) was correlated with a small maximum of $\delta^{13}C$ values during the lower *Dicarinella algeriana* Biozone of the Upper Cenomanian.

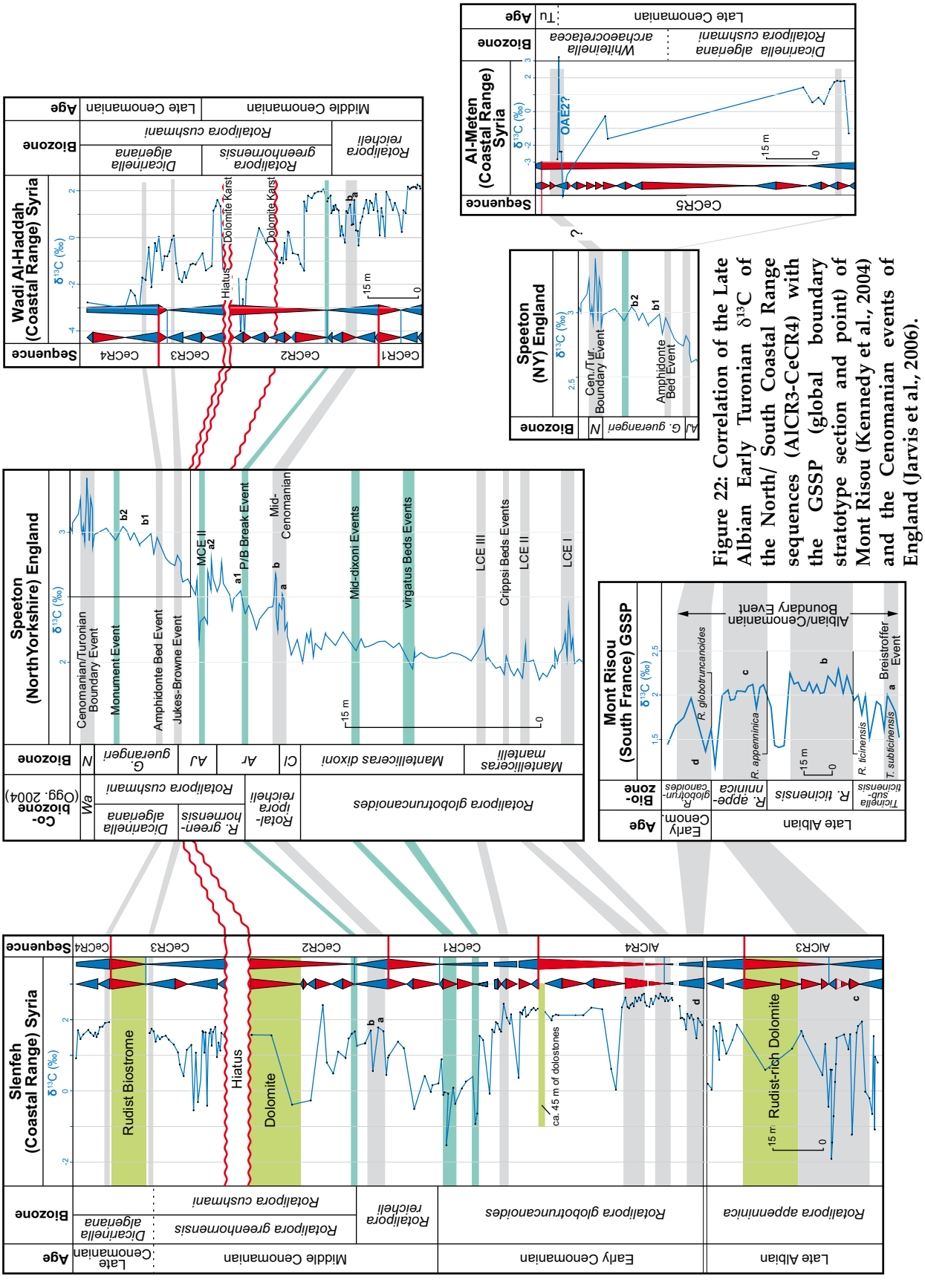

Figure 22: Correlation of the Late Albian Early Turonian $\delta^{13}C$ of the North/ South Coastal Range sequences (AlCR3-CeCR4) with the GSSP (global boundary stratotype section and point) of Mont Risou (Kennedy et al., 2004) and the Cenomanian events of England (Jarvis et al., 2006).

Maximum $\delta^{13}C$ values occur in the uppermost platy limestones of Sequence CeCR4 of the MT Section (Figure 22) that were correlated with the Cenomanian/Turonian Boundary Event (OAE2).

Major Oceanic Events of the Coastal Range: OAE1d, LCE I to LCE III, MCE and P/B Break Events

The combination of various biostratigraphic markers (benthonic and planktonic foraminifera, this study), ammonites, inoceramid bivalves (Sornay et al., 2001; Krasheninnikov et al., 2005) with carbon-isotope signals is employed to establish a high-resolution correlation of the uppermost Albian to the Upper Cenomanian successions of the North and South Coastal Range of northwest Syria.

OAE1d Event

In the studied succession, a double positive peak near the Albian/Cenomanian Boundary (ACB) is correlated with "peak c" of the GSSP (Global boundary stratotype section and point) of Mont Risou (Gradstein et al., 2012; Kennedy et al., 2004). This correlation is supported by the FO of *Rotalipora appenninica* in the North CR (Figure 22), while the FO of *Rotalipora globotruncanoides* of the SL Section (North CR) correlates to "peak d" of the GSSP. The uppermost Albian to lower Cenomanian transition in northwest Syria is characterized by a thick interval from the pelagic limestones of unit 12 to the pelagic marls of unit 17 with the massive dolostones rich in rudists in between (Figure 22).

Lower Cenomanian Events (LCEs) I-III

The Lower Cenomanian $\delta^{13}C$ curve of the CR is marked by three well-defined positive excursions. In the SL Section, LCE I reaches 2.73‰ and occurs in light gray marls with *Neostlingoceras cracitanensis* (Sornay et al., 2001) equal to the lower *Mantelliceras mantelli* Zone (Jarvis et al., 2006). Following a short decline at the top of the marls above, LCE II attains $\delta^{13}C$ values of up to 2.72‰; this excursion is equivalent to chalk-like clayey soft limestones (rich in calcispheres) with flint and cauliflower nodules at the top. In the lower part of the SL Section, LCE III occurs within marly limestones of unit 20 (Figure 4) with positive $\delta^{13}C$ values (up to 2.47‰); it is supplemented biostratigraphically by a characteristic macrofauna (*Mantelliceras mantelli, Sharpeiceras laticlavium, Neithea quinquecostata*, *Inoceramus lynchi* after Krasheninnikov et al. (2005) and planktonic foraminifera (upper *R. globotruncanoides* Zone (Figures 7 and 22).

The Mid-Cenomanian Event (MCE)

The Mid-Cenomanian Event is documented from sections in England (Jarvis et al., 2006), Germany (Wilmsen, 2007), Spain (Paul et al., 1994), Morocco (Gertsch et al., 2010) and Italy (Luciani and Cobianchi, 1999), where it corresponds to the lower part of the middle Cenomanian *Rotalipora reicheli* Biozone (Paul et al., 1994; Jarvis et al., 2006; Gertsch et al., 2010). The $\delta^{13}C$ signature of the MCE in both the South and North CR is represented by small $\delta^{13}C$ peaks (+1.8‰), which correlate to the MFS of the first cycle of CeCR2. The marker bed of this event is characterized by a thin bed of clay with *Rotalipora reicheli*.

Planktonic/Benthonic (P/B) Break Event

The P/B Event is characterized by a rapid increase of planktonic foraminifera marking the base of *Rotalipora greenhornensis* Subzone (*R. cushmani* Biozone) (Paul et al., 1994; Jarvis et al., 2006). However, in the Coastal Range of Syria decreasing $\delta^{13}C$ values exhibit an increase of planktonic foraminifera in this interval and above it. *Rotalipora* becomes much more abundant within the planktonic foraminiferal assemblages (Jarvis et al., 2006). *Rotalipora cushmani* and *R. greenhornensis* first appear at this level marking the base of the *R. greenhornensis* Subzone (*R. cushmani* Zone). The marker bed of this event is characterized by the occurrence of small bivalve *Lyropecten* (*Aequipecten*) *arlesiensis* and large *Inoceramus pictus* (South CR, Figure 5d3) together with the *Rotalipora* spp. in both CR areas.

Jukes-Browne Event

The middle Upper Cenomanian is marked by a small maximum in $\delta^{13}C$ values between the lower *Dicarinella algeriana* Subzone and the upper *R. greenhornensis* Subzone (Figures 7 and 22). It represents a good reference for the base of the Upper Cenomanian (Jarvis et al., 2006).

Amphidonte Bed Event

The lower Upper Cenomanian of the Coastal Range is marked by oyster beds with *Amphidonte* sp. (North CR, Krasheninnikov et al., 2005). A similar Upper Cenomanian oyster event, is also present in the South CR in both MT and AH sections (Figure 22). The $\delta^{13}C$ excursion of the oyster event may equivalent to the *Amphidonte* Bed Event of Jarvis et al. (2006).

Cenomanian/Turonian Boundary Event (OAE2)

The Cenomanian/Turonian Boundary Event (OAE2) carbon-isotope record is poorly known from shallow-water environments. However, the lagoonal carbonate rocks of Coastal Range correlate with a similar platform position in Italy, Portugal, western Morocco, Spain and Mexico. The $\delta^{13}C$ excursion is comparable with deep-water sections (Parente et al., 2007; Parente et al., 2008; Elrick et al., 2009; Gertsch et al., 2010). Regardless of the negative diagenetic values, the maximum positive $\delta^{13}C$ value may span the Cenomanian/Turonian Event (Jarvis et al., 2006). The $\delta^{13}C$ curves of the MT Section show abrupt breaks such as a pronounced positive excursion of 3.2‰ correlating to shallow-marine platy limestones within the *Whiteinella archaeocretacea* Biozone interval (Figures 7 and 22).

CONCLUSIONS

This regional stratigraphic review of the Aptian–Early Turonian succession made use of the largest database available to date in the Coastal Range of Syria. The biozonation schemes allow for a much-improved regional understanding in the particular phylogenetic lineages of the benthonic and planktonic foraminifera. Benthonic foraminifera are presented in seven associations from Aptian to Early Turonian:

(1) Early– early Middle Aptian *Pseudocyclammina vasconica* partial-range zone;
(2) Late Middle–Late Aptian *Sabaudia capitata* interval zone;
(3) Early–Middle Albian *Mesorbitolina subconcava* range zone;
(4) Late Albian *Neoiraqia convexa* taxon-range zone;
(5) Early Cenomanian *Praealveolina iberica* interval zone;
(6) Middle Cenomanian *Chrysalidina gradata* partial range zone;
(7) Late Cenomanian *Vidalina radoicicae* range zone.

Six planktonic foraminiferal biozones are identified from the latest Albian to Early Turonian:

(1) latest Albian *Rotalipora appenninica* Zone;
(2) the Early–early Middle Cenomanian *Rotalipora globotruncanoides* Zone;
(3) the Middle Cenomanian *Rotalipora reicheli* Zone;
(4) the late Middle–Late Cenomanian *Rotalipora cushmani* Zone (including the late Middle Cenomanian *Rotalipora greenhornensis* Subzone and the early Late Cenomanian *Dicarinella algeriana* Subzone);
(5) the latest Cenomanian–earliest Turonian *Whiteinella archaeocretacea* Zone;
(6) the Early Turonian *Helvetoglobotruncana helvetica* Zone.

The larger diversities of the Aptian–Albian benthonic foraminifera in the North CR are in contrast to low diversities in the coeval strata of the South CR (probably due to shallower water depths). The lower transgressive and the early highstands of the Middle Cenomanian–Early Turonian sequences (South CR) are characterized by high diversities and abundance of larger benthonic foraminifera. Furthermore, the Late Cenomanian late highstands of the South CR are characterized by thick rudist biostromes. For the North CR, in contrast, deeper shelf conditions are assumed.

Our new stratigraphic observations of the Aptian–Early Turonian carbonate platforms of the northwestern Arabian Plate in Syria (Coastal Range and the Palmyrides (Ghanem et al., 2012) permit comparisons with those of the eastern Arabian Plate (van Buchem et al., 2011) and Jordan (Schulze et al., 2004; Powell and Moh'd, 2011). Although the detailed lithologic evolution and depositional geometry of these areas differ, the timing of many flooding surfaces and major incisions are similar. In contrast to the eastern Arabian Plate, with extended shallow platforms (including clastic-dominated

successions e.g. during the Albian), coeval platforms of the northwestern Arabian Plate (e.g. Syria, Jordan and Sinai) are much narrower with a steeper gradient; as a consequence, the extended sandy accumulations of the eastern Arabian Plate favored flourishing *Orbitolina* assemblages that are, however, of minor importance in the northwestern Arabian Plate. Therefore, the biotic communities of Syria record many faunal similarities with those of the South European platforms, described for example from the Adriatic Plate.

A composite $\delta^{13}C$ isotope reference curve is proposed for the Coastal Range in Syria, which is calibrated by biostratigraphic controls in both shallow-marine (benthonic foraminifera) and hemipelagic deposits (planktonic foraminifera). Several isotopic events of the CR are recognized and can be correlated with global biotic and abiotic events: OAE1d, LCEs, MCE, P/B Break, Jukes-Browne, Amphidonte Bed and OAE2.

The exceptional outcrop quality displays detailed facies patterns from peritidal to mid-ramp environments. The regional correlation of Coastal Range with the Levant, Arabian Plate and Tethyan realm reveal similar large-scale depositional patterns, within the limits of the biostratigraphic resolution. These correlations suggest that each of the major episodes of the second-order sea-level rise are comparable with MFS K80 to MFS K140 of the Arabian Plate (Sharland et al., 2001; Haq and Al-Qahtani, 2005; van Buchem et al., 2011).

Calibrating our sequence-stratigraphic model with global sequences (Hardenbol, et al., 1998; Gradstein et al., 2012), only the Cenomanian sequences boundaries CeCR1 to CeCR5 appear to have clear inter-basinal equivalents, while ApCR1, AlCR1, AlCR3 CeCR4 and CeCR5 are delineated by major disconformities.

ACKNOWLEDGEMENTS

The authors sincerely thank Prof. Dr. Esmeralda Caus (Barcelona) for her support in analyzing benthonic foraminifera. Our thanks are extended to Dr. Christian Scheibner (Bremen) for his suggestions to an earlier version of the manuscript, to Prof. Dr. Armin Tröger (Freiberg) for determinations of some molluscs, and to Ralf Bätzel for his help in preparing thin sections. We wish to thank the Syrian Petroleum Company for their generosity in providing data used in this study. The DAAD (Bonn) is thanked for financial support. The authors thank GeoArabia's Assistant Editors, Kathy Breining, for proofreading the manuscript and Heather Paul-Pattison for designing the paper.

REFERENCES

Allan, J.R. and R.K. Matthews 1982. Isotope signatures associated with early meteoric diagenesis. Sedimentology, v. 29, p. 797-817.

Alsharhan, A.S. and A.E.M. Nairn 1997. Sedimentary Basins and Petroleum Geology of the Middle East. Elsevier, Amsterdam, 843 p.

Bachmann, M. and J. Kuss 1998. The Middle Cretaceous carbonate ramp of the northern Sinai: Sequence stratigraphy and facies distribution. In V.P. Wright and T.P. Burchette (Eds.), Carbonate Ramps. Geological Society Special Publication 149, p. 253-280.

Bachmann, M., M.A.A. Bassiouni and J. Kuss 2003. Stratigraphic modelling, graphic correlation and cyclicities of mid-Cretaceous platform carbonates - northern Sinai, Egypt. Palaeogeography, Palaeoclimatology, Palaeoecology, v. 200, p. 131-162.

Bachmann, M., J. Kuss and J. Lehmann 2010. Controls and evolution of facies patterns in the Upper Barremian–Albian Levant Platform in North Sinai and North Israel. In C. Homberg and M. Bachmann (Eds.) Evolution of the Levant Margin and Western Arabia Platform since the Mesozoic). Geological Society of London, Special Publication no. 341, p. 99-131.

Banner, F.T. and M.D. Simmons 1994. Calcareous algae and foraminifera as water depth indicators: An example from the early Cretaceous carbonates of northeast Arabia. In M.D. Simmons (Ed.), Micropalaeontology and Hydrocarbon Exploration in the Middle East. British Micropalaeontology Society Publications Series, Chapman and Hall, London, p. 243-252.

Boudagher-Fadel, M.K. 2009. The taxonony and evolution of the foraminiferal genus *Buccicrenata* Loeblich and Tappan. Micropaleontology, v. 47, no. 2, p. 168-172.

Chowns, T.M. and J.E. Elkins 1974. The origin of quartz geodes and cauliflower cherts through the silicification of anhydrite nodules. Journal of Sedimentary Petrology, v. 44, no. 3, p. 885-903.

Dunham, R.J. 1962. Classification of carbonate rocks according to depositional texture. In W.E. Ham (Ed.), Classification of carbonate rocks, A symposium. American Association of Petroleum Geologists Memoir, v. 1, p. 108-171.

Elrick, M., R. Molina-Garza, R. Duncan and L. Snow 2009. C-isotope stratigraphy and paleoenvironmental changes across OAE2 (mid-Cretaceous) from shallow-water platform carbonates of southern Mexico. Earth and Planetary Science Letters, v. 277, no. 3-4, p. 295-306.

Flexer, A, A. Rosenfeld, S. Lipson-Benitah and A. Honigstein 1986. Relative sea-level changes during the Cretaceous in Israel. American Association of Petroleum Geologists Bulletin, v. 70, p. 1685-1699.

Flügel, E. 2004. Microfacies of Carbonate Rocks: Analysis, Interpretation and Application. Springer-Verlag, Berlin, Heidelberg, New York, 976 p.

Gale, A.S., W.J. Kennedy, J.A. Burett, M. Caron and B.E. Kidd 1996. The Late Albian to Early Cenomanian succession at Mont Risou near Rosans (Drome, SE France): An integrated study (ammonites, inoceramids, planktonic foraminifera, nannofossils, oxygen and carbon isotopes). Cretaceous Research, v. 17, p. 515-606.

Gerdes, K.D., P. Winefield, M.D. Simmons and C. Van Oosterhout 2010. The influence of basin architecture and eustacy on the evolution of Tethyan Mesozoic and Cenozoic carbonate sequences. Geological Society of London, Special Publications, v. 329, no. 1, p. 9-41.

Gertsch, B., T. Adatte, G. Keller, A.A.A.M. Tantawy, Z. Berner, H.P. Mort and D. Fleitmann 2010. Middle and late Cenomanian oceanic anoxic events in shallow and deeper shelf environments of western Morocco. Sedimentology, v. 57, no. 6, p. 1430-1462.

Ghanem, H., M. Mouty and J. Kuss 2012. Biostratigraphy and carbon-isotope stratigraphy of the uppermost Aptian to Late Cenomanian strata of the South Palmyrides, Syria. Geoarabia, v. 17, no. 2, p. 155-184.

Gradstein, F.M., J.G. Ogg, M. Schmitz and G. Ogg 2012. (Eds.). The Geologic Time Scale 2012. Elsevier, 1,144 p.

Grötsch, J., I. Billing and V. Vahrenkamp 2002. Carbon-isotope stratigraphy in shallow-water carbonates: Implications for Cretaceous black-shale deposition. Sedimentology, v. 45, no. 4, p. 623-634.

Hajikazemi, E., I.S. Al-Aasm and M. Coniglio 2010. Subaerial exposure and meteoric diagenesis of the Cenomanian–Turonian Upper Sarvak Formation, southwestern Iran. Geological Society, London, Special Publications, v. 330, no. 1, p. 253-272.

Haq, B.U. and A.M. Al-Qahtani 2005. Phanerozoic cycles of sea-level change on the Arabian Platform. GeoArabia, v. 10, no. 2, p. 127-160.

Hardenbol, J., J. Thierry, M.B. Farley, T. Jacquin, P. -C. de Graciansky and P.R. Vail 1998. The Mesozoic and Cenozoic sequence chronostratigraphic framework of European basins. In P.-C. de Graciansky, J. Hardenbol, T. Jacquin and P.R. Vail (Eds.), Mesozoic and Cenozoic Sequence Stratigraphic Framework of European Basins. Society of Economic Paleontologists and Mineralogists Special Publication no. 60, p. 3-13.

Jarvis, I., A.S. Gale, H.C. Jenkyns and M.A. Pearce 2006. Secular variation in Late Cretaceous carbon isotopes: A new $\delta^{13}C$ carbonate reference curve for the Cenomanian– Campanian (99.6– 70.6 Ma). Geological Magazine, v. 143, p. 561-608.

Jenkyns, H.C., A.S. Gale and R.M. Corfield 1994. Carbon- and oxygen-isotope stratigraphy of the English Chalk and Italian Scaglia and its palaeoclimatic significance. Geological Magazine, v. 131, p. 1-34.

Kennedy, W.J., A.S. Gale, J.A. Lees and M. Caron 2004. The global boundary stratotype section and point (GSSP) for the base of the Cenomanian Stage, Mont Risou, Hautes-Alpes, France. Episodes, v. 27, no. 1, p. 21-32.

Krasheninnikov, V.A., J.K. Hall, F. Hirsch, C. Benjamini and A. Flexer (Eds.), 2005. Geological framework of the Levant, Volume I: Cyprus and Syria, p. 165-416.

Kuss, J. 1992. The Aptian-Paleocene shelf carbonates of northeast Egypt and southern Jordan: Establishment and break-up of carbonate platforms along the southern Tethyan shores. Zeitschrift der deutschen geologischen Gesellschaft, v. 143, p. 107-132.

Kuss, J. and M. Bachmann 1996. Cretaceous palaeogeography of the Sinai Peninsula and neighbouring areas. Comptes Rendus Académie des Sciences Paris, v. 322/ser. IIa, p. 915-933.

Le Nindre, Y.-M., D. Vaslet, S.S. Maddah and M.I. Al-Husseini 2008. Stratigraphy of the Valanginian? to Early Paleocene succession in central Saudi Arabia outcrops: Implications for regional Arabian sequence stratigraphy. GeoArabia, v. 13, no. 2, p. 51-86.

Loeblich, A.R., Jr. and H. Tappan 1988. Foraminiferal genera and their classification. Van Nostrand Reinhold Company, New York, 970 p.

Luciani, V. and M. Cobianchi 1999. The Bonarelli level and other black shales in the Cenomanian–Turonian of the northeastern Dolomites (Italy): Calcareous nannofossil and foraminiferal data. Cretaceous Research, v. 20, p. 135-167.

Maurer, F., F.S.P. van Buchem, G.P. Eberli, B.J. Pierson, M.J. Raven, P.H. Larsen, M.I. Al-Husseini and B. Vincent 2012. Late Aptian long-lived glacio-eustatic lowstand recorded on the Arabian Plate. Terra Nova, v. 25, p. 87-94.

Mouty, M. and P. Saint-Marc 1982. Le Crétacé Moyen du Massif Alaouite (NW Syrie). Cahiers de Micropaléontologie, v. 3, p. 55-69.

Mouty, M., D. Delaloye, D. Fontignie, O. Piskin and J.J. Wagner 1992. The volcanic activity in Syria and Lebanon between Jurassic and actual. Schweizerische Mineralogische und Petrographische Mitteilungen, v. 72, p. 91-105.

Nader, F.H., A.F.M. Abdel-Rahman and A.T. Haidar 2006. Petrographic and chemical traits of Cenomanian platform carbonates (central Lebanon): Implications for depositional environments. Cretaceous Research, v. 27, p. 689-706.

Ogg, J.G. and G. Ogg 2008. Mid-Late Cretaceous Charts. <https://engineering.purdue.edu/Stratigraphy/charts/Timeslices/4_Mid-Cret.pdf> <https://engineering.purdue.edu/Stratigraphy/charts/Timeslices/3_Late_Cret.pdf>.

Parente, M., G. Frijia and M. Di Lucia 2007, Carbon-isotope stratigraphy of Cenomanian–Turonian platform carbonates from the southern Apennines (Italy): A chemostratigraphic approach to the problem of correlation between shallow-water and deep-water successions. Journal of the Geological Society, London, v. 164, no. 3, p. 609-620.

Parente, M., G. Frijia, M. Di Lucia, H.C. Jenkyns, R.G. Woodfine and F. Baroncini 2008. Stepwise extinction of larger foraminifers at the Cenomanian–Turonian boundary: A shallow-water perspective on nutrient fluctuations during Oceanic Anoxic Event 2 (Bonarelli Event). Geology, v. 36, no. 9, p. 715-718.

Paul, C.R.C., S.F. Mitchell, J.D. Marshall, P.N. Leafy, A.S. Gale, A.M. Duane and P.W. Ditchfield 1994. Palaeoceanographic events in the Middle Cenomanian of Northwest Europe. Cretaceous Research, v. 15, no. 6, p. 707-738.

Powell, J.H. and B.K. Moh'd 2011. Evolution of Cretaceous to Eocene alluvial and carbonate platform sequences in central and south Jordan. GeoArabia, v. 16, no. 4, p. 29-82.

Premoli Silva, I. and D. Verga 2004. Practical manual of Cretaceous planktonic foraminifera. In D. Verga, R. Rettori (Eds.), International School on Planktonic Foraminifera: Perugia, Italy, Tipografia Ponte Felcino, Universities of Perugia and Milan, 3rd Course, p. 283.

Premoli Silva, I., M. Le Caron, R.M. Leckie, M.R. Petrizzo, D. Soldan and D. Verga 2009. Paraticinella Gen and Taxonomic Revision of Ticinella Bejaouaensis Sigal 1966. Journal of Foraminiferal Research, v. 39, no. 2, p.126-137.

Schroeder, R., F.S.P. van Buchem, A. Cherchi, D. Baghbani, B. Vincent, A. Immenhauser and B. Granier 2010. Revised orbitolinid biostratigraphic zonation for the Barremian–Aptian of the eastern Arabian Plate and implications for regional stratigraphic correlations. In F.S.P. van Buchem, M.I. Al-Husseini, F. Maurer and H.J. Droste (Eds.), Barremian–Aptian stratigraphy and hydrocarbon habitat of the eastern Arabian Plate. GeoArabia Special Publication 4, Gulf Petrolink, Bahrain, v. 1, p. 49-96.

Schulze, F., Z. Lewy, J. Kuss and A. Gharaibeh 2003. Cenomanian-Turonian carbonate platform deposits in west central Jordan. International Journal of Earth Sciences, v. 92, p. 641-660.

Schulze, F., A.M. Marzouk, M.A.A. Bassiouni and J. Kuss 2004. The late Albanian–Turonian carbonate platform succession of west-central Jordan: Stratigraphy and crises. Cretaceous Research, v. 25, p. 709-737.

Schulze, F., J. Kuss and A. Marzouk 2005. Platform configuration, microfacies and cyclicities of the upper Albian to Turonian of west-central Jordan. Facies, v. 50, p. 505-527.

Sharland, P.R., R. Archer, D.M. Casey, R.B. Davies, S.H. Hall, A.P. Heward, A.D. Horbury and M.D. Simmons 2001. Arabian Plate sequence stratigraphy. GeoArabia Special Publication 2, Gulf PetroLink, Bahrain, 371 p., with 3 charts.

Sharland, P.R., D.M. Casey, R.B. Davies, M.D. Simmons and O.E. Sutcliffe 2004. Arabian Plate Sequence Stratigraphy. GeoArabia, v. 9, no. 1, p. 199-214.

Simmons, M.D., J.E. Whittaker and R.W. Jones 2000. Orbitolinids from Cretaceous sediments of the Middle East – a revision of the F.R.S. Henson and Associates Collection. In M.B. Hart, M.A. Kaminski and C.W. Smart (Eds.), Proceedings of the Fifth International Workshop on Agglutinated Foraminifera. Grzybowski Foundation Special Publication 7, p. 411-437.

Sornay, J., M. Mouty and H. Gauthier 2001. Les ammonites du Cénomano-Turonien de la Chaîne côtière (Jibal As-Sahilyeh) de Syrie. Géologie Méditerranéenne, v. 28, p. 243-257.

Vahrenkamp, V.C. 1996. Carbon isotope stratigraphy of the upper Kharaib and Shu'aiba Formations; Implications for the Early Cretaceous evolution of the Arabian Gulf region. American Association of Petroleum Geologists Bulletin, v. 80, no. 5, p. 647-662.

Vahrenkamp, V.C. 2010. Chemostratigraphy of the Lower Cretaceous Shu'aiba Formation: A $\delta^{13}C$ reference profile for the Aptian Stage from the southern Neo-Tethys Ocean. In F.S.P. van Buchem, M.I. Al-Husseini, F. Maurer and H.J. Droste (Eds.), Barremian–Aptian Stratigraphy and Hydrocarbon Habitat of the Eastern Arabian Plate, GeoArabia Special Publication 4, Gulf PetroLink, Bahrain, v. 1, p. 107-137.

van Buchem, F.S.P., M.I. Al-Husseini, F. Maurer, H.J. Droste and L.A. Yose 2010. Sequence-stratigraphic synthesis of the Barremian–Aptian of the eastern Arabian Plate and implications for the petroleum habitat. In F.S.P. van Buchem, M.I. Al-Husseini, F. Maurer and H.J. Droste (Eds.), Barremian–Aptian Stratigraphy and Hydrocarbon Habitat of the Eastern Arabian Plate. GeoArabia Special Publication 4, Gulf PetroLink, Bahrain, v. 1, p. 9-48.

van Buchem, F.S.P., M.D. Simmons, H.J. Droste and R.B. Davies 2011. Late Aptian to Turonian stratigraphy of the eastern Arabian Plate – depositional sequences and lithostratigraphic nomenclature. Petroleum Geoscience, v. 17, p. 211-222.

Velić, I. 2007. Stratigraphy and Palaeobiogeography of Mesozoic Benthic Foraminifera of the Karst Dinarides (SE Europe). Geologia Croatica, v. 60, no. 1, p. 1-113.

Verga, D. and I. Premoli Silva 2002. Early Cretaceous planktonic foraminifera from the Tethys: the genus Leupoldina. Cretaceous Research, v. 23, no. 2, p. 189-212.

Vicedo, V., A. Calonge and E. Caus 2011. Cenomanian Rhapydioninids (Foraminifera): Architecture of the shell and stratigraphy. Journal of Foraminiferal Research, v. 41, p. 41-52.

Wendler, J., J. Lehmann and J. Kuss 2010. Orbital time scale, intra-platform basin correlation, carbon isotope stratigraphy and sea-level history of the Cenomanian–Turonian Eastern Levant platform, Jordan. In C. Homberg and M. Bachmann (Eds.), Evolution of the Levant Margin and Western Arabia Platform since the Mesozoic. Geological Society of London, Special Publication no. 341, p. 171-186.

Wilmsen, M. 2007. Integrated stratigraphy of the upper Lower – lower Middle Cenomanian of northern Germany and southern England. Acta Geologica Polonica, v. 57, no. 3, p. 263-279.

Wilmsen, M. and E. Nagm 2012. Depositional environments and facies development of the Cenomanian–Turonian Galala and Maghra el Hadida formations of the Southern Galala Plateau (Upper Cretaceous, Eastern Desert, Egypt). Facies, v. 58, no. 2, p. 229-247.

Wilmsen, M. and E. Nagm 2013. Sequence stratigraphy of the lower Upper Cretaceous (Upper Cenomanian–Turonian) of the Eastern Desert, Egypt. Newsletters on Stratigraphy, v. 46, no. 1, p. 23-46.

Wilmsen, M., B. Niebuhr and M. Hiss 2005. The Cenomanian of northern Germany: Facies analysis of a transgressive biosedimentary system. Facies, v. 51, no. 1-4, p. 242-263.

ABOUT THE AUTHORS

Hussam Ghanem *is currently a member in the North Africa Group, Bremen, Germany, and joined the University of Homs (Syria). He received his PhD in Geology in 2012 from the University of Bremen (Germany). In his project he has been working on carbonate sedimentology, sequence stratigraphy, biostratigraphy and the tectonic evolution of the Palmyrids and the Coastal Range of Syria. He obtained an MSc in Geology and worked for Petro-service Syria.*

Hussam_ghanem@yahoo.com

Jochen Kuss *was awarded a PhD in 1983 by Erlangen University in Germany following studies on Upper Triassic ramp deposits in the northern Calcareous Alps. From 1983 to 1991 he was an Assistant Professor at the Technical University of Berlin (Germany) and undertook sedimentologic and stratigraphic work in Egypt and Jordan. In 1991 Jochen joined the University of Bremen (Germany). His main research interests are field work-based studies of marine Cretaceous to Paleogene successions in North Africa and the Middle East. Methods used include petrography, (micro) biostratigraphy, geochemistry, remote sensing and basin modeling.*

kuss@uni-bremen.de

Manuscript submitted July 22, 2012

Revised February 10, 2013

Accepted March 1, 2013